Location-Aware Mechanism for Efficient Video Delivery over Wireless Mesh Networks

by

Quang Le-Dang

A Dissertation submitted in fulfilment of the requirements for the award of Doctor of Philosophy (Ph.D.)

Dublin City University

School of Electronic Engineering

Supervisor: Dr. Gabriel-Miro Muntean

Dr. Jennifer McManis

April, 2015

Declaration

I hereby certify that this material, which I now submit for assessment on the programme of study leading to the award of Ph.D is entirely my own work, and that I have exercised reasonable care to ensure that the work is original, and does not to the best of my knowledge breach any law of copyright, and has not been taken from the work of others save and to the extent that such work has been cited and acknowledged within the text of my work.

Signed: _____

Student ID:_____12210460_____

Date: _____24/07/2015_____

Acknowledgement

My first and foremost thank is given to my dearest parents, who have been sparing their best things in life to raise me up. It is their strongest and warmest support that enables me to get over the toughest moments in the past. Special thanks to my dearest wife, Nhi Le-Quynh, who has always been with me through many ups and downs through our life. Since we got married, the time we have spent together is less than that apart due to my PhD. It is her endless and unconditioned love that makes me feel like she was right beside me and taking care of me throughout my PhD journey. They have always been and will forever be my beloved ones.

An extra special acknowledgement goes to my two supervisors, Dr. Gabriel-Miro Muntean and Dr. Jennifer McManis, who have always been extremely kind, helpful and patient during my PhD study. It would not have been possible for me to complete this doctoral thesis without their help and support. They always tried to encourage me to achieve higher standards at every stage, to show me new possibilities for my research, and also to provide me with constructive critics and comments. I would like to pay my greatest respect and regard to Gabi and Jenny, who have been and will always be my dearest advisors and friends.

Big thanks go to my colleagues in DCU PEL, including Zhenghui, Shengyang, Irina, Ronan, Longhao, Ting, Martin, Lejla, Bogdan, Ramona, Faisal, Aarthy, Ruiqi, Yang. Together, we discussed and shared many things including difficulties in our research, and even in our personal life. It is their friendliness and help that make me feel like I am at home with my brothers and sisters and not feeling lonely in a different country. I will never forget our monthly birthday celebrations, our PEL badminton champion League, our visit to Wicklow mountain and our tiring but wonderful 10-km hiking to the top of the Sugarloaf. It has been a wonderful time working with you guys in the DCU PEL family.

Dublin, April 2015

Quang Le-Dang

List of Publications

[Journals]

- Quang Le-Dang, Jennifer McManis, and Gabriel-Miro Muntean, "Location-Aware Chord-based Overlay for Wireless Mesh Networks", *IEEE Transaction on Vehicular Technology*, .Vol. 63, no. 3, pp. 1378-1387, Mar. 2014.
- Quang Le-Dang, Jennifer McManis, and Gabriel-Miro Muntean, "A Location Coordinate-based Video Delivery Scheme over Wireless Mesh Networks", *Accepted to ACM/Springer Wireless Networks*, .Vol. 21, 2015.

[Conferences]

- Quang Le-Dang, Jennifer McManis, and Gabriel-Miro Muntean, "User Location-Aware Video Delivery over Wireless Mesh Networks", *IEEE International Symposium on Broadband Multimedia Systems and Broadcasting*, pp.1-6, London, UK, June, 2013.
- Quang Le-Dang, Jennifer McManis, and Gabriel-Miro Muntean, "Link Quality-Aware Overlay for Video Delivery over Wireless Mesh Network", *Accepted to IEEE International Symposium on Broadband Multimedia Systems and Broadcasting*, Ghent, Belgium, June, 2015.

Table of Contents

List of Figures

List of Tables

List of Algorithms

List of Abbreviations

AODV: Ad hoc On-Demand Distance Vector

AVL: Adelson-Velskii and Landis.

CAN: Content Addressable Network.

CBR: Constant Bit Rate.

CPU: Central Processing Unit.

DSIS: Double Stimulus Impairment Scale

DSR: Dynamic Source Routing.

DSDV: Destination Sequenced Distance Vector Routing.

DSR: Dynamic Source Routing.

DTH: Distributed Hash Table.

EDSR: Enhanced Dynamic Source Routing.

ETX: Expected Transmission Count.

FACC: File Acceptance.

FREQ: File Request.

GHT: Geographic Hash Table.

HTTP: HyperText Transfer Protocol.

IEEE: Institute for Electrical and Electronics Engineers.

ITS: Institute of Telecommunication Science.

ITU: International Telecommunication Union.

LTE: Long Term Evolution.

MANET: Mobile Ad-hoc Network.

MC: Mesh Client.

MChord: Mobile Chord.

MHT: Mobile Hash Table.

MIMO: Multiple Input/Multiple Output.

MOS: Mean Opinion Score.

MPCP: Mobile Peer Control Protocol.

MPP: Mobile Peer-to-Peer.

MPR: Multipoint Relay.

MR: Mesh Router.

MSE: Mean Square Error.

MSM: Multiplication Selector Metric.

MSU: Moscow State University.

NAS: Network-attached Storage.

NUS: National University of Singapore.

OLSR: Optimized Link State Routing.

ORION: Optimized Routing Independent Overlay Nework.

P2P: Peer-to-Peer.

P2PSI: P2P file sharing system over MANET based on Swarm Intelligent.

PSNR: Peak Signal to Noise Ratio.

QAM: Quadrature-Amplitude-Modulation.

QoE: Quality of Experience.

QoS: Quality of Service.

QUVoD: User-centric solution for VoD services.

RREQ: Route Request.

RREP: Route Reply.

RERR: Route Error.

RTSP: Real-Time Streaming Protocol.

RTP: Real-Time Transport Protocol.

SCACJ: Stimulus Comparison Adjectival Categorical Judgement

SINR: Signal to Interference plus Noise Ratio.

SNR: Signal to Noise Ratio.

SSIM: Structural Similarity Index.

SURFNET: SUpeRchunk-based Fast search Network

TC: Topology Control.

TSAR: Tiered Storage ARchitenture for sensor networks.

TTL: Time to Live.

UDP: User Datagram Protocol.

TCP: Transmission Control Protocol.

VANET: Vehicular Ad-hoc Network.

VLC: Video LAN Client.

VMQ: Video Quality Metric.

VoD: Video on Demand.

VoD: Video on Demand.

Wi-Fi: Wireless Fidelity.

WILCO: Wireless Location-aware Chord-based Overlay mechanism for WMN.

WLAN: Wireless LAN.

WLO: Wireless Link quality-aware Overlay peer selection mechanism.

WMN: Wireless Mesh Network.

ZP2P: Zone-based P2P.

Abstract

Due to their flexibility, ease of use, low-cost and fast deployment, wireless Mesh Networks have been widely accepted as an alternative to wired networks for last-mile connectivity. When used in conjunction with Peer-to-Peer data transfer solutions, many innovative applications and services such as distributed storage, resource sharing, live TV broadcasting or Video on Demand can be supported without any centralized administration. However, in order to achieve a good quality of service in such variable, error-prone and resource-constrained wireless multi-hop environments, it is important that the associated Peer-to-Peer overlay is not only aware of the availability, but also of the location and available path link quality of its peers and services.

This thesis proposes a **wireless location-aware Chord-based overlay mechanism for Wireless Mesh Networks (WILCO)** based on a novel geographical multi-level ID mapping and an improved finger table. The proposed scheme exploits the location information of mesh routers to decrease the number of hops the overlay messages traverse in the physical topology. Analytical and simulation results demonstrate that in comparison to the original Chord, WILCO has significant benefits: it reduces the number of lookup messages, has symmetric lookup on keys in both the forward and backward direction of the Chord ring and achieves a stretch factor of $O(1)$.

On top of this location-aware overlay, a **WILCO-based novel video segment seeking algorithm** is proposed to make use of the multi-level WILCO ID location-awareness to locate and retrieve requested video segments from the nearest peer in order to improve video quality. **An enhanced version of WILCO segment seeking algorithm (WILCO+)** is proposed to mitigate the sometimes suboptimal selection of the WILCO video segment seeking algorithm by extracting coordinates from WILCO ID to enable location-awareness. Analytical and simulation results illustrate that the proposed scheme outperforms the existing state-of-the-art solutions in terms of PSNR and packet loss with different background traffic loads.

While hop count is frequently strongly correlated to Quality of Service, the link quality of the underlying network will also have a strong influence on content retrieval quality. As a result, **a Cross-layer Wireless Link Quality-aware Overlay peer selection mechanism (WLO)** is proposed. The proposed cross-layer mechanism uses a Multiplication Selector Metric (MSM) to select the best overlay peer. The proposed MSM overcomes the two issues facing the traditional summation-based metric, namely, the difficulty of bottleneck link identification and the influence of hop count on behavior. Simulation results show that WLO outperforms the existing state-of-the-art solutions in terms of video quality at different background loads and levels of topology incompleteness. Real life emulation-based tests and subjective video quality assessments are also performed to show that the simulation results are closely matched by the real-life emulation-based results and to illustrate the significant impact of overlay peer selection on the user perceived video quality.

CHAPTER 1: Introduction

1.1. Research Motivation

Since their first introduction and commercialization in 1997, the Institute for Electrical and Electronics Engineers (IEEE) 802.11 Wi-Fi (Wireless Fidelity) standards [1] have become the most widely used wireless data access network standards worldwide. As illustrated in Figure 1.1, a survey conducted by Cisco in 2013 [2] shows that Wi-Fi was the predominant access technology for mobile devices. According to this figure, except in the smartphone category, 80% of the devices in other categories are now connecting exclusively through Wi-Fi. More importantly, the popularity of Wi-Fi connections is predicted to increase in the future. Another figure on the Cisco Virtual Network Index [3] clearly shows this trend by pointing out that by the end of 2018, only about 40% of all tablets will be equipped with a cellular connection; while Wi-Fi will still be the must-have type of connection on this type of device. Not only numerous in number are WiFi enabled devices, users tend to prefer Wi-Fi over cellular network when accessing the Internet. Even in the smartphone category, where cellular is a built-in technology, users tend to prefer Wi-Fi connections more. According to the Cisco Global Mobile Data Traffic Forecast [3], by 2018, it is predicted that an average smartphone user will have 52% of his data usage on Wi-Fi, noticeably increased from 44% in 2013. All the above statistics illustrate that from the user point of view, Wi-Fi is the first choice in terms of technology.
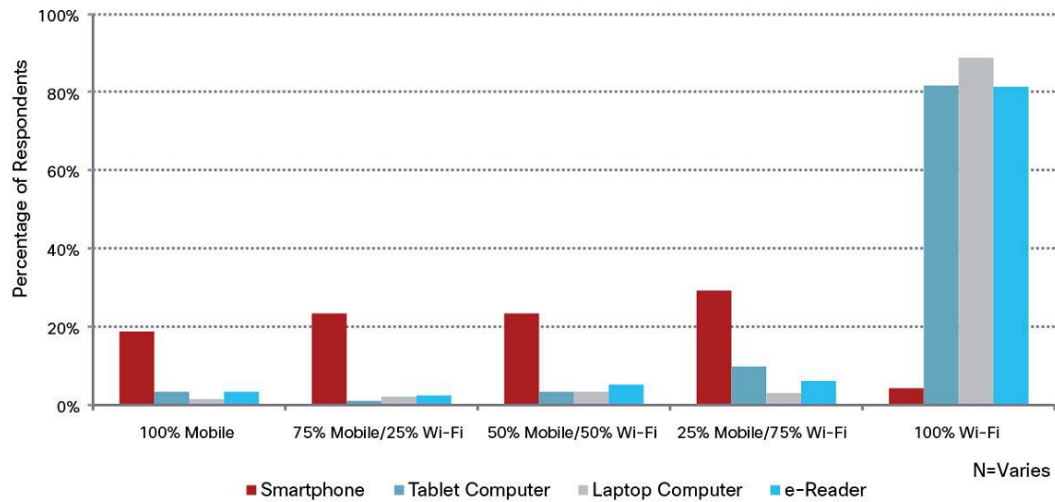
Figure 1.1: Distribution of network connectivity by Time, 2013 [2].

The reasons for the success of Wi-Fi are mostly due to its many benefits in comparison to its cellular technology rival. According to [2], users prefer to use Wi-Fi due to its superior in network speed, reliability, low cost and ease of use. In terms of speed, there have been non-stop bandwidth upgrades for both the IEEE 802.11 and cellular technologies; however, until now, 802.11 standards have always a head start in this benchmark. For instance, the latest 802.11 standard (802.11ac [4]) is capable of providing bandwidth of up to 6.77Gbps while the state-of-the-art on the side of the cellular counterpart (Long Term Evolution – LTE [5]) can only provide up to 300Mbps downlink and 75Mbps uplink. Moreover, the wider coverage range of a cellular cell with more subscribers would further reduce the achievable bandwidth of cellular networks. As a matter of fact, according to Cisco study [3], the Wi-Fi off-load traffic is higher on 4G networks (56%) than on lower speed networks such as 2G (40%) and 3G (49%) networks. The device and data usage cost is another major advantage of Wi-Fi over cellular networking. Regarding the device cost, while it costs almost nothing to have a Wi-Fi module on a mobile device, there is a significant gap between the same mobile device model with and without a cellular module, for instance, the price difference between an iPad tablet with and without cellular connection could be as much as 120 euros[1]. Regarding the data usage fee, although the cellular data cost per Megabyte has reduced significantly recently, the drastically increase in size of contents such as high

---

[1] Comparisons of iPad models - http://www.apple.com/ie/ipad/compare/

quality video and audio makes the monthly data usage significant and sometimes unaffordable to some users such as students. On the other hand, the use of Wi-Fi networks is more or less free most of the time. Not only it is free in coffee shops or restaurants, but also it gradually becomes free in public areas and public transportations (e.g. Dublin Bus free Wi-Fi[2]) in big cities around the globe. With these inevitable benefits, it is unlikely that some other technologies could replace Wi-Fi in its leading role for mobile access networks in the near future.

However, there are also disadvantages of Wi-Fi. One of the most substantial drawbacks of Wi-Fi is its limited coverage. While Wi-Fi can cover indoor scenarios such as in an apartment or a floor of a hotel quite well, its coverage outdoors is quite limited. As Wi-Fi hotspots generally require a wired connection of uplink traffic, it is very expensive to deploy a single operated Wi-Fi network in a large scale scenario such as in a city-wide community network. While the number of Wi-Fi hotspots is undoubtedly increasing on a daily basis, they are operated under different administration and use different wired networks (in terms of operators, network speed, etc.). As a result, in the eyes of users, they appear to be just a collection of isolated "data oases" and not a coherent ubiquitous data access network.

To overcome this problem, in other words, to build a ubiquitous coverage network which is capable of providing seamless data connectivity to users, these "data oases" need to be connected together to form an infrastructure. One of the promising and practical ways of building this infrastructure is to link these Wi-Fi hotspots wirelessly and to incorporate into this infrastructure wireless routing to remove the need for wired connections. This idea is the major motivation behind Wireless Mesh Network (WMN) solutions. WMNs are last-mile access networks which are used for providing wireless Internet access or other services for a large coverage area. A typical WMN includes two types of components: Mesh Routers (MR) and Mesh Clients (MC). MRs connect to each other to form a wireless multi-hop backbone. Some of the MRs have wired connections to the Internet or other networks. MCs are user devices which connect to the WMN through theses MRs to gain access to the provided network resources.

---

[2] Dublin Bus notice on July, 03, 2014: Dublin Bus launches Free Wi-Fi -
http://www.dublinbus.ie/en/News-Centre/Media-Releases-Archive1/All-aboard-Dublin-Bus-with-Free-Wi-Fi-on-all-routes/
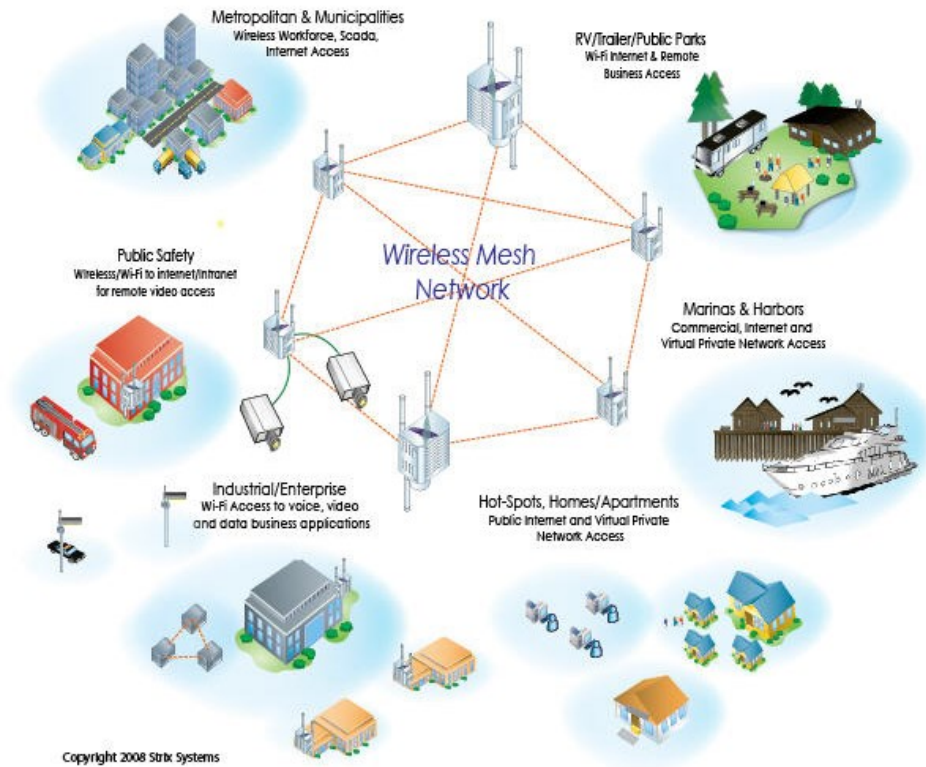
Figure 1.2: Wireless Mesh Network applications[3].

Due to their many advantages such as flexibility, ease of use, low-cost deployment and capability of providing high throughput, WMNs have been widely deployed for last-mile connectivity. From the very few self-constructed and operated WMN such as the National University of Singapore (NUS) Wireless Mesh Testbed[4] with less than 50 nodes, metro-scale Wi-Fi mesh networks have now passed the experimental phase and are well into operation and commercial phases. According to Muniwireless[5], the authority on public Wi-Fi networks worldwide, there is an increasing number of metro-scale Wi-Fi mesh projects currently underway or in the planning stage, all of which are carefully planned and are well supported by governments or enterprises. These deployments open up a new horizon of opportunities for many useful applications. These applications cover a wide range from the municipality access networks to intelligent

---

[3] Image source: http://www.strixsystems.com

[4] NUS Wireless Mesh Testbed - http://mesh.ndslab.net/home/index.html

[5] Muniwireless - http://www.muniwireless.com/category/city-county-wifi-networks/

transport management systems and public safety applications as shown in Figure 1.2. For instance, in the case of intelligent transport systems, WMN is a cost-effective scalable and flexible solution for the information delivery system to control public transportation services. With a citywide WMN and a mesh connection on each of the busses, this system allows anybody to display real-time information on transportation services such as where his/her bus currently is, its ultimate destination and when it is scheduled to arrive. Additionally, statistics of the busses (such as current number of passengers, live video feed of the onboard camera, etc.) can be reported to the bus central office, enabling adaptive allocation and scheduling of buses on each of the routes. Such a system could alleviate transportation congestion problems, reduce pollution, improve transportation safety, security and greatly enhance passengers' experience.
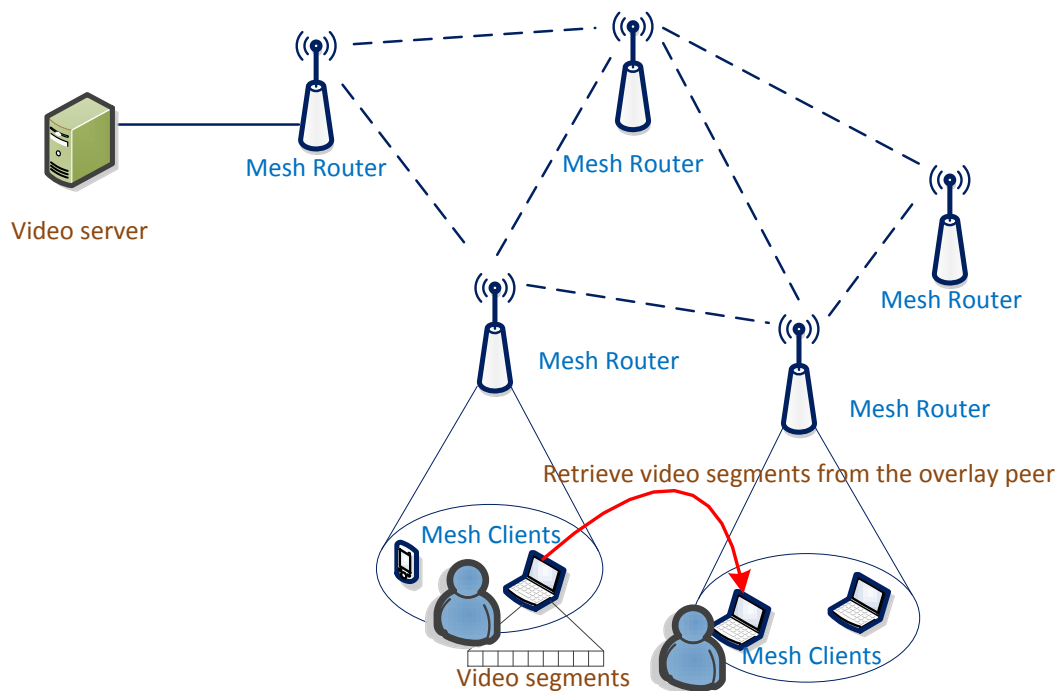
Figure 1.3: VoD overlay over WMN.

Moreover, with the recent evolution of smartphones and tablets, which are now equipped with powerful Central Processing Units (CPU) and higher resolution displays, users are no longer using their devices only for basic Internet access such as web

browsing, email, chat, etc., but also for entertainment purposes with high quality contents. According to Cisco [3], video traffic is forecasted to account for 70% of the overall traffic by 2018. As a result, besides being a common access network, WMN also needs to support the increasing user demands for new, innovative applications such as resource sharing, video on demand (VoD) exchange. The introduction of these types of applications suggests that the combination of peer-to-peer (P2P) overlay network and WMN provides a promising technical solution and is therefore worthy of investigation.

In P2P VoD application for instance such as CoolStreaming[6], many users may watch the same video at the same time but at different progress points in the video. As a result, the same video segment may be simultaneously available at several places in the network. In this context, by making use of the existing user community and getting the video segment from an overlay peer as shown in Figure 1.3, the server load could significantly reduce making P2P VoD a more scalable solution. Moreover, in comparison with the non-P2P approach, by getting the content from the overlay peer instead of the server, the traffic balance in the network would be greatly enhanced instead of concentrating at MRs with wired connections, making bottlenecks in the network. In addition, with the supplement of overlay peers, there are more options of where to get the content from. If the overlay mechanism is also integrated with an intelligent content fetching algorithm, the quality of the provided service could be greatly enhanced.

However, the integration of P2P overlay network over WMN imposes two challenges: how to efficiently deploy P2P overlay network over WMN and how to provide good quality services, especially for video traffic to the users.

1.2. Problem Statement

In contrast to wired connections, wireless channels are error-prone, time varying and bandwidth limited. These critical characteristics of WMN introduce two main challenges for integrating WMN and peer-to-peer overlay networks.

---

[6] CoolStreaming - http://www.coolstreaming.us/

First, the combination of WMN at lower layer and overlay network at higher layer is not straightforward. The current overlay protocols are designed for resource-rich wired networks and require high maintenance traffic for ensuring the correctness and integrity of the overlay. This amount of maintenance traffic increases with the number of overlay peers. While this maintenance overhead may not be a problem in wired networks and is usually ignored when introducing these solutions, it is a big issue in the error-prone and bandwidth limited wireless multi-hop networks when the traditional overlay protocols are used "as is". As the overlay network increases in size the problem gets worse as overlay control messages may have to travel across the physical network many times to reach their destination peers. Consequently, **there is a need for an overlay protocol that is capable of enabling efficient overlay communications on the resource constrained WMNs**.

Second, it is well-known in wireless multi-hop networks that the achievable bandwidth and packet loss performance degrade sharply with many factors such as the number of intermediate nodes between the source and the destination [6], network load, etc. As a result, getting the content from just any overlay peer may result in very bad quality of service as content or resource can be retrieved from a very remote peer. This is especially true for video delivery applications which require critical network conditions for bandwidth, delay and packet loss and a small variation in one of these conditions can significantly degrade the video quality. Hence, a content delivery overlay service for WMN such as VoD should integrate **a mechanism to enable the requesting peer to select the best peer among all the capable peers to retrieve the resource or content it needs for the best quality of service**.

1.3. Contributions

The main contributions of this thesis focus on the design, analysis, simulation and performance evaluation of an efficient location-aware overlay to combine WMN at lower layer and overlay network at higher layer. On top of this, a location-aware and a link quality-aware overlay for video delivery overlay are proposed to improve the overlay retrieval video quality. The specific contributions of this thesis include:

- **Wireless Location-aware Chord-based Overlay mechanism for WMN (WILCO).** The location–awareness of the proposed mechanism is realized through a novel geographical multi-level Chord-ID assignment to the MRs on WMNs. An improved finger table is proposed to make use of the geographical multi-level ID assignment to minimize the underlay hop count of overlay communications. An analytical framework is developed to analyse the lookup efficiency of WILCO. Analytical and experimental results demonstrate that the lookup efficiency and message overhead of WILCO are significantly superior to the state-of-the-art solutions.

- **WILCO-based novel geographical location-aware video segment seeking algorithm.** The proposed video segment seeking algorithm makes use of the multi-level WILCO ID location-awareness to locate and retrieve video segments from the closest peer to improve video delivery quality. An enhance version of this video segment seeking algorithm (WILCO+) is proposed to mitigate the suboptimal selection of the WILCO video segment seeking algorithm by extracting coordinates from WILCO ID to enable location-awareness. Simulation results illustrate that the proposed video segment seeking algorithms can greatly enhance the retrieved video quality in terms of PSNR and packet loss with different background traffic load.

- **Cross-layer Wireless Link Quality-aware Overlay peer selection mechanism (WLO)**. The proposed peer selection mechanism aims at providing the requesting peer a measure at link quality level of the path to overlay peers so that the requesting peer can select the best peer to get the video segment from. A novel Multiplication Selector Metric (MSM) is proposed to overcome the two drawbacks of the traditional summation based metric (i.e., bottleneck link identification and imitating the hop count behaviour). Then, WLO cross-layer mechanism is proposed to select the best overlay peer based on MSM. Simulation results show that WLO outperforms the existing state-of-the-art solutions in terms of video quality at different background loads and levels of topology incompleteness.

1.4. Thesis Structure

The thesis is structured in chapters as follows.

- *Chapter 1* – introduces the motivation of the research, states the research issues and lists the contributions of the research

- *Chapter 2* - presents the background technologies on wireless access protocols and video quality evaluation mechanisms.

- *Chapter 3* - presents a detailed review of the related works and their contributions in the research area of this thesis.

- *Chapter 4* - describes the overall system architecture that is used throughout the report to enable location-aware overlay and geographical video segment seeking.

- *Chapter 5* - presents the proposed WILCO overlay along with the analytical framework, simulation setups and results.

- *Chapter 6* - presents the two proposed WILCO-based geographical video segment seeking algorithms, the segment retrieval efficiency analysis and simulation setups and results.

- *Chapter 7* – presents the Cross-layer Wireless Link Quality-aware Overlay peer selection mechanism, the simulation setups and results. Real-life emulation-based experiments with subjective tests are also conducted to confirm the simulation results and to show the significant impact of overlay peer selection on the user perceived video quality.

- *Chapter 8* - concludes the thesis and presents possible future work directions.

1.5. Chapter Summary

This chapter illustrated the growing trend of WMN from both the user's and service provider's point of view. The motivation of combining WMN with P2P overlay network, the problem statement, the research contributions to advancement of the state of the art as well as the thesis structure are also included.

CHAPTER 2: Technical Background

Abstract

This chapter introduces the technical background of the work presented in this thesis. The chapter starts by presenting different architectures of wireless access networks and the technologies behind them. An overview of wireless multi-hop routing protocols is also introduced. The concept of an overlay network is then illustrated. As multimedia traffic is the main type of traffic considered in this work, multimedia delivery methods are briefly discussed and video quality assessment techniques are described. The chapter concludes with a short summary.

2.1 Wi-Fi Technologies and Network Structures

Wireless communications have evolved very fast over the last 30 years; wireless technologies have shaped and changed our lives drastically in many ways. Network-connected smartphones, laptops, tablets, eBook readers, etc. have now become indispensable devices which are extensions of ourselves and accompany us everywhere from office to home. Despite having many shortcomings in comparison to wired networks such as lower bandwidth and unreliability, the benefits of wireless networks including mobility, cost-effectiveness, ease of use and fast deployment, are very important especially in terms of user-friendliness. These benefits have made wireless access networks the user's first choice for everyday use [2].

2.1.1 The IEEE 802.11 family

In the mid-1990s, with the advent of portable computing devices such as the laptop, users demanded a more convenient way of accessing network support without a physical wire attachment. Foreseeing this increasing demand, the IEEE 802.11 workgroup [7] was formed to draw up a wireless LAN (WLAN) standard. Not very long after this initial attempt, the 802.11 standard [8] was introduced in 1997. Using the unlicensed 2.4GHz spectrum, the first version of Wi-Fi was capable of providing up to 2Mbps bit rate. In comparison with the widely used 10Mbps 802.3 wired Ethernet at the time, this data rate was an impressive achievement.

After this first launch, the IEEE 802.11 workgroup has been constantly working on enhancing the standard, not only in terms of data transfer rate improvement, but also to add value to the existing WLAN such as Quality of Service (QoS) or security. After nearly 20 years of technology evolution, many amendments have made their ways to user devices. A list of 802.11 standards, amendments and supplements is shown in Table 2.1. 802.11a [9] is the first enhancement to the original 802.11 which enables data rates up to 54Mbps over the unlicensed 5GHz frequency band. However, due to the high equipment cost and poor performance, 802.11a devices were not widely adopted in the consumer space. When manufacturers managed to overcome the technical issues and be able to make cheaper 802.11a wireless cards, 802.11b [10] products were already widely available on the market. Operating at 2.4GHz frequency band and providing data rates up to 11Mbps only, 802.11b gained its popularity in the consumer space due to its low-cost. The next Wi-Fi amendment, the 802.11g [11] uses the same 2.4GHz frequency band and is backward compatible with 802.11b. However, 802.11g is capable of providing a much higher data rate of up to 54Mbps. The reliability, high bit rate communication and inexpensive manufacturing cost of 802.11b/g devices made Wi-Fi a big success and led to its widespread adoption in both consumer and enterprise market [2]. Today, this success is so apparent that no laptop is shipping without a Wi-Fi card, while the wired connections may be left out to achieve thinner body, portability and mobility, especially for ultra-books such as Apple Macbook Air[7] and Dell XPS[8].

---

[7] Apple Macbook Air - http://store.apple.com/ie/buy-mac/macbook-air
[8] Dell XPS laptop - http://www.dell.com/ie/p/xps-13-9333/pd?ref=PD_OC

Table 2.1: Overview of 802.11 standard amendments and supplements.

Standard	Year of release	Specifications
802.11	1997	Data rate: 1Mbps and 2Mbps Frequency band: 2.4GHz and infrared Modulation schemes: FHSS, DSSS and IR
802.11a	1999	Data rate: up to 54Mbps Frequency band: 5GHz Modulation schemes: OFDM
802.11ac	2013	Provide very high throughput of up to 1Gbps over the 5GHz spectrum band. 802.11ac uses better modulation scheme, wider channel and multi-user MIMO in comparison with 802.11n.
802.11b	1999	Data rate: up to 11Mbps Frequency band: 2.4GHz Modulation schemes: DSSS
802.11c	2001	Bridge operation procedures
802.11d	2001	International roaming extensions
802.11e	2005	QoS Enhancements and periodization of data packets
802.11f	2003	Inter-Access Point Protocol
802.11g	2003	Data rate: up to 54Mbps Frequency band: 2.4GHz (compatible with 802.11b) Modulation schemes: OFDM
802.11h	2004	Spectrum Managed 802.11a for European compatibility
802.11i	2004	Enhanced Security
802.11j	2004	Extensions for Japan
802.11k	2008	Radio Resource Measurement
802.11m	2007, 2012	Standard maintenance, technical and editorial corrections and improvements
802.11n	2009	Data rate: up to 600Mbps Frequency band: 2.4Ghz and 5GHz (compatible with 802.11a, b, and g) Modulation schemes: MIMO-OFDM
802.11p	2010	Wireless Access for the Vehicular Environment (WAVE)
802.11r	2008	Fast BSS transition
802.11s	2011	Mesh Networking
802.11u	2011	Interworking with non-802 networks such as cellular

The 802.11n amendment [12], which was released in 2009, uses both the unlicensed band of 2.4GHz and 5GHz and is backward compatible with all the 802.11a/b/g devices. The new standard uses Multiple Input/Multiple Output (MIMO) technology and improved modulation schemes which promise an enhancement in the data rate by up to 10 times that of 802.11g with improved reliability and coverage. With the continuous evolution of technology today, there are open doors for many

possibilities. Products of the just-published 802.11ac amendment are already available in the market[9]. Embedded with the state-of-the-art technologies such as extended channel binding, increased MIMO spatial streams, multi-user MIMO and high-density modulation of up to 256 Quadrature-Amplitude-Modulation (QAM), 802.11ac devices are capable of providing very high throughput of up to 1Gbps, which is currently on par with a low-end server wired connectivity.

2.1.2 Wi-Fi Access Network Architectures

Regarding network structures, Wi-Fi access networks are arranged in one of the three ways illustrated in Figure 2.1, i.e., the infrastructure, ad-hoc and wireless mesh architectures.

- *Infrastructure network*. In this type of network architecture, an access point acts as a central exchange point of the network and mediates all the communications between the wireless clients and between the clients and the outside world. The access point usually has a wired connection allowing wireless clients to connect to the Internet or to other networks. This type of network is very simple to deploy in a small scale scenario, easy to manage, with a centralized point of management. Infrastructure networks are also very stable, as the access point is usually stationary and is connected to a wall socket which offers unlimited and uninterrupted power. This type of network is also the most widely used in home and office scenarios due to its simplicity, ease of maintenance and cost effectiveness.

- *Ad-hoc network*. This type of network architecture allows direct communications between the wireless clients without the need of an access point. In other words, ad-hoc networks are decentralized and do not depend on a pre-existing infrastructure to operate which make them extremely flexible to deploy. However, the disadvantages of ad-hoc networks include limited bandwidth and highly dynamic network topology due to client mobility. Moreover, by default, the IEEE 802.11 ad-hoc mode supports only

---

[9] Cisco Meraki wireless - https://meraki.cisco.com/solutions/80211ac

direct point-to-point connection and does not support multi-hop routing. As a result, in order to enable data exchange in a large network consisting of many nodes, routing mechanisms must be integrated on all the nodes. This integration may not be desirable in many cases due to energy constraints, the increase in overhead or computation complexity.

a) Infrastructure Network

b) Ad-Hoc Network

c) Wireless Mesh Network
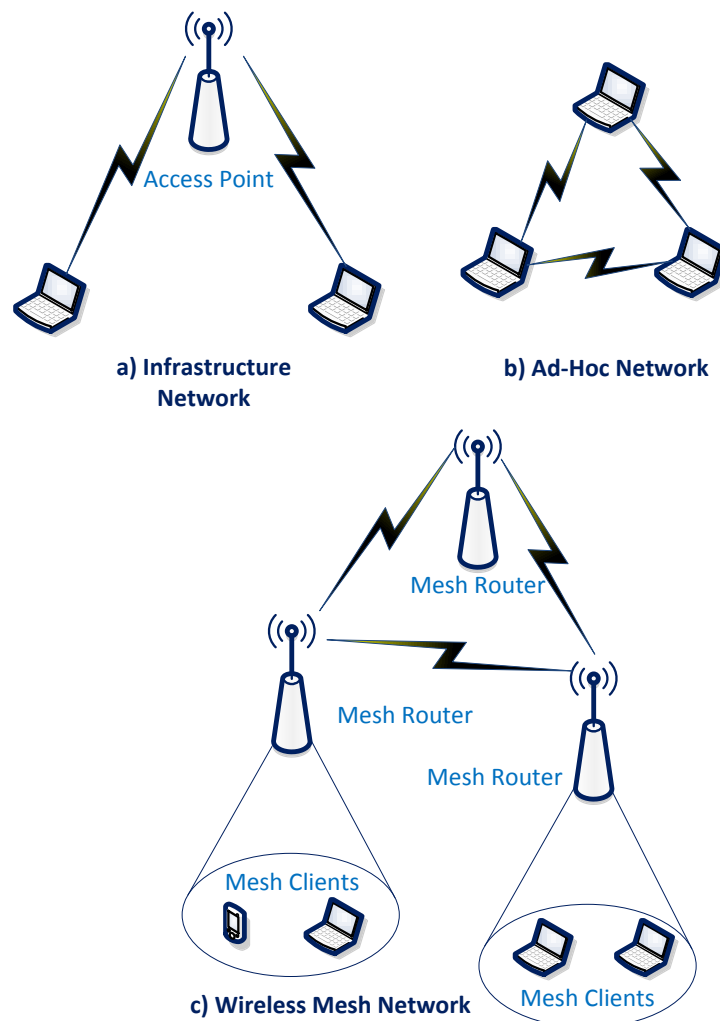
Figure 2.1: Architectures of wireless access networks.

- *Wireless Mesh network.* This type of network architecture is a hybrid combination of infrastructure and ad-hoc network. A typical mesh network consists of two types of devices: Mesh Routers (MR) and Mesh Client (MC).

MRs are stationary, power-unlimited network devices which are used for forwarding the network traffic from the source to the destination. The MRs connect to each other to form a wireless backbone which acts as the wireless backbone infrastructure of the network. Multi-hop routing is integrated into the MRs to enable multi-hop communications. Some of the MRs have wired connections to the Internet or other networks. These MRs are often referred to as gateways to be distinguished from the wireless-only MRs. MCs are user devices, which connect to the WMN through these MRs to gain access to the provided services. The use of the wireless backbone and the mesh topology offers reliability to communication services as the network can self-heal the failure of some of the nodes.

Comparing the above three network architectures, it can be seen that infrastructure networks are suitable for providing network access in small areas such as homes, shopping malls or public Wi-Fi hotspots. The fast installation, ease of usage, reliability and high-speed connection have made infrastructure networks widely available in small size deployments, from houses with a single broadband connection to campus-size or enterprise networks where the access points are connected to an already existed wired infrastructure. However, in large-scale deployments such as the wireless metropolitan networks, the need for wired connection at every access point introduces a substantial installation cost. Beside the budget limitation, in some scenarios such as the rural areas, it is still impossible to have a wired connection at every access point since the wired infrastructure may not exist. In addition, this type of large-scale network lacks of the self-heal ability due to the operational independence among the access points. If the wired connection on a certain access point is not operational for some reasons, all the communications under that access point will cease until the wired connection is restored even if the wireless is still on. Management complexity is another big issue with this type of network when deploying in large-scale.

Ad-hoc networks on the other hand are totally different to the infrastructure counterpart where the network is self-constructed by the wireless clients only. At first look it seems to be a very good solution for large scale networks, given that some multi-hop routing is integrated on all the connected devices, and due to the fact that its size can be automatically adjusted to the user population. However, since the users and their devices move constantly, the ad-hoc network topology changes rapidly. Due to this rapid

change in topology, the life of wireless links in the network is relatively short, making the whole network unstable and hence this type of network is unsuitable for transmitting high traffic loads. The limited bandwidth of user devices is another significant drawback of this type of network structure. In order to maximize mobility capability, most user devices are optimized for minimum battery usage by using a small radio card and antennas which offer very limited bandwidth, capacity and efficiency in comparison with even a home access point. As a result, ad-hoc structure with multi-hop routing is only suitable for small-scale deployments or low-bandwidth and limited processing applications such as wireless sensor networks and not wireless metropolitan area networks.

For large-scale networks, such as metropolitan area networks, connectivity is just one of the requirements. With the increasing demand in data traffic, users also demand high bandwidth at a reasonable cost. In this context, wireless mesh becomes the most promising network structure that is suitable for large-scale wireless access deployment. With the wireless infrastructure built by stationary, power-unlimited MRs, WMN provides a solid and stable backbone, which is capable of providing high-speed, uninterrupted services for the MCs. As opposed to infrastructure networks which are used for public access (Wi-Fi hotspots), where each access point has to have a wired connection, in WMN, only 10-20% of the MRs require a direct connection to the wired backhaul network for an adequate service [13]-[14]. This relaxation enables flexible and fast deployment of WMNs at a significantly reduced cost. Moreover, with the mesh wireless backbone, the network traffic can be dynamically rerouted in response to the failure of some MRs (even with the failure of a MR with wired connection) making the network self-healing and fault-tolerant. It is noted that the power requirements of MRs are rather easy to fulfil as modern MRs are small and versatile enough to be mounted on streetlights or traffic lights and use the available power source. Moreover, the power consumption of these MRs is generally very small; in extreme cases, they can operate independently without any available infrastructure by mounting outside of buildings or on trees with a solar panel and batteries.

Technology-wise, the solution of using dedicated MRs for backbone connections enables the WMN to be upgradeable and customisable to user and operator needs without changing anything in the MC devices. In particular, the MRs can be upgraded in hardware with multi-channel, multi-radio or directional antennas which can further

extend the coverage, significantly increase the backbone/access bandwidth and reduce wireless interference [15]-[17]. Moreover, MRs can also be customized in firmware to enable sophisticated resource allocation techniques for improving the quality of service and supporting user or operator specific services such as VoIP or video streaming [15], [18]-[19].

For its many advantages, it is believed that WMNs are the appropriate answer to the question of enabling metropolitan-scale networks to provide seamless and ubiquitous network access to users [2].

2.2 Overview of Wireless Routing Protocols

In order to enable multi-hop communications in networks such as WMNs, it is important that the MRs in the network are aware of the route between the source and destination so that they can correctly redirect the packet stream towards the destination. As a result, one of the essential components of a wireless multi-hop network is routing. Without multi-hop routing, the network cannot be deployed on a large scale and cannot self-heal against node failures. In contrast to a wired network where the topology is fixed for a relatively long time, nodes in wireless multi-hop networks need to be able to connect to other nodes dynamically due to node mobility or fluctuations in communication channels which may be considered arbitrary. Consequently, in wireless multi-hop networks, nodes are not familiar with the topology of their networks and they have to discover it before any communications can take place. Typically, the discovery process includes broadcast-based advertisement messages from recently joined nodes about their presence. By listening to these advertisement messages, a node learns about its neighbours and may advertise that it can reach them too, so that a two-way relationship can be established. For routing to take place, each node behaves as a router and takes part in the discovery and maintenance of routes to other nodes in the network.

Depending on how this route discovery and maintenance process is conducted, the wireless routing protocols can be classified into two main categories: reactive or on-demand routing protocols and proactive or table driven routing protocols. Essentially, in proactive routing protocols, consistent and up-to-date routing information to all nodes is

maintained at each node even when this information is not needed for routing the current traffic. In reactive routing protocols, the routes are discovered when they are needed to route the traffic only and this process is started by the source host.

2.2.1 Reactive Routing Protocols for Wireless Multi-hop Networks

In reactive routing protocols, route discovery mechanisms run when necessary only, i.e., when there is traffic to be sent to a distant node and there is not an already established route to that node. The triggering traffic has to wait in the buffer of the sending node until the complete route to the destination node is discovered or the timeout expires. In case the route is discovered, the traffic will be sent along the discovered route, otherwise, these packets are discarded. Once a route is established, it is maintained by the route maintenance procedure until either the source does not need the route any longer or the destination node is unreachable for some reasons along that route.

Since a route is discovered when needed only, wireless nodes stay silent most of the time when there is no traffic. As a result, protocol overhead and energy consumption is significantly reduced. However, since a route is discovered on-demand, there is always a delay for this procedure to finish before the traffic can be sent. For a large network, this procedure can be long and a high rate traffic source can overrun the node's buffer causing packet loss.

Among the available reactive routing protocols, such as Dynamic Source Routing (DSR) [20], Ad hoc On-Demand Distance Vector (AODV) [21]-[22]; the AODV routing protocol is perhaps the most commonly used and is widely mentioned in the literature.

Overview of Ad-hoc On-Demand Distance Vector (AODV) routing protocol [21]

AODV is an efficient reactive routing protocol designed for wireless multi-hop networks. In AODV, each node maintains a neighbour table of all the directly connected neighbours in order to provide quick response for new route establishment requests and for routing maintenance. For route discovery, AODV uses a broadcast-based route discovery mechanism in which a route request is broadcast from the source node across

the network. When the route request message reaches the destination node or a node that knows the route to the destination node, a route reply is unicasted back to the source node. Routing information is built at intermediate nodes based on the forwarding of route request and route reply messages. The detailed operation process of AODV can be summarized in five processes: Local Connectivity Management, Route Discovery, Reverse Route Setup, Forward Route Setup and Route Maintenance.

- **Local Connectivity Management**

AODV enables nodes to learn about their neighbours and establish a bidirectional connectivity with them by periodically broadcasting "Hello" messages. Each "Hello" message includes the sending node identity and the identities of all of its neighbours. Whenever a node receives a broadcast "Hello" message from a neighbour, the receiving node updates the sending node identity to its local neighbour tables, which includes all its directly connected neighbours. In the subsequent "Hello" messages, the receiving node also adds the newly discovered neighbour to its list of neighbours. If a node receives a "Hello" message with itself in the neighbour list, it declares the link to sending neighbour as a bidirectional link. In an AODV "Hello" message, the time to live (TTL) value is set to 1 to prevent the message from being rebroadcasted outside the neighbourhood of the node.

If a node fails to receive a predefined consecutive number of "Hello" messages from a neighbour, the node assumes that neighbour is down and removes it from its neighbour table. In the case the failed neighbour is part of an active link, the active neighbours using that next hop will be notified of the link failure. This link failure notification belongs to the route maintenance process which will be described latter.

- **Route Discovery**

The AODV path discovery process begins when a source node needs to communicate with another node for which it has no routing information in its routing table. The source node initiates route discovery by broadcasting a "Route Request" (RREQ) message. The RREQ contains the following fields:

<source_addr, source_seq_no, broadcast_id, dest_addr, dest_seq_no, hop_cnt>

source_addr and *dest_addr* are the source and destination address, respectively. Together they uniquely identify a RREQ. *broadcast_id* is incremented whenever the source issues a new RREQ.

The *source_seq_no* is used to maintain freshness information about the reverse route to the source. The *dest_seq_no* is the last destination sequence number known to the source and this number specifies how fresh a route to the destination must be before it can be accepted by the source. The *source_seq_no* and the *dest_seq_no* are used in the Reverse Route Setup and the Forward Route Setup which will be shown next.

Upon receiving the RREQ, each node in the network either sends a "Route Reply" (RREP) message to the source node, if it has the routing information to the destination or re-broadcasts the RREQ after increasing the *hop_cnt*. If a node does not have the routing information for the RREQ, it also keeps track of the *dest_addr*, *source_addr*, *broadcast_id*, *source_seq_no*, and the expiration time for the reverse path route entry of the RREQ in order to process the reverse and forward path setup procedures. Together, the *source_addr* and *broadcast_id* are also used to eliminate redundant packets in case a node receives multiple copies of the same broadcast RREQ packet.

- **Reverse Route Setup**

As the RREQ travels from a source node to various intermediate nodes, the reverse route back to the source is automatically set up at each of these intermediate nodes which received the RREQ. This reverse route is constructed by recording the address of the neighbour from which the first copy of the RREQ was received. The reverse route entries are maintained for a predefined expiration time which is at least long enough for the RREQ to traverse the network and for the reply to get back. Figure 2.2 illustrates the reverse route pointers that points back to the neighbours from which the RREQ was received. In this figure, S and D are the source and destination node, respectively.
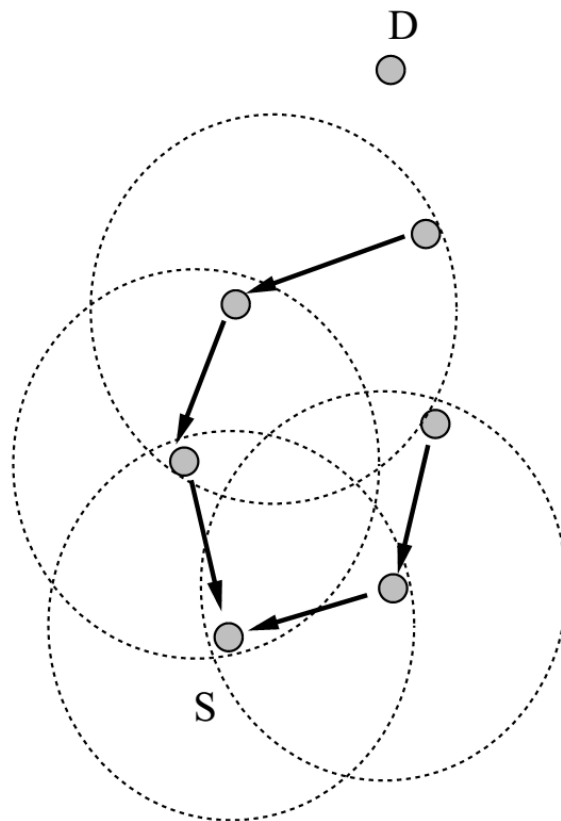
Figure 2.2: AODV reverse route setup. [21]

- **Forward Route Setup**

If the RREQ was received from a bidirectional link, when the RREQ arrives at the destination node or a node that knows the route to the destination, the forward route setup procedure starts. If the receiving node is an intermediate node to the destination, it first determines if the routing information it has is current by comparing the *dest_seq_no* in its own route entry with that in the RREQ. If the *dest_seq_no* in the RREQ is higher, the intermediate node considers its own routing information out of date and rebroadcasts the RREQ without sending the RREP. If the *dest_seq_no* in the route entry of the intermediate node is greater or equal to that in the RREQ and the RREQ has not been processed previously (use *source_addr* and *broadcast_id* to eliminate the redundant packets), the intermediate node will unicast a RREP to the source node through the neighbour from which it receives the RREQ. The RREP contains the following fields:

<source_addr, dest_addr, dest_seq_no, hop_cnt, lifetime>
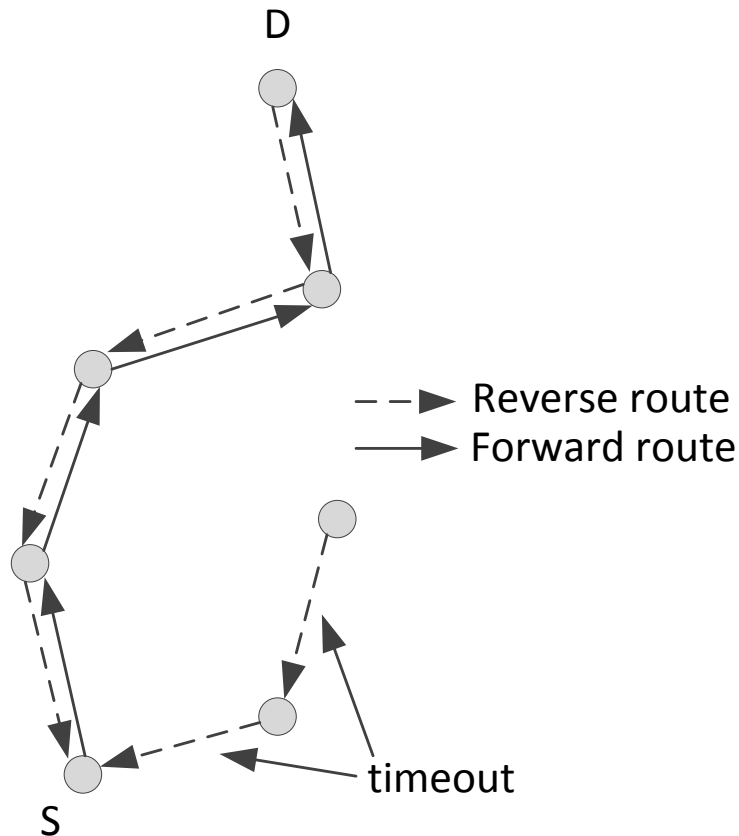
Figure 2.3: AODV forward path formation. [21]

Since the reverse route was already setup when the RREQ travels the network using the pointers in the Reversed Route Setup Procedure, the RREP follows this reverse route to travel back to the source node. As the RREP travels back to the source node, each node along the path sets up a forward pointer to the node from which the RREP was received. The timeout information and the latest *dest_seq_no* are also updated.

Figure 2.3 illustrates the forward route setup from the destination node D to the source node S. The solid arrows are the forward pointers to the destination. The dotted arrows are the reverse route pointers which are constructed during the propagation of the RREQ. Since the RREQ broadcasts to the whole network, multiple reverse paths are

built, even between nodes that are not along the route to the destination. However, these reverse routes will be deleted after a predetermined timeout duration.

An intermediate node propagates the first RREP for a given source node through the reverse path towards that source. It suppresses all further RREP for this source node unless the RREP contains either a greater *dest_seq_no* or the same *dest_seq_no* but with a smaller hop count. In this case, it updates its routing information and propagates this better RREP. The source node can start data transmission as soon as the first RREP is received and can latter update its routing table with a better route.
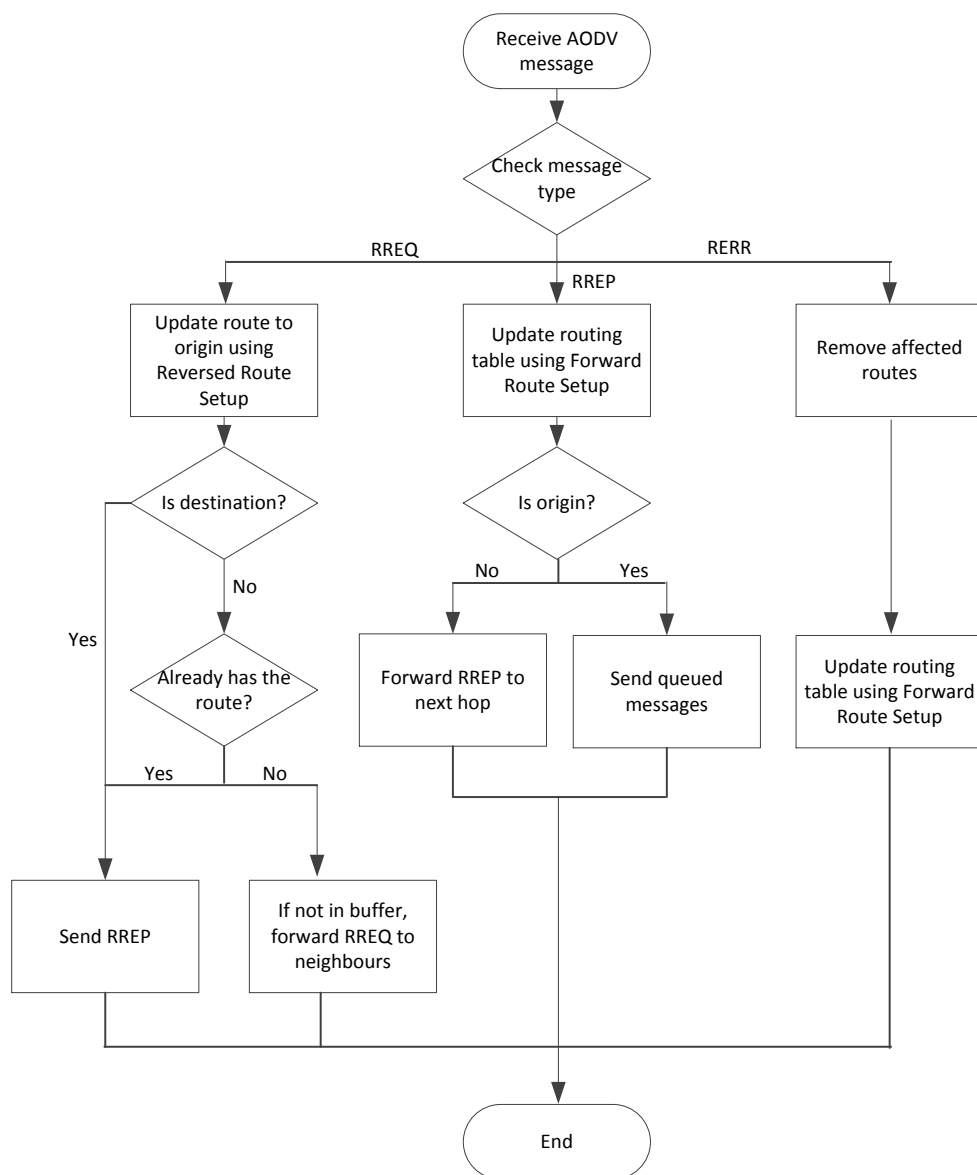
Figure 2.4: AODV operation flowchart.

- **Path Maintenance**

A route is considered active as long as there are data packets travelling from the source to the destination along that path. Once the route becomes idle, the reverse and forward pointers will time out and be deleted from the intermediate node routing tables.

As long as the route remains active, each intermediate node monitors the links towards the source and the destination by monitoring its neighbours on the paths using the local connectivity management mechanism described earlier. If a link break occurs at an intermediate node while the route is active, the node propagates a Route Error (RERR) message to the source node to inform it of the now unreachable destination(s). Upon receiving this notification of a broken link, the source node can restart the discovery process if it still requires a route to the destination.

Figure 2.4 summarizes the basic operations of AODV in the form of a flowchart when processing different types of AODV messages. HELLO messages are excluded from the diagram for brevity

2.2.2 Proactive routing protocols for wireless multi-hop networks

Proactive routing protocols take a totally different approach than reactive routing protocols, as they are based on periodic exchange of control messages. Some of these messages (which are similar to AODV "Hello" messages) are exchanged locally between network nodes to provide participating network nodes the information about their local neighbourhood. Beside these locally exchanged messages, there are types of messages that are sent to the entire network in order to exchange knowledge of network topology among the nodes in the network. By using this information, each and every node in the network can construct the topology of the whole network and have the optimized routing information to all the nodes in the network.

Since the routing information is already available whenever data packets need to be sent, there is no routing delay and no packet loss of buffer overrun due to this delay. However, since the routing information is calculated beforehand, periodic topology

24

updates cause additional overhead even when the routing information is not needed or when there is no data traffic for routing.

Among the available proactive routing protocols such as Destination-Sequenced Distance Vector routing (DSDV) [23], Optimized Link State Routing (OLSR) [24]-[25], the OLSR protocol is perhaps the most commonly used and widely mentioned in the literature.

Overview of Optimized Link State Routing (OLSR) routing protocol [24]-[25]

OLSR is an efficient proactive routing protocol for wireless multi-hop networks. As its name suggests, OLSR uses the link-state scheme to diffuse and calculate routing information. However, instead of flooding the link-state information throughout the network, in order to preserve network bandwidth, OLSR-enable nodes elect a subset of their directly connected neighbours as their Multipoint Relays (MPR). By using these MPRs as their communication gateway for both routing information and data exchange to the rest of the network, OLSR greatly reduces the routing messaging overhead. OLSR MPR, neighbour sensing, MPR selection, MPR information declaration and routing table calculation will be discussed next to give an overview of OLSR protocol.

- **OLSR Multipoint relays (MPR)**

The motivation behind multipoint relays is to minimize the flooding broadcast of routing packets in the network by reducing the duplicate retransmissions in the same region. Each node selects its multipoint relays, i.e., the multipoint relay set, among its one hop neighbours so that the set of selected nodes covers all the nodes that are two hops away. These multipoint relays of a node N, called $MPR(N)$, are a subset of N's bidirectional neighbours in which every node in the two hop neighbourhood of N must have a bidirectional link towards $MPR(N)$.
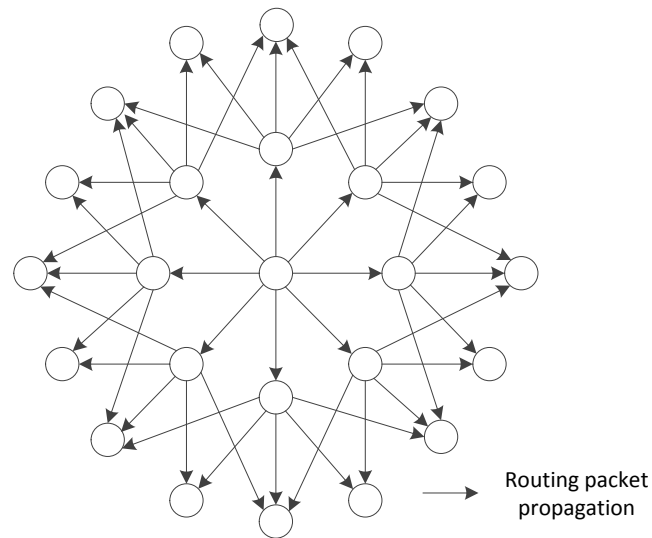
a. Flooding a packet in a wireless multi-hop network without MPRs.
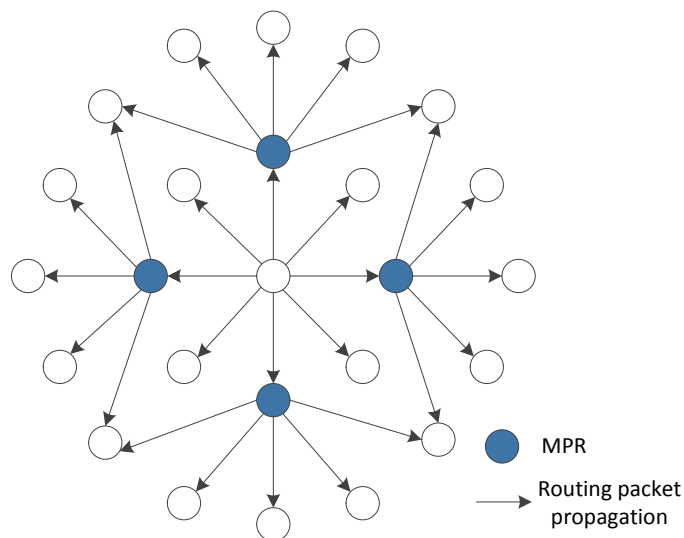
b. Flooding a packet in a wireless multi-hop network with MPRs (solid filled nodes).

Figure 2.5: Flooding a packet in a wireless multi-hop network with and without MPRs

Only nodes in $MPR(N)$ process and retransmit the routing information received from node N. Other neighbours of N process the packet, but do not retransmit the packet. Figure 2.5 illustrates the significant reduction of duplicated packets by using MPR when

26

flooding the routing information in a wireless multi-hop scenario. OLSR-enable nodes also use these multipoint relays to calculate routes to other nodes in the network.

- **Neighbour sensing**

To discover bidirectional neighbours in the neighbourhood, each node periodically broadcasts its "Hello" messages. The TTL of these "Hello" messages is set to 1 so that they can be received by all one hop neighbour, but they are not retransmitted any further. A "Hello" message contains the list of addresses of all the bidirectional neighbours of the transmitted node and the list of addresses of the neighbours which are heard by this node (a Hello has been previously received) but the link is not yet bidirectional.

When receiving a "Hello" message from a neighbour, if a node finds its own address in the Hello message, it considers the link to the sender node as a bidirectional link.

Since the "Hello" message contains information about the one hop neighbours of a node, it allows each node to learn the knowledge of its neighbours of up to two hops. Based on the exchange of "Hello" messages, each node maintains a neighbour table about its one hop neighbours and a list of two hop neighbours that these one hop neighbours give access to. Each of the one hop neighbours in the neighbour table is marked with a link status of either unidirectional, bidirectional or MPR (the selection of MPR will be discussed later). Each entry in the neighbour table also would be removed if its associated holding time expires.

- **MPR selection**

Each node in the network selects its own MPR set independently so that all the members of the MPR set cover the entire two hop neighbour set of the node. The MPR set does not need to be optimal, but it should be small enough for the benefit of the multipoint relays.

The MPR set is recalculated when a change in the neighbourhood is detected (either a bidirectional neighbour fails or a new bidirectional neighbour is added) or when there is a change in the two hop neighbour set (with a bidirectional link).

After it is calculated, the MPR set information is also embedded into the "Hello" messages so that the MPRs can receive this information as well. When a node receives a "Hello" message with itself as a MPR, it adds the sending neighbour into its MPR selector table.

- **MPR information declaration**

In order to build the topology table, a "Topology Control" (TC) message is sent periodically by each node in the network to declare its MPR Selector set. The TC message contains the list of neighbours who have selected the sender node as a multipoint relay. The TC messages are forwarded as broadcast messages to the entire network. A node with an empty MPR selector set, i.e. no other node selects it as a multipoint relay, does not generate any TC message. A TC message could be sent earlier than the predefined interval if there is a change in its MPR Selector set during this duration.

Upon receiving these TC messages, each node in the network populates its topology table with the multipoint relays of other nodes obtained from the received TC messages. Each entry in the topology table also has a holding time after which the entry is removed.

Each entry in the topology table consists of a pair of addresses [*last-hop*, *node*] where the *node* is the address of the MPR selector in the received TC message and *last-hop* is the originator of the TC message. This information in the topology table is then used to calculate the routing table at each node.

- **Routing table calculation**

The routing table is calculated independently at each node from its topology table and neighbour table and contains all the routing information for the node to reach other nodes in the network.

Since the entries in the topology table are in the form of pairs of [*last-hop*, *node*] addresses, the routing table is constructed by tracking the connected pairs of nodes in the topology table. The tracking starts from the source node, through its neighbours (specified in the neighbour table) and spreading outwards to all the possible destination nodes in the network. In order to restrict to the optimal paths, the source node selects the

connected pairs on the minimal path only. Each of the final route entries in the routing table consists of the destination address, next hop address, and the estimated distance to the destination.

Since the routing table is calculated based on the information contained in the neighbour and the topology tables, if there is any change in either of these tables, the routing table is recalculated to update the routing information. It is remarked that the recalculation of the routing table is the result of the changes in the neighbour table or the topology table, this recalculation does not generate any packet to be transmitted.

2.2.3 Routing Protocol Discussion

With both many advantages and disadvantages, it is hard to tell whether proactive or reactive protocols are best suited for all wireless multi-hop scenarios. Perhaps, it depends on the specific use case that the advantages of one protocol are more noticeable than those of the others.

Since the reactive protocols explore routes when they are needed only, if the communication demand is not high, the nodes in the network stay quiet most of the time. As a result, reactive routing protocols like AODV require only a small amount of energy to operate. This low energy consumption can significantly prolong the battery life of the participating nodes which is very important in wireless scenarios. In addition, the routing procedures of reactive protocols are fairly simple in terms of calculation complexity and do not require a large amount of memory to store routing database of the whole network such as the topology database of the proactive routing protocols. These benefits make it easier to implement reactive protocols at low cost for sensor networks.

On the other hand, since the routing information is always available beforehand, proactive routing protocols can start transmitting the data packets as soon as they arrive without any additional delay. This is extremely beneficial when the network is under constant load, since in reactive protocols the network latency tends to result in dropped packets due to buffer overflow while the routing protocol is still computing the route to the destination. Moreover, having the full topology information of the network, it is easier for proactive routing protocols like OLSR to optimize the routing information. As

a result, the routing entries in the routing table always indicate the best route which can significantly improve the performance of the whole network.

In a metropolitan wireless mesh network, the node density is quite high with a large number of hosts and sporadic but high volume traffic. In this scenario, the proactive routing protocols have an edge over the reactive protocols due to their low delay in route setup and optimized routing information. Indeed, in [26] the authors show that the OLSR protocol is more efficient in networks with high density, large number of hosts and high but sporadic traffic. In [27], the authors further show that OLSR exhibits the best performance in terms of data delivery rate and end-to-end delay in comparison to reactive protocols such as AODV and DSR [28]. Moreover, in a dense network with high traffic load, the network-wide flooding style of reactive protocols can lead to network clogging. In [29], the authors demonstrate how for vehicular networks (VANET), OLSR has smaller routing overhead, end-to-end delay and route lengths than AODV protocol.

Considering the advantages and disadvantages of proactive and reactive routing protocols as discussed above, OLSR is chosen to use throughout the tests as the underlay routing protocol in this dissertation.

2.3 Overview of Peer-to-Peer (P2P) Overlay Networks

An overlay network is a virtual computer network which is built on the top of another physical network. Nodes in the overlay are connected by virtual or logical links which may be realised by one or more physical paths in the underlying network. A P2P overlay network is a content-sharing overlay network where peers come together and help each other to store and distribute the content. The peers in overlay networks are often simple home computers, laptops or any network-enabled devices, such as Network-attached storage (NAS) devices or a micro-computer such as the raspberry pi[10], which are capable of installing the overlay client application. Unlike the client-server paradigm, there is no dedicated infrastructure or a central point of control in a peer-to-peer network. Instead, each and every peer participates in the task of storing and distributing the content. Thus, there is no dedicated infrastructure making P2P overlay networks scalable,

---

[10] Raspberry Pi - http://www.raspberrypi.org/

self-organizing and self-healing with the join and leave of peers. A second advantage of P2P overlay networks is that the capacity of the network scales with the number of peers. Since each peer plays both the role of the client and server at the same time (uploading and downloading simultaneously), all the capacity of the peers can be used efficiently to distribute content. In other words, P2P overlay networks are self-scaling: the more peers participate in the overlay, the more capacity the overlay can offer. These distinctive advantages of overlay networks have made them very well received by internet users from their first introduction in 1999.

Peer-to-peer overlay networks can be classified into two types based on their structure, namely unstructured overlay and structured overlay. Both of these types will be briefly introduced next. It is remarked that from this point on, the term "overlay" is used to refer to P2P overlay.

2.3.1 Overview of Unstructured Overlay

Just as its name implies, unstructured overlay imposes no rigid structure on the relationship between the overlay topology and where the resources are stored. Instead, in an unstructured P2P network overlay, the links between the peers are established arbitrarily. Among the unstructured overlays protocols, BitTorrent [30] is the most commonly used and accounts for the most P2P traffic on the Internet [31].
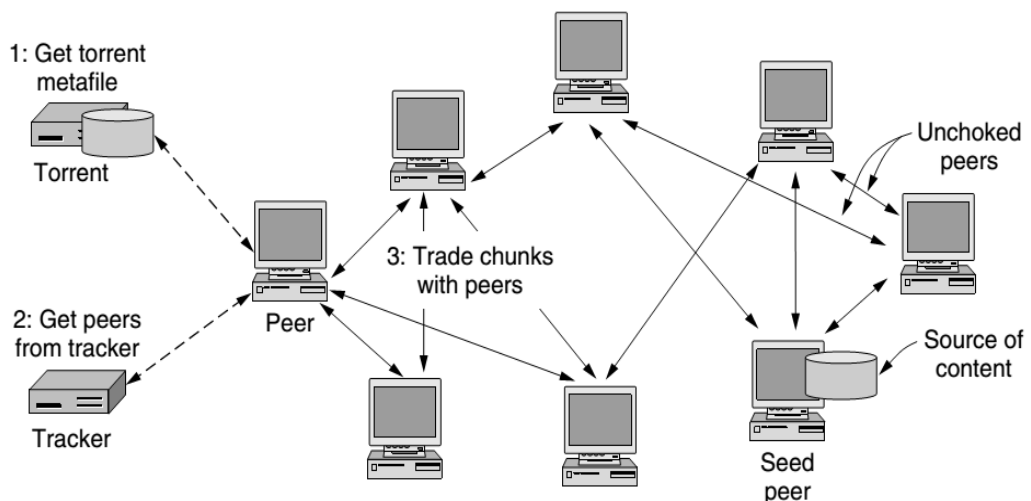
Figure 2.6: The operation of BitTorent [32].

31

Figure 2.6 illustrates the operation of BitTorrent. In BitTorrent, for each piece of shared contents, a content description (torrent) is created. The torrent, which is the metadata of the content and is much smaller than the content itself, contains the information about a server (tracker) that keeps track of the peers that are actively downloading and uploading the content and a list of equal-sized pieces (chunks) of the content. In order to download the content, a peer first contacts the tracker to get the list of the peers storing the content. The requesting peer then starts downloading and exchanging the chunks of data with the peers in the list. To prevent bottleneck traffic, the chunks are not downloaded in order of play but instead, rare chunks are chosen to be downloaded first. This strategy has three main benefits. First, it ensures all the chunks will be widely available in the network after a short time. Second, as the peers simultaneously download chunks that they do not have and upload the chunks which are already available in their storage, this strategy makes better use of the network capacity since all the peers participate in the chunk exchange. Third, since rare chunk are prioritized to download first, the departure of a peer does not greatly affect the content distribution process.

Variations of unstructured overlay protocols such as Gnutella [33] and Freenet [34] replace the central directory tracker by a flooding process to search for the content. In this process, each computer connects to random peers and sends queries for content to these neighbours. If a neighbour peer has the content, it sends a reply to the requesting peer, otherwise, it keeps on propagating the query. This process continues until the query is resolved. Since there is no rigid structure, unstructured overlays are simple, easy to implement and deploy. However, due to the reliance on either a centralized tracker or an expensive process of flooding the network to find the shared content, unstructured overlays are not scalable when deployed in wireless scenarios. The search operation may take a long time and consume significant network resources.

2.3.2 Structured overlay

The centralized tracker in unstructured overlays introduces the problem of a single point of failure while the flood-based request process is network intensive; thus both solutions are not scalable. In other words, although the upload and download

32

processes are fully distributed, the unstructured overlays are only partly decentralized or are fully decentralized but are not efficient. The need for a fully distributed P2P overlay without the disadvantages of unstructured overlays drives the motivation of the study of a new type of overlay – the structured overlay.

In structured overlays, to implement a fully distributed directory service, each peer is assigned an identifier and a structure is imposed on the overlay topology. In order to enable routing on the overlay, an overlay routing table is systematically built and maintained at each of the peers. The routing table for each peer is different and covers only a small part of the overlay network, but allows the peer to query another arbitrary peer in the overlay within a limited number of requests (usually $\log N$, where N is number of peers on the overlay). As the result, structured overlays are also called Distributed Hash Tables (DHT). The imposed structure and routing strategy allows the constructed overlay to be fully distributed, scalable and performs well without any centralized point of management or network-wide flooding process. First, since the routing table of each peer is relatively small, the routing table maintenance is quick and not very expensive. Second, the usually small number of requests to resolve a query ensures the lookup process is quick and accurate. Last but not least, since each node stores routing information about only a small subset of the overlay network nodes, the joining and leaving of peers does not seriously affect the structural integrity of the overlay.

Among the proposed structured overlays, Chord [35] is the most widely used. In this thesis, Chord is also used as the base overlay protocol due to its simplicity and popularity. An overview of Chord protocol is performed next as a background material to our study.

Overview of Chord Protocol

In the Chord protocol, in order to identify peers and resources on the overlay, an m-bit ID space is used (to avoid ambiguity, from this point on, the term *key* is used for the resource identity while *ID* implies peer identifier). The IDs are ordered in an ID circle of modulo 2^m positions (the Chord ring). Each key is managed by a peer with the smallest ID greater or equal to that key. In order to enable routing on the overlay and efficiently locate a key, a peer with ID i builds and maintains a finger table which stores

the IP addresses of m other peers at ID $(i + 2^k) mod\ 2^m$ ($1 \leq k \leq m$) (the finger ID). Each entry in the finger table has a structure of

<finger ID, IP address of the peer at the finger ID>

To locate a key, the peer sends a lookup message to the peer in the finger table with the greatest ID less than or equal to the key. Upon receiving the lookup message, the receiving peer checks if it manages the key; if so, it sends back a reply, otherwise it forwards the lookup message to its finger peer with the greatest ID less than or equal to the key. The process continues until the lookup message reaches the peer that manages the key.
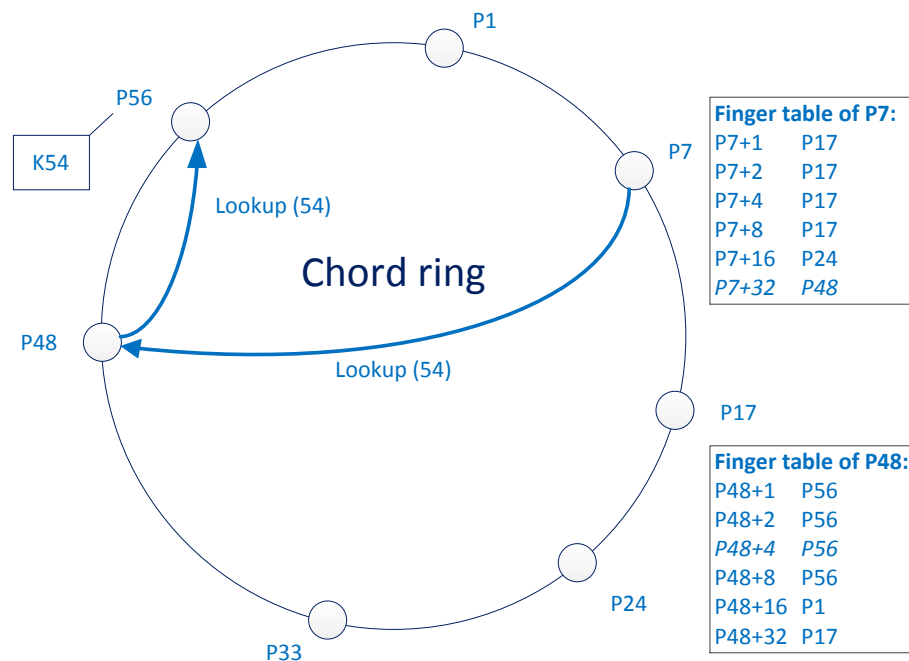
Figure 2.7: Overview of Chord operations for *m*=6.

Figure 2.7 shows an illustrative example of Chord operations with *m*=6. The Chord ring comprises of 7 peers: P1, P7, P17, P24, P33, P48 and P56 (the indexes of the peers are also their Chord IDs). A resource identified by key 54 will be managed at P56 since 56 is the smallest ID greater or equal to 54. As an example, the Chord finger tables for P7 and P48 pointing to other peers at ID $(i + 2^k) mod\ 2^m$ ($1 \leq k \leq 6$) are also shown. Since keys 8, 9, 11, 15 are managed by P17, these entries in the finger table of P7 point to P17. Suppose that P7 wants to retrieve the resource at key 54, it sends a lookup message to its finger peer with the greatest ID less than or equal to the key (P48) to

locate the key. As P48 does not manage K54, it forwards the lookup query to its finger peer (P56), according to its finger table, in the same manner as described for P7. Since P56 manages K54, P56 sends a reply to P7 after receiving the lookup message. This reply finishes the lookup process.

It is proved in [35] that this approach of lookup-through-finger table can resolve a lookup within $O(m)$ messages to other peers. However, since the finger table of Chord contains only IDs on half of the Chord ring entries in the forward direction (the increasing IDs direction of the Chord ring), Chord lookup is not symmetric (i.e., a lookup for a key close to the requested peer in the forward direction travels through much less intermediate peers than that in backward direction of the Chord ring). Another remark is that the Chord overlay IDs and the finger tables are independent of the physical topology and hence Chord is not location-aware. Consequently, lookup and overlay maintenance messages may travel across the entire physical topology many times and tremendously increase the overlay overhead and response time. In the case of wireless multi-hop network, these problems can severely affect the performance of other co-existing traffic and degrades the performance of Chord itself. More details about the related works will be presented in Chapter 3. The study in this dissertation seeks to overcome these drawbacks of Chord in the context of WMN to improve the lookup efficiency, to reduce the lookup delay and also to reduce the overlay overhead.

2.4 Multimedia Content Delivery and Quality Evaluation

Over the years, multimedia has evolved and becomes an essential part of modern life. Youtube[11], Daily Motion[12] and Vimeo[13] are just some of the most popular video content providers that are available on the Internet. People subscribe to Youtube channels not only for entertainment content such as movies or videos but also for technical contents. From cooking recipes, instructions on a do-it-your-self project or how to fix common issues around the home, to tutorials for a computer programming language, how to build a server or complete lectures for university courses. Perhaps, the main

---

[11] Youtube - http://www.youtube.com/
[12] Daily Motion - http://www.dailymotion.com/
[13] Vimeo - https://vimeo.com/

motivation that drives the development of communication technology is this explosion of media-rich content with a non-stop increase in bandwidth demand. However, transporting multimedia content, especially, videos is not easy and the quality of the content can be significantly degraded depending on network conditions. Even if the network throughput is sufficient for transporting the video, network related parameters such as delay, jitter and packet loss could negatively affect the quality of the received video.

In this section, multimedia delivery methods and some of the most important the network related parameters that could affect the quality of received videos will be discussed. In addition, metrics for evaluating video user perceived quality are also described.

2.4.1 Multimedia Delivery Methods

High-quality video streaming has become the core component of media-rich content. Typically, streaming protocols are associated with the Real-Time Streaming Protocol (RTSP) [40] and the Real-Time Transport Protocol (RTP) [41]. RTP is designed for real-time streaming between end-to-end devices, which requires timely rich-media content delivery. Due to its real-time requirement, RTP is normally used with connectionless transport layer protocols like User Datagram Protocol (UDP) instead of connection-oriented transport protocols like Transmission Control Protocol (TCP). RTP uses timestamps for synchronization and sequence number for packet loss detection and reordering. Synchronization between media streams is handled by the RTSP. RTSP is used to provide remote media playback controls such as play/pause commands from user devices. In RSTP, the playback state on the device is monitored by the streaming server during the connection period so that the server can encode the multimedia content at a suitable rate according to the available bandwidth of the user.

2.4.2 Quality of Service (QoS)-related parameters

When streaming multimedia through a network, especially in a dynamically changing environment resulting from network fluctuation or user mobility, the quality of the received video depends largely on a number of network related QoS parameters such as end-to-end delay, jitter and packet loss. These QoS parameters and their influences on multimedia streaming are described as follows.

End-to-end Delay

End-to-end delay refers to the time taken for a packet to be transmitted across a network from the source to the destination. End-to-end delay is a summation of the three components as shown in (2.1): transmission delay, propagation delay and processing delay.

end-to-end delay = transmission delay + propagation delay + processing delay   (2.1)

- *Transmission delay*. Transmission delay is the time taken to transmit a packet into a medium. Transmission delay is negligible when the transmission is over a high bandwidth link but is very significant when the bandwidth is low, e.g., the transmission delay of a packet of 1500 bytes is $12\mu s$ over a 1Gbps link and over 23ms on a 512Kbps modem line.

- *Propagation delay*. Propagation delay refers to the time to deliver a bit over the transmission medium. Propagation delay depends on the characteristics of the medium, such as materials (copper wire, optical fiber, wireless, etc.) or the length of the link (e.g., propagation delay over a 1km fiber is nearly negligible while propagation delay on satellite links are noticeable).

- *Processing delay*. Processing delay is the summation of the time taken to process a packet at the destination or at intermediate networking devices. The processing delay at the destination includes the decoding delay, buffering delay, etc. The processing delay at intermediate devices consists of queuing delay, routing processing delay, etc.

In real-time applications as considered in this thesis, such as live streaming or interactive services, long end-to-end delay can severely affect the user perceived quality. For instance, a long wait between conversations in video Internet calling service would negatively affect user experience although the voice and video quality could be perfect.

Jitter

Jitter or packet delay variation refers to the difference between the current packet delay and the delay of the reference packet which usually is the packet with the lowest delay in the packet stream. Jitter is caused by many reasons but mainly by the network dynamics. Since the network is changing constantly, different packets belonging to the same video stream may experience different queuing delays and processing delays on the intermediate nodes even if they are taking the same path. Moreover, since different packets in the same packet stream may have different sizes, especially for video packets, their end-to-end delay may be very different from each other.

In multimedia transmission, the effect of jitter is even worse than end-to-end delay. High jitter may result in distortion or jerkiness videos, both of which would severely affect user perceived quality.

Packet loss

Packet loss is the percentage of the packet stream which gets lost during the transmission through the network. Generally, during a transmission session, a packet might be lost due to one of the following reasons:

- Queue drop caused by network congestion or buffer overflow at intermediate network nodes.
- Erroneous channels, especially in wireless communications.
- Channel contentions and collisions.
- Expired packets, i.e., packets that are received after its deadline has passed and hence is useless and is discarded.
- Device failure.

Since video frames are typically split over multiple packets, when a packet is lost, this loss is amplified to the inability to recover a part or a whole video frame and the received multimedia quality can be greatly impaired.

Throughput

Network throughput is the rate of successful message delivery over a communication channel. Throughput is usually measured in bits per second or packets per second. Network throughput relies heavily on the physical network capacity and the network condition at the point of measurement:

- Physical network capacity, i.e., the physical bit rate limitation that a network can accommodate in perfect propagation conditions.

- Network condition. In a multi-access network such as wireless network, the network usage of one user can lead to network contention and collisions which would greatly reduce the network throughput of other users. Bad or noisy channels also affect the achievable throughput.

Low network throughput can cause long transmission times and low user perceived quality, especially for real-time services.

Network Requirements for Common Applications

Table 2.2: Y.1541 IP network performance requirements for different applications [42].

Network performance parameters	Class 0	Class 1	Class 2	Class 3	Class 4	Class 5
Delay	100ms	400ms	100ms	400ms	1s	-
Jitter	50ms	50ms	-	-	-	-
Packet loss ratio	10^{-3}	10^{-3}	10^{-3}	10^{-3}	10^{-3}	-
Applications	Real-time, Highly interactive, Delay variation sensitive (VoIP, video conference, VoD)	Real-time, Interactive, Delay variation sensitive (VoIP)	Transaction Data, highly interactive (signalling)	Transaction data, interactive	Low loss only (short transactions, bulk data)	Traditional application of default IP networks

"-" means unspecified in this table.

Different applications have different demands on the discussed above network parameters in order to achieve a good quality of service. Table 2.2 illustrates the network performance requirements for common IP applications according to the International Telecommunication Union (ITU).

2.4.3 Approaches for Measuring Video quality

To evaluate the perceived satisfaction of viewers regarding the delivered video content, different methods have been developed to quantify the received video quality. It is important to note that video quality refers to the user perception while all of the network requirements, as listed in the previous part, are purely technical concepts and improving the network requirements does not always guarantee better video quality retrieval.

Table 2.3: ITU MOS quality and impairment scale [44].

MOS Scale	Quality	Impairment
5	Excellent	Imperceptible
4	Good	Perceptible but not annoying
3	Fair	Slightly annoying
2	Poor	Annoying
1	Bad	Very annoying

There are two major approaches for evaluating video quality, namely subjective and objective quality methods. For both of the methods, the most commonly used metric in assessing the video quality is Mean Opinion Score (MOS). The MOS scale includes five quality levels representing human quality impression on the video. The five levels are from 5 (excellent quality) to 1 (bad quality) as shown in Table 2.3[44].

2.4.3.1 Subjective Quality Evaluation

In subjective methods, video quality measurement is performed by human by letting human subjects watch the actual videos and mark the video quality based on their own perception. Typically, each viewer is asked to rate the videos based on the MOS scale.

The International Telecommunication Union-Telecommunication Standardisation Sector (ITU-T) has defined standards and recommendations for subjective assessment. These standards recommend the viewing conditions and the assessment procedures. For instance, the ITU-R BT-500 [42] proposes tests for assessing the video quality of television images.

Subjective methods are accurate since they truly reflect human perception about the video quality; however, they are extremely costly, highly time consuming, and require a lot of human resources to conduct the tests and process the results. Moreover, in subjective methods special equipment is normally needed. These disadvantages make it impossible to conduct subjective video assessment in real time applications or at a large scale.

2.4.3.2 Objective Quality Evaluation

On the other hand, objective methods are automated methods based on mathematical models and algorithms that try to approximate human perception. Objective methods are relatively inexpensive, fast and do not require a lot of manpower to accomplish; however, the results from these methods could be incorrect due to the possibility of poor correlation with the human perception.

The metrics used in objective quality assessment can be classified into three types based on the presence of the reference videos: full reference, reduced reference and no reference. The full reference metrics rely on the comparison between the original video (before transmission) and the received video. The reduced reference metrics require a feature vector derived from the statistical model of the reference video for quality evaluation. No reference metrics use information contained in the received video only, which make it easy to implement in real-time tests. The quality evaluation result is more precise for full reference metrics in comparison with the reduced/no reference metrics; however the computation complexity involved also increases. As the full reference metrics are more precise, they will be discussed in more detail in this Section. Some of the most known full reference objective metrics including Peak Signal to Noise Ratio (PSNR), Video Quality Metric (VQM), Structural Similarity Index (SSIM), etc.

The **PSNR metric** is the most commonly and widely used metric for assessing video quality. The PSNR can be calculated as shown in equation (2.2).

$$PSNR_{dB} = 20 \log_{10} \frac{255}{\sqrt{MSE}} \qquad (2.2)$$

Where Mean Squared Error (MSE) represents how the original video is different from the received one. The popularity of PSNR is due to its low computational complexity. However, PSNR does not consider the effect of visual masking, i.e., any pixel error will cause a decrease of PSNR even if it is not perceived [46].

In [47], another estimation model for PSNR is proposed using only the network related parameters such as the received and transmitted bit stream. According to [47], the PSNR can be estimated using only the transmitted and received bit rate as in (2.3)

$$PSNR = 20 \log_{10} \left(\frac{Bitrate}{\sqrt{(EXP_{Thr} - CRT_{Thr})^2}} \right) \quad (2.3)$$

Where:

- $Bitrate$ is the average bit rate of the data stream transmitted.
- EXP_Thr is the average throughput expected to be obtained.
- CRT_Thr is the actual average measured throughput.

For the simulations in this thesis, PSNR is used as the video quality measurement metric and the estimated PSNR value of simulated video streaming service is evaluated using (2.3).

Table 2.4: PSNR to MOS conversion [48].

PSNR [dB]	MOS
>37	5 (Excellent)
31-37	4 (Good)
25-31	3 (Fair)
20-25	2 (Poor)
<20	1 (Bad)

In [48] the authors proposed that PSNR metric values can be mapped to MOS scale by using the conversion table as in Table 2.4.

SSIM metric [49] is another known full reference objective metrics which aims at being more consistent with the human vision by comparing the similarities between two frames based on luminance, contrast and structural similarity. The SSIM metric sits between [0, 1] where 0 means there is no correlation with the original video frame (totally different frames) and 1 means full correlation (identical frames). SSIM metrics is highly correlated with subjective quality assessment methods; however, the computational complexity of SSIM is also much higher than that of PSNR.

42

VMQ metric [50] is a novel objective video assessment metric developed by The Institute of Telecommunication Science (ITS). In VMQ, the perceptual effects of video impairments such as blurring, noise and distortion are assessed and combined. The computational complexity of VMQ is even higher than SSIM, yet the correlation with subjective quality assessment method is better.

2.5 Chapter summary

This chapter presents an overview of the main technical background information related to this thesis, including Wi-Fi access network technologies and architectures, wireless multi-hop routing protocols, structured and unstructured overlay networks and subjective/objective quality assessment methods for video streaming services. Considering the advantages and disadvantages of proactive and reactive routing protocols, OLSR was chosen to be used as the underlay routing protocol in this dissertation and therefore was used in the tests. In addition, acknowledging the drawbacks of overlay protocols in wireless scenarios, this thesis aims at finding a solution to improve overlay communication for wireless multi-hop scenarios. Finally, both subjective and objective approaches for measuring video quality were also summarized and discussed.

CHAPTER 3: Related Work

Abstract

This Chapter discusses the research works related to the proposed solutions including methods for overlay construction and techniques to improve overlay content delivery in the context of wireless multi-hop networks. For each study, the advantages and disadvantages of the proposed mechanisms are highlighted. The methods for constructing the overlays over wireless multi-hop networks are categorized as either unstructured or structured. The techniques for improving overlay content delivery include link-aware methods and solutions for enhancing seek and jump operations for Video on Demand (VoD) services.

3.1 Overlay Network Construction over Wireless Multi-hop Network

Due to the common nature of their distributed components (wireless nodes in multi-hop networks and peers in overlay networks), P2P overlay networks and wireless multi-hop networks share many common characteristics such as self-organization and decentralization. Moreover, in both kinds of networks, nodes can join and leave the network at any given time, and the degree of dynamicity is very high. When integrating an overlay network on top of a wireless multi-hop network, these similarities impose an additional layer of complexity in order to accommodate topology changes in both the overlay and physical network. As a result, designing an overlay protocol that is efficient

and well-suited to wireless multi-hop networks is a challenging task to be solved. The suitability of applications that rely on P2P overlay architecture over a wireless multi-hop network introduces several technical challenges including accommodating bandwidth and reliability issues, the overlay maintenance overhead, and overlay routing stretch, which will be discussed next.

Bandwidth and reliability issues. P2P overlays were initially designed for the Internet which mostly relies on wired networks where bandwidth is plentiful and connections are in general reliable. In contrast to wired networks, wireless multi-hop networks are limited in bandwidth. In addition, wireless channels are changing constantly and wireless transmission is error prone due to collisions and multipath fading. These critical characteristics of wireless multi-hop networks make the implementation of overlay networks very challenging. If existing overlay protocols for wired networks are used without modification in wireless multi-hop networks, the high volume of their maintenance traffic eventually overwhelms the network capability, imposing excessive delay and packet loss on overlay data exchange and other types of background traffic.

Overlay maintenance overhead. In order to enable routing on the overlays and also keep the overlay structure consistent, overlay peers have to exchange overlay control messages with other peers. This maintenance traffic contributes to congestion and collisions on the underlay network. Moreover, since the overlay network is built on top of the physical network, it imposes another layer of complexity for overlay maintenance. In addition to the dynamicity at the overlay network due to leave and join of peers, changes in the physical network topology could also indirectly affect the overlay consistency. These two layers of dynamicity further increase the maintenance overhead over the resource-constrained wireless multi-hop networks.

Overlay routing stretch. In wireless multi-hop scenario, whenever an overlay peer wants to contact a neighbour peer, the query message may have to go through multiple wireless hops across the network. For instance, when routing a query message to a destination through Chord, the node selects and forwards the message to its finger neighbour which is closest in the ID space towards the destination peer. When the message reaches the overlay neighbour, it repeats the same overlay routing procedure until the message reaches the destination peer. As a result, routing an overlay message happens at two levels: overlay routing from one neighbour peer to another according to

the overlay routing strategy and underlay routing through the hop-by-hop wireless multi-hop routing protocols. Since the overlay is constructed independently of the physical topology, the overlay routing from one neighbour peer to another could travel across the whole network, which is highly inefficient.

Overlay routing stretch is defined as the ratio between the cost of the route from the source to the destination peer using the overlay routing relative to the cost of the optimal path routing using the underlay wireless multi-hop routing protocol if the source and the destination peers are known. A small overlay routing stretch means that the overlay route is efficient in comparison to the shortest underlay path. Minimizing overlay route stretch could significantly reduce the overlay resource consumption, increase the overlay reliability and therefore, make the overlay network more scalable.

Because of the different possible strategies and also the numerous techniques and approaches involved, in this chapter the related proposed overlay construction solutions are categorized into two wide categories, namely unstructured and structured.

3.1.1 Unstructured Overlay Construction over Wireless Multi-hop Networks

As previously described in Chapter 2, unstructured overlay imposes no rigid structure on the relationship between the overlay topology and where the resources are stored. Resource searches in an unstructured overlay are normally based on flooding mechanism where the peer asks its neighbours for the resource, these neighbour peers in turn asks their neighbours until the resource is found. In this Section, the different solutions to deploy unstructured overlay network over wireless multi-hop networks are presented. The discussions on these solutions are then shown in Section 3.2.3.

In [51] A. Klemm et al. proposed *Optimized Routing Independent Overlay Nework (ORION)* for P2P file sharing on MANET (Mobile Ad-hoc Network) based on the Gnutella protocol. ORION comprises an algorithm for on-demand (reactive-like) overlay construction in which route discovery of network layer could be integrated with an application-layer query process to reduce the overlay and routing overhead. In ORION, query messages are flooded to the whole network to search for the requested file. Based on the response messages, each peer in the network along the path to the

requesting peer builds a file routing table containing the next hop nodes on the paths to the shared file. Based on this routing table, overlay messages and data packets can be routed efficiently between the overlay nodes towards the requested node. A packet scheduling scheme was further introduced to replace the TCP transport mechanism, aiming at reducing retransmission overhead when there is a change in physical topology. The ORION packet scheduling scheme divides the sharing files into equal size blocks, each block is transferred and received independently (not necessarily in order) and only lost blocks are re-requested. Simulation results show that ORION outperforms Gnutella with TCP transport mechanism in search accuracy and reduces overlay overhead. However, in the proposed mechanism, in the case that there is more than one peer containing the requested file, there is no indication of how to select the best peer to get the file from. Moreover, for large networks with high dynamicity, the flooding process is network intensive and may take a long time, during which the route to the shared file may have already changed, which makes the file routing table inaccurate.
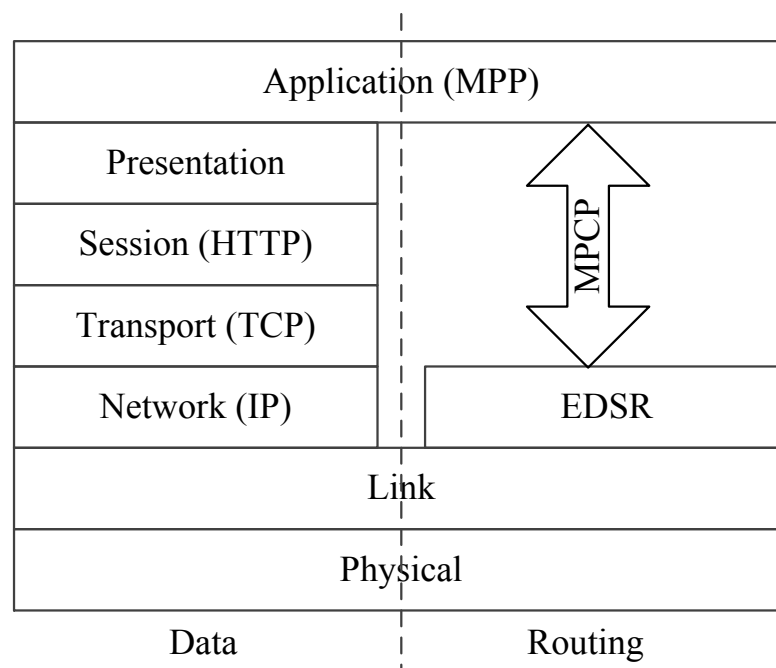
Figure 3.1: Layered architecture of Mobile Peer-to-Peer (MPP) [52]

I. Gruber et al. proposed *Mobile Peer-to-Peer (MPP)* [52] as a file sharing system in MANET. In contrast to ORION, MPP introduces cross-layer communication between

the network layer and P2P application layer to adapt the overlay structure to the physical structure of MANET. As shown in Figure 3.1, MPP includes a file sharing application at the application layer, a P2P extended Enhanced Dynamic Source Routing (EDSR) at the network layer for both overlay and underlay network routing and a Mobile Peer Control Protocol (MPCP) which acts as an interlayer communication protocol between the MMP and EDSR. At the network layer, EDSR combines Gnutella-style flooding and Dynamic Source Routing (DSR) [20] for overlay search as well as underlay routing. In MPP, when a node wants to locate a desired file, it issues a search request that is flooded throughout the MANET using the route discovery mechanism of DSR with additional fields for the search string. Intermediate peers add their own addresses to the search request to create a DSR-style route while the search request is flooded throughout the network. At the destination, a response message is sent back to the requester using the reverse route. At the application layer, MPP uses HyperText Transfer Protocol (HTTP) to provide file transfer service to support download resume. Simulation results show that MPP can reduce overlay overhead in comparison with ORION. However, the flooding-style request would result in a network-wide broadcast which is bandwidth intensive and is not suitable for large scale networks with high request rate.

C. C. Hog et al. proposed a *P2P file sharing system over MANET based on Swarm Intelligence (P2PSI)* [53] to enable efficient and scalable file sharing. The proposed P2PSI is based on a hybrid push-pull approach, which comprises of advertisement (push) and discovery (pull) processes to locate shared files on the network. In the advertisement process, peers periodically broadcast advertisement messages about their shared files. The advertisements are bounded in a limited area using TTL to prevent broadcast storms. In the discovery process, a peer sends a request message to look for the shared file and based on the reply message, each intermediate peer builds and maintains a pheromone table which records reply message intensity through its neighbours. The pheromone table is used to forward subsequent queries. The pheromone table entries are reinforced with each subsequent reply and are also periodically evaporated to help reflect network changes. The authors further proposed a cross-layer architecture to integrate P2PSI with swarm-based ARA routing protocol [54] to integrate the overlay discovery process with the routing process. This integration combines the overlay discovery and the underlay route establishment processes, further reducing route establishment overhead. Simulation results show that in comparison with existing cross-layer design using DSR

and Destination Sequenced Distance Vector Routing (DSDV) [23], P2PSI achieves better performance in terms of control overhead, request success ratio and path length. However, the overhead of pheromone table may have a significant negative impact on the peer operation when the number of shared items increases. Besides, it is not clear from the paper how to choose a suitable parameter set, such as the limit of broadcast range, pheromone evaporate parameters, etc., for different network sizes and levels of mobility.

W. Kellerer et al. proposed the **Zone-based P2P (ZP2P)** [55] to reduce the overlay maintenance traffic and to replace the network-flood approach of Gnutella. In the proposed scheme, each overlay peer builds and maintains a zone around its vicinity (in terms of hop count). A peer periodically exchange advertisement messages, which includes all its shared resources and routing information with all the peers in its zone. Through this advertisement exchange, each peer knows the complete P2P overlay network topology and the available content in its zone. To search for a piece of content, a peer first searches among the available content in its zone. If the searched content is not found locally, the peer issues request messages to the peers at the border of its zone. The search process proceeds in a similar way, step by step, until the content is found. Simulation results illustrate that the proposed ZP2P outperforms the conventional Gnutella protocol in terms of overlay maintenance overhead. It can be seen that this zone-based approach can reduce some broadcast traffic as the node-to-node flooding process is transformed into zone-to-zone propagation. However, to a certain degree, this zone-to-zone search process behaves the same way as the flooding search and the utility of local zones will not scale with growing network sizes. Besides, the periodic content update of peers in a zone will further introduce some traffic overhead to the protocol. Moreover, peer mobility is not considered in the proposed scheme which may severely affect the performance of ZP2P.

C.L. Liu et al. proposed **Mobile Chord (MChord)** [56] to enhance the P2P performance over vehicular ad hoc networks (VANET). MChord removes the overlay structure of Chord by replacing the Chord finger table structure with an overlay table containing all other nodes which are currently in the P2P overlay. An overlay peer keeps the overlay table updated by periodical exchanging its overlay table with all its one-hop neighbours by making use of the broadcast nature of the wireless channel. To speed up the overlay synchronization process, the overlay table is further piggybacked into overlay

messages, such as query messages. MChord also makes use of the broadcast nature of the wireless channel so that all the overlay messages passing through a peer are investigated even if they are not destined for the peer and overlay knowledge is harvested. Using this piggyback and cross-layer information harvesting, all intermediate peers along the forwarding path of an overlay message can update their overlay information upon receiving a message. Simulation results show that MChord outperforms Chord in the number of overlay forwarding steps, success query ratio, and query delay. However, for large networks, it would be impossible to maintain a consistent overlay table across all the peers, especially in high dynamic scenarios. Besides, the periodic one-hop broadcast of overlay tables occurs at a network wide scope, therefore is similar to the flooding mechanism, and can significantly increase the overlay maintenance overhead. Moreover, piggybacking the overlay table into all overlay messages may cause excessive overhead on the network, which would increase dramatically as the number of overlay peers increases, making the scheme un-scalable. Complexity is another issue as each and every message have to be inspected according to the cross-layer mechanism.

G. Ding et al. proposed *OverMesh* [57] - an architecture to deploy services across mobile nodes in WMN. The proposed architecture is built over IEEE 802.11s and includes four components: Central, Gateway, Mesh nodes and Clients. The Central component is a dedicated machine which is responsible for centralized overlay management and node authorization. The Gateway component is a network device which is used for connecting the mesh network to external networks such as the Internet or other wireless networks. The Mesh nodes provide wireless multi-hop communication and overlay services. Mesh nodes are also partitioned into multiple virtual machines, where each virtual machine provides a service to an overlay. These virtual machines are managed by the Central. The Clients connect to the nearest Mesh nodes to gain access to the overlay services, but they do not contribute to providing of overlay services. Another contribution of the study is the proposal of a cross-layer searching method. In OverMesh, each of the queries for resource content is broadcasted to the whole network. This broadcast-based query replaces the query mechanism in the Distributed Hash Table (DTH) protocols to reduce the search complexity and response time. Making use of the network layer broadcast, the cross-layer mechanism allows nodes to look into the broadcasted queries received (even if they are not the destination) and reply if the nodes know routing information about the queried key. However, the centralized management

in this study does not scale well over a large-scale deployed WMN. Besides, the broadcast-based queries are inefficient as the query messages flood the whole network. Moreover, the authors have not investigated the effect of node failures to the performance of the proposed scheme.

3.1.2 Structured Overlay Construction over Wireless Multi-hop Networks

As previously described in Chapter 2, structured overlays such as the Chord Ring [35] impose a structure on the overlay topology. In order to enable routing on the overlay, an overlay routing table is maintained at each of the peers. This routing table for each peer is different and covers only a small part of the overlay network, but allows the peer to query another peer in a limited number of overlay steps. In this Section, the different solutions to deploy structured overlay network over wireless multi-hop networks are presented. The discussions on these solutions are also shown in the next Section.

S. Ratnasamy et al. proposed ***Data-Centric Storage*** [58]-[60], an overlay-based data dissemination method for sensor networks aiming at minimizing communication costs. In their works, the authors first assume that sensor data can be classified into events (based on some combination of sensor readings) and the data can be summarized (such as count of events, average values, etc.) to provide meaningful indicators about the network. In the proposed scheme, each data event is named with a key, a unique identifier, and the communications regarding the data event (storage and retrieval of an event) are performed using this key rather than the actual node addresses. The authors then proposed Geographic Hash Table (GHT) to hash the keys into geographic coordinates. The data associated with the key is stored at the sensor node in the vicinity of this location using Greedy Perimeter Stateless Routing (GPSR) [61] (assuming each sensor node knows its own location a priori). To make the key available in case of node failure, the key-data combination is duplicated to the node's neighbours. The communication cost of the proposed scheme is analysed and compared with the External Storage scheme (when all data are sent for storage at an outside external node) and Local Storage scheme (when data is stored at the observed sensor and queries for data are done through flooding). An analysis framework is provided to show that the Data-Centric

Storage scheme is superior in terms of overlay communication overhead to External Storage and Local Storage especially when summaries of the data events are required instead of a listing of all the individual data events. Nevertheless, since data is only replicated to nodes near the location of the key, it is not geographically distributed and failure of nodes in a certain area would result in loss of all information associated with the key. Moreover, a centralized storage at one sensor node for a certain type of data for the whole sensor network, although promising for handling queries, may overwhelm the sensor storage and deplete the battery of the node due to excessive communications.

Using the same principle of GHT, O. Landsiedel et al. propose **Mobile Hash Table (MHT)** [62] to integrate a DHT into mobile ad-hoc networks. This integration allows resource sharing when experiencing frequent changes in physical topology due to node mobility. In order to make MHT feasible, each node in the overlay periodically broadcasts its own position, speed and direction to the surrounding nodes. In this scheme, each data item is assigned a key that indicates its position in the physical network and is stored on a mobile node that is closest to this position and is within the transmission range. When the node which stores the data item moves away from the data's position, the data will be transferred to another node in the vicinity of the data item's original position. In order to query a data item, the requesting node computes the item's position using its key. Each query contains the data location for reaching the stored node, and the current position, speed and direction of the requesting node for the response. In order to adapt to the direction changes of the requesting node, whenever the requesting node changes its direction or speed, a temporary data item (a buoy) is generated to store the change in node's movement and is placed at the current positon of the source and moves with the old direction and old speed of the source. The authors also proposed a traffic adaptation method for reducing data transfer overhead in which the data item is moving around its location along traffic paths shaped by roads. Local redundancy and global redundancy solutions are also proposed to ensure the availability of data items. However, the proposed scheme is strongly relyant on the movement data (direction and movement speed) which is hard to collect and may not be reliable. Moreover, as a data item transfers among the mobile nodes to retain its location, it would cause excessive communications and can lead to network congestion or may not be possible when the data is large and the node is moving at high speed.

P. Desnoyers et al. proposed ***Tiered Storage ARchitecture for sensor networks (TSAR)*** [63] – a two-tier storage architecture for Wireless Sensor Networks. In TSAR, an Interval Skip Graph, a distributed indexing structure, was proposed for efficiently supporting both temporal queries and queries for sensor data in a certain range. The architecture includes two tiers: the proxy tier and the sensor tier. The sensor tier comprises energy-limited sensors which store data locally and send only summary of data (metadata) to the proxies for indexing. This metadata includes only the time stamp interval of the sensor data and the coarse description of the sensor data, such as the max-min data values in the interval. The proxy tier consists of resource-rich proxy nodes which exchange the metadata received from the sensors to provide a unified logical view of all data in the system. In order to index the metadata for further queries from users, the authors propose the Interval Skip Graph – a multi-resolution ordered distributed index structure. The metadata is ordered using the summary information and $\log_2 n$ pointers (n is the number of the data elements) are constructed for each of the metadata in order to enable overlay search with $O(\log_2 n)$ messages. Since the data elements can be indexed using the range values in the summary, this interval-based data structure allows data range queries instead of searching for a particular value. However, the authors have not investigated the effect of proxy failures on the framework performance. Moreover, since the overlay structure is indexed by the data values which are likely to change drastically with each update, the overlay maintenance at the proxy tier could be very significant.

L. Galluccio et.al. proposed ***Georoy*** [64], an algorithm for efficient retrieval of information for overlay networks on WMN. The Georoy algorithm is based on Viceroy protocol [65] for the basic lookup mechanism. The authors introduced a two-tier overlay architecture design. The lower-tier includes leaf peers which provide overlay services. The upper-tier comprises super peers (access points) which manage a distributed catalogue of available resources and maintain the overlay structure. In order to make the overlay nodes aware of the physical topology, the author introduced a super peer - location ID mapping scheme. This location-aware ID exploits the location information of the super peers to speed up the search process. The geographical ID mapping is shown in Figure 3.2 and mathematically formulated by equation (3.1) in which node IDs are marked based on their x and y coordinates sequentially on each Δ slide which define the granularity of the location awareness. Intuitively, the Georoy ID assignment divides the deployment region into slides and assigns ID to nodes in each slide consecutively

according to x coordinate in each slide; the ID assignment order is reversed in the next slide to preserve the location proximity. This geographical ID mapping aims at enabling nodes close together physically lay in an ID range close together. The paper also illustrates mobility management procedures including joining/leaving of leaf nodes, update distributed resource catalogue, retrieval of information and handoff management. However, the proposed scheme is not designed with data replication and failure of a super peer that manages the resources would make the resource unavailable globally. Moreover, since resources are mapped to keys which are fixed, failure or joining of a super peer would lead to key transfer and movement of the data associated with the transferred key which may lead to congestion in dynamic networks. Besides, the mapping scheme although is location-aware, can lead to ID duplication which is not mentioned in the paper.

Δ   Location awareness granulariry

S   Side of the deployment region

—▶   Order of ID assignment
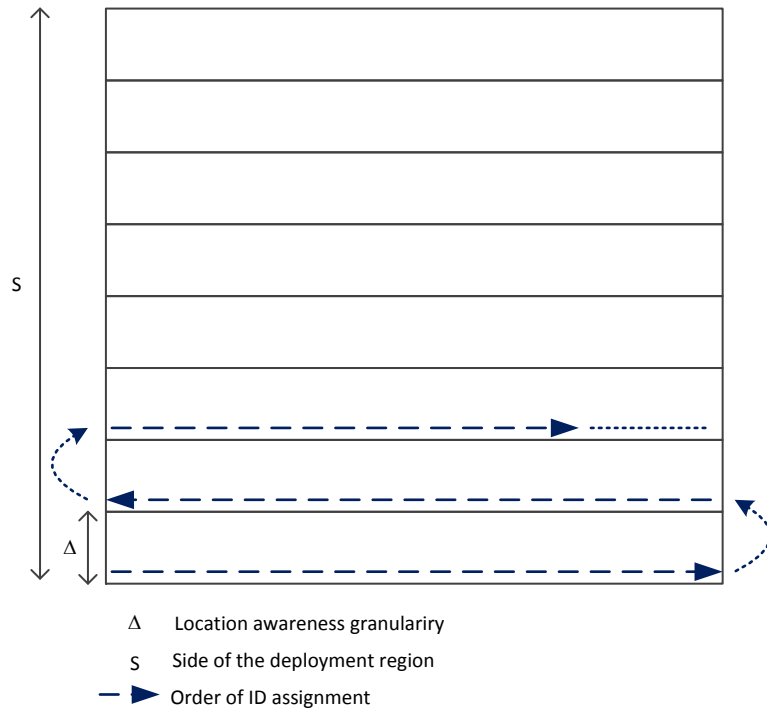
Figure 3.2: Node ID assignment of Georoy [64].

$$ID(x,y) = \begin{cases} \dfrac{x\Delta}{s^2} + \left\lfloor\dfrac{y}{\Delta}\right\rfloor \dfrac{\Delta}{s}, & if \ \left\lfloor\dfrac{y}{\Delta}\right\rfloor is \ even \\ \dfrac{(s-x)\Delta}{s^2} + \left\lfloor\dfrac{y}{\Delta}\right\rfloor \dfrac{\Delta}{s}, & if \ \left\lfloor\dfrac{y}{\Delta}\right\rfloor is \ odd \end{cases}$$

(3.1)

where

ID(x, y) is the ID of a peer with coordinates (x, y).

s is the side of the deployment region.

Δ is a parameter which defines the granularity of location awareness.

C. Canali et al proposed *MeshChord*. [66] - [68], an efficient overlay mechanism for peer-to-peer resource sharing in WMN with reduced overlay message overhead and improved overlay lookup performance. The proposed scheme adopts the two-tier design and includes location aware ID assignment, which is the same as in [64], to incorporate location information into node-ID assignment. However, instead of using Viceroy, MeshChord uses the Chord overlay protocol. Another contribution of the paper includes a MAC layer cross-layer mechanism to speed up the lookup process. In this cross-layer mechanism, overlay nodes examine all the received messages at the data-link layer (even those not destined for them) and answer to lookup requests if they can resolve the lookup locally. The authors also proposed the *stretch factor* as a metric to measure how close the overlay to the physical topology. The stretch factor is calculated the same way as the overlay routing stretch which was mentioned in Section 3.2. Their analysis results show that the stretch factor of MeshChord is $O\left(\sqrt{N \log N}\right)$, i.e., an overlay lookup traverses $O\left(\sqrt{N \log N}\right)$ times on average through overlay routing more than the hop count between the two overlay peers in the physical network. The performance evaluation shows that location-awareness could greatly reduce message overhead while cross-layering could decrease the response time. However, the study is basically an extension of [64] and hence shares the weaknesses of [64]. Besides, the cross-layer mechanism would introduce an additional processing overhead and delay on intermediate peers as all messages relaying through an intermediate node have to be examined for overlay query. With an increase in the size of the network this processing overhead increases dramatically which makes the scheme not scalable.

F. Delmastro et al. proposed *CrossROAD* [70], an optimized solution which exploits a cross-layer architecture to reduce the communication overhead introduced in Pastry [37]. The authors first evaluate the messaging overhead influence of Pastry on an actual Mobile ad hoc test bed. The tests show that Pastry overlay introduces a heavy overhead in ad hoc networks, reducing the overall system performance. The authors then

proposed CrossROAD to integrate the overlay operations with the underlay routing protocol. Making use of this integration, CrossROAD exploits additional information at routing layer to optimize the overlay management. In particular, additional overlay information fields are embedded in the OLSR routing packets. These fields include overlay service information and are periodically sent by the OLSR instances in the wireless nodes. In this way, each node in the network becomes aware of the other peers in the overlay network as well as aware of underlay network changes with only a marginal increase in network overhead. This piggyback approach seems promising in reducing overlay overhead, however, CrossROAD requires the routing layer of the protocol stack to be changed accordingly, which may not be practical in real networks and can lead to incompatibility issues between devices. Besides, this integration only works with proactive wireless multi-hop routing protocols which also limits the usage scope of the scheme. Last but not least, in this study, the authors only illustrated the concept of CrossROAD, and no scenario-based testing and verifications were presented to show the overlay performance metrics of CrossROAD.

3.1.3 Discussions and Architectural Design Decisions

A summary of the advantages and disadvantages of unstructured and structured overlay mechanism over wireless networks is illustrated in Table 3.1.

- *Underlay Network Structure Choice*

    In order to achieve efficiency when deploying an overlay network over a wireless multi-hop network, a suitable underlay network structure must be carefully selected. As shown below, this choice of underlay network structure seriously affects the overlay performance.

    In terms of underlay network structure, among the various overlay solutions, two underlay network structures are commonly used, namely Mobile Ad-hoc Network (MANET) and Wireless Mesh Networks (WMN). MANETs are composed of the wireless clients only and allow direct communications between them. On the other hand, WMNs include two types of network devices: the Mesh Routers (MRs) and the Mesh Clients (MCs). MRs are stationary, power-unlimited network devices which are used for forwarding the network traffic from the source to the destination. The MRs

connect to each other to form a wireless backbone which acts as the wireless backbone infrastructure of the network. Multi-hop routing is integrated into the MRs to enable multi-hop communications. MCs are user devices, which connect to the WMN through these MRs to gain access to the provided services.

Table 3.1: Summary of advantages and disadvantages of unstructured and structured overlay schemes over wireless scenarios.

Category	Scheme	Advantages	Disadvantages
Unstructured overlay	ORION [51]	Integrates route discovery into overlay communications	Uses flooding based search which is not efficient
	MPP [52]	Integrates overlay communication into DSR routing	Uses flooding based search which is not efficient Needs to modify existing routing protocol
	P2PSI [53]	Uses pheromone table to maintain the freshness of shared files' location information	Introduces additional networking and computational overhead
	ZP2P [55]	Uses zones to reduce overlay messaging overhead	Still uses flooding process in each zone to search for shared items
	MChord [56]	Piggybacks overlay table into query message to reduce overlay messaging	Has difficulty maintaining consistent overlay table in large networks
	OverMesh [57]	Uses cross-layer mechanism to speed up the query process	Uses flooding based search which is not efficient
Structured overlay	Data-Centric Storage [58]	Stores data at geographic coordinates to reduce overlay communications	Is sensitive to node mobility and node failure
	MHT [62]	Integrates node position, speed and direction into overlay messages to support mobility	Introduces additional networking overhead
	TSAR [63]	Uses a two-layer architecture Support summary of data	Is sensitive to node failure
	Georoy, MeshChord [64]-[68]	Uses a two-layer architecture Uses location-aware ID to speedup search process	The location-aware ID mapping could be improved
	CrossROAD [70]	Integrates overlay communications into OLSR to avail physical information on the overlay	Requires the change of existing routing protocols No scenario-based testing to verify the idea.

For deploying overlay networks, the low capability and highly dynamic nature of wireless clients of MANETs make them un-scalable and inapplicable. First, wireless clients are normally battery-powered user devices which are not designed for relaying traffic. Their small wireless card and power-constraints clearly puts a limit on the offered bandwidth and transmission range. Besides, the power-limited characteristic also puts a constraint on their operational lifetime. On top of this, wireless clients could be highly mobile which leads to frequent connection disruptions. These characteristics make the underlay network unreliable for high volume traffic such as videos. Deploying overlay network over such unreliable underlay structure would cause instability in overlay connections. This instability in overlay connections makes the overlay communication inefficient and also results in constantly excessive overlay maintenance traffic trying to maintain overlay consistency. This effect can be illustrated by the lookup success rate of less than 50% for large network or high mobility scenarios in [53]-[55], [72]-[73].

On the other hand, in WMNs, the stationary wireless backbone constructed by the MRs offers a more suitable facility to deploy overlay networks over. With the hardware highly specified for traffic relaying tasks and an unlimited power source, MRs offer a much higher bandwidth at a much wider coverage of up to hundreds of meters. By deploying the overlay network on top of these MRs, the MCs only connect to the MRs to access the overlay resources or to share their own resources as in [63], [65]-[67]. In this way, the control messages can be kept to minimal as the underlay and overlay networks do not change much. Moreover, since the overlay is deployed over the MRs, the overlay maintenance traffic remains constant regardless of the number of the MCs. Besides, in the WMN scenario, mobility of MCs would not overly affect the overlay performance due to the wide area coverage of the MRs. For instance, assume that the coverage radius of one MR is 100m, a MC with average moving speed of 10m/s will stay connected to one MR at least for 10 seconds, which is sufficient for a transfer session of small pieces of data (a video segment or a block of data). Moreover, it is easier to install and maintain overlay applications on the MRs to provide services for the MCs

than install them on all MC devices and expect the users to maintain the overlay application. In recent research works, even wireless sensor network have begun to make a switch to a layered network structure [63].

Due to the many of the advantages described above, it is believed that ***deploying an overlay on top of a WMN*** with overlay maintenance conducted on the MRs is the most scalable and efficient approach. Hence, this type of underlay network architecture is chosen to be employed throughout this study.

- ***Overlay Structure Choice***

When deploying overlay services over a resource-constrained wireless multi-hop network, a direct use of legacy P2P protocols would lead to high maintenance overhead and scalability problems since they operate independently of the underlay network topology. As a result, in order for an overlay protocol to perform efficiently over a wireless multi-hop network such as WMN, it should not only operate at the application layer alone, but also integrate the underlay physical network topology into the overlay structure and operations.

Unstructured overlays have been proved to work very well in wired networks. However, when deploying over wireless multi-hop scenarios, their flooding-based query becomes a severe weakness. The network wide flooding process for each resource search from one peer will result in a network wide traffic burst. This traffic burst makes the overlay network un-scalable, especially when many peers search for resources at the same time. Although many studies have tried to improve the efficiency of the unstructured overlay by integrating overlay protocol with underlay routing [51]-[52], using swarm-based intelligence [53] or dividing the network into multiple zones [55], the basic searching process is still based on network flooding which could lead to network wide broadcast storms, network congestion and disruption of other services.

On the other hand, in structured overlays, each peer builds and maintains a small overlay routing table. These distributed routing tables ensure overlay communications between any two peers that are accomplished within a predetermined number of overlay forwarding steps. It is remarked that these overlay queries are unicast based on the structure of the overlay routing table and are much less network intensive than the flooding based query of the unstructured overlay protocols. Of course, in order to maintain this overlay routing table, some level of maintenance traffic is required. However, different from the bursty traffic of unstructured overlay, structured overlay maintenance traffic is unicast periodically. As each overlay peer has its own overlay routing table, the effect of increasing query rate is much less network intensive than the flooding-based query of unstructured overlay.

However, if there is no linkage between the overlay network and the physical underlay topology, overlay routing table may point to distant peers in the underlay network. As a result, the overlay routing process towards the destination peer could route an overlay message across the entire physical network many times. As illustrated above, this lack of underlay network awareness could result in inefficient underlay routing, significantly increasing the protocol overhead and a high overlay routing stretch. Not only affecting the underlay performance, this inefficiency could also significantly degrade the overlay performance and efficiency, as well as seriously affect the transport of other types of traffic.

Based on the above discussions, *the structured overlay* is chosen as the overlay protocol to be studied in this thesis. An integration mechanism between overlay network and physical topology is further proposed. This overlay-underlay integration mechanism makes use of the stationary characteristics of MRs to realize a location-aware overlay for locating and retrieving resources and contents.

3.2 Improving Peer-to-Peer Overlay Content Delivery over Wireless Multi-hop Networks

One of the most significant aspects of original overlay networks is that the P2P overlay is independent of the underlay network topology. This means the overlay identification of a peer is only used to uniquely identify the peer in the overlay network and the true identity of the peer (such as IP address) stays anonymous. However, this independence also results in a drawback: two peers whose identifications are close to each other in the overlay network are not necessarily close to each other in the physical topology. This characteristic is not a serious problem for deploying P2P networks across the Internet, which is the initial idea of P2P, as topology-awareness across the Internet, through many continents, is hard to achieve and connections across the Internet are usually wired-based which are resource-rich and very reliable.

However, when deploying overlay applications in a wireless multi-hop scenario with bandwidth-limited, dynamically changing and error-prone links, this independence becomes a significant disadvantage. In particular, in an overlay network, overlay content such as a data item or a video segment can be available at many peers in the network. If the requesting peer selects a peer to download the content from at random, the data retrieval performance could be very bad as it is well-known that the achievable bandwidth of a wireless multi-hop network degrades quickly with the number of hops between the source and destination node [2]. Especially, in multimedia applications, such as video streaming, Video on Demand (VoD), etc., this data retrieval degradation is very noticeable as it often results in a very poor Quality of Service (QoS) and a poor viewing experience for the users. As a result, how to select the best peer to get the content from in order to improve the overlay content delivery in a dynamic wireless multi-hop scenario is an open question to be studied.

In this dissertation, the methods in the literature for improving peer-to-peer content delivery over wireless multi-hop scenarios are classified into two main categories, namely link aware methods and solutions for improving VoD through seek and jump operations.

3.2.1 Link Quality-aware Methods

E. Karasabun et al. proposed **Wi-Share** [74], a path quality aware P2P file sharing protocol for mobile Ad-hoc networks. The scheme integrates a P2P file sharing application with reactive wireless multi-hop routing at network layer to enable efficient search and download of shared files. In Wi-Share, search requests for shared files are broadcast to the entire network. As the search request message travels the network, the list of traversed nodes is recorded so that the route establishment at network layer to the requesting node is not needed. The authors further introduce additional parameters to quantify the quality of the path. These additional parameters include the current available power, path length to the requesting node and the current traffic rate at each node along the path. These parameters are appended to the search request at each of the intermediate nodes which receives the search request. These parameters are used as the routing metrics to build the routing table to the requesting node. These additional parameters are also included in the response packet back to the requesting node by the nodes that stored the requested file. The requesting node uses these parameters to calculate the path cost to each of the matching files as follows:

$$Path\ Cost = C_h \times HopCount + C_b \times (100 - Battery_{min}) \\ + C_t \times Traffic_{max} \tag{3.2}$$

Where C_h, C_b, C_t are constants.

$HopCount$ is the number of hops between the nodes,

$Battery_{min}$ is the battery level of the node with the least battery power on the path.

$Traffic_{max}$ is the traffic load of the node with the highest load.

The requesting node uses this path cost to select the best peer to get the file from. Path costs are also calculated as in equation (3.2) in intermediate nodes to select the best path for routing. During a download session, a periodic search request mechanism is introduced to update routing tables with the most recent path cost and also to enable newly joined nodes to contribute to the download session. The performance of Wi-Share is evaluated on a real test bed of nine nodes. However, in the proposed scheme, the

constant to calculate the path cost is topology dependent and a general method or a learning mechanism to determine these parameters is not shown. Besides, as discussed in the previous section, the broadcast based request is not suitable for large networks with high content request rates.

A. A. Asaad et al. proposed **P2PMesh** [75], a structured-based P2P overlay for file sharing over WMN. The authors first proposed a two-level architecture to deploy an overlay network over WMN. On the top level, a structured P2P protocol is constructed on the MRs. The constructed overlay takes advantage of the stationarity of the MRs to reduce overlay overhead and mitigate the end-user mobility. In addition, the MRs are also equipped with high storage capabilities to cache the shared files from the users. At the bottom level, end user devices connect to the MRs to upload the shared files and to download the needed files. To select the best file provider, the MR to which the requester is connected sends file request messages (FREQ) to all the potential providers. Upon receipt the FREQ message, the potential provider replies with a file acceptance message (FACC). The FACC message also includes the list of all the routes to each of the other peers that the provider is uploading the same file to. Based on this information, P2PMesh enables peers that are downloading the same file from the same provider at the same time to share wireless links, thus minimizing route coupling, hop distance and number of disjoint nodes. In addition, a file segment retrieval algorithm is proposed to minimize wireless transmissions. The requester selects the best provider as above to be its main source and other sources as secondary sources. The requester tries to collect segments from secondary sources and only requests the missing segments from its main source. However, since the routes between sources and requesters may not always overlap, the proposed scheme requires many requesters to request the same file from the same provider to have a significant efficiency improvement which may not be feasible in practice. Besides, it is not clear from the paper how minimizing route coupling, hop distance and number of disjoint nodes can be done at the same time, as it is very hard to do so in a general scenario.

N. Mastronarde et al. proposed a distributed framework for transmitting delay-sensitive multimedia among multiple peers over WMN [76]. The authors first partition all the video flows in the network into sub-flows or quality layers. Upon receiving a video sub-flow at the destination peer, it is assumed that the quality of the video can be incrementally increased. The authors further assume that the underlying Signal to

Interference plus Noise Ratios (SINR) of all the intermediate nodes along the path to the destination node are known a priori so that the expected goodput at those intermediated nodes can be determined. The authors define two utility functions: one for maximizing the total quality of all video flows and one for maximizing the minimum quality for all video flows to determine the end-to-end system performance. Using the incremental quality of each sub-flow and the goodput at the intermediate nodes along the path to the destination, a collaborative and a non-collaborative path provisioning algorithms for sub-flow admission control are proposed to determine which sub-flow can be admitted into the network to maximize the desired utility function. In the collaborative path provisioning algorithm, source peers exchange information about the relative importance (in terms of the quality) of each sub-flow, and perform the optimization for each sub-flow. In the non-collaborative path provisioning algorithm, a source node resolve the paths for its sub-flows without considering the sub-flows of other nodes. Simulation results illustrate that the collaborative distributed scheme outperforms the non-collaborative case and is close to the performance of a centralized optimal scheme. However, the proposed study requires all wireless peers to perform optimization and be aware of video's service layers which would result in extreme computational complexity and high volume of network overhead in a topology with many nodes or when there are many video flows to be transmitted.

H. Luo et al. proposed a cross-layer optimized scheduling algorithm for peer-to-peer video streaming applications over multi-hop Wireless Mesh Networks [77]. In the proposed scheme, the requesting peer sends query messages to all of its peers which have the requested video. As shown in Figure 3.3, the queries include the link information (SNR, queue length, etc.) of the requesting peer and all the intermediate nodes along the path. The requested peer jointly optimizes the video transmission at different layers using this information in order to minimize the video distortion. The parameters for the optimization include the quantization step and prediction mode at application layer, the frame size at MAC layer and the modulation and channel coding mode at the physical layers of all the nodes along the path. The requesting node then uses the optimized values from all the requested peers to select the best peer to get the video from. Using the parameters for optimization as described above, a video distortion –delay optimization problem is formulated under the constraint of the packet playback deadline. To reduce the computation complexity, an algorithmic solution to the formulated problem based on

dynamic programming is provided. The simulation results in NS-2 [94] showed that an enhancement of 5-15dB in terms of PSNR can be achieved using the proposed algorithm.
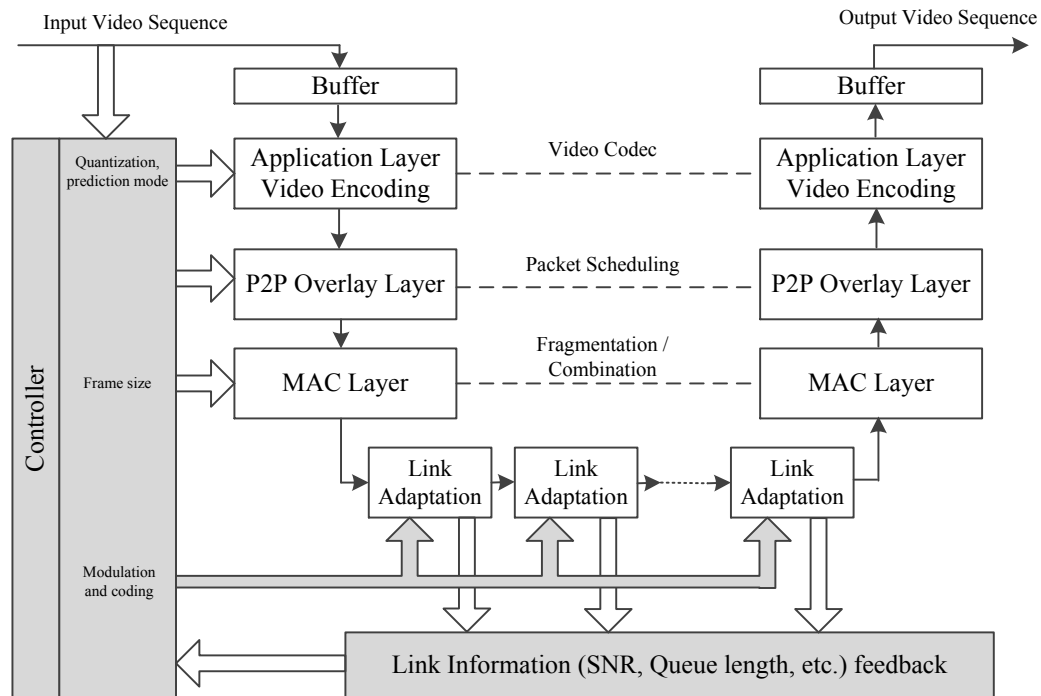
Figure 3.3: System architecture of the scheduling algorithm in [77]

However, for wireless multi-hop networks, the SNR and queue length of the intermediate nodes could vary dynamically with channel conditions and the network traffic. As a result, the optimized link adaptation on all the intermediate nodes along the path is impractical in reality. Besides, the cross-layer optimization mechanism requires fine tuning parameters on the entire protocol stack in order to improve the video quality, i.e., it requires the modification of the entire protocol stack to integrate the scheme, which is very hard for implementation.

3.2.2 Methods for Improving VoD Seek and Jump Operations

D. Wang et al. studied intra and inter-video VoD operations [78]-[79] to reduce the latency of user seek and jump operations by exploiting the locality of reference in user access patterns. In order to support P2P VoD, each video is divided into blocks of equal size and a set of continuous blocks are grouped into a chunk. The chunks are indexed in the overlay network using DHT to enable content searching. A chunk holder updates its chunk ownership to peers whose IDs are closest to the hash of the chunk for redundancy. Since a chunk holder also knows about γ peers closest to the hash of the chunk (which is called a *publish cache*), a cached publish scheme is proposed to reduce the overlay lookup time. In this scheme, upon receiving an overlay query, a peer can forward the query to the destination directly if it knows the destination peer through its publish cache, skipping the DHT routing in order to speed up the lookup process.

For intra-video seeking, the authors claimed that video delivery can be improved without doing an overlay search by using the set of neighbours the peer is currently downloading the video segment from. First, the authors argue and prove that if a peer is downloading a video chunk from a set of neighbouring peers who hold the chunk, it is highly probable that its next video chunk is also available in that set of neighbours even in the case of a user doing a seek operation within the video. As a result, the requesting peer can request the next segment from this set of neighbours without issuing a lookup request.

In addition, in order to reduce the jump delay, the authors use association rules learning to discover the reference in inter-video access patterns from other peers to predict the videos that are likely to be watched next. Knowing this information enables the peer to do lookup or even pre-fetch the content of the predicted next video in advance in order to avoid long delay. The proposed scheme however, does not show how to choose the best peer from the available peers which holds the video chunk for the best video quality retrieval.

W-P. K. Yiu et al. proposed *VMesh* [80], a distributed P2P VoD streaming scheme for supporting random user seeking functionality. VMesh utilizes the aggregate storage capacity of peers to amplify the supply of video segments to achieve user scalability. VMesh utilizes DHT to locate the video segments, however in order to

66

support faster user interactivity, each peer keeps a list of the peers who have the previous and the next segment depending on the segment it currently stores, as shown in Figure 3.4. The authors argue that since the segment access order of users is highly correlated, i.e, a user who is accessing the current segment also wants to access the next segment, using this list could enhance the overlay search efficiency. The authors further argue that even if the seek point is not far from the current playing point, traversing this list to find the provider of the sought segment is faster than looking up through the DHT network. To enable load balancing, each peer also keeps a list of peers storing the same segment so that when a supplier peer is overloaded, it can direct some of the new requests to other peers storing the same requested segment. To reduce maintenance overhead for these lists, a feedback-based maintenance mechanism is proposed in which the requesting peer validates the pointers in the lists returned by the requested peer and feeds back to the requested peer if the percentage of invalid pointers is large.
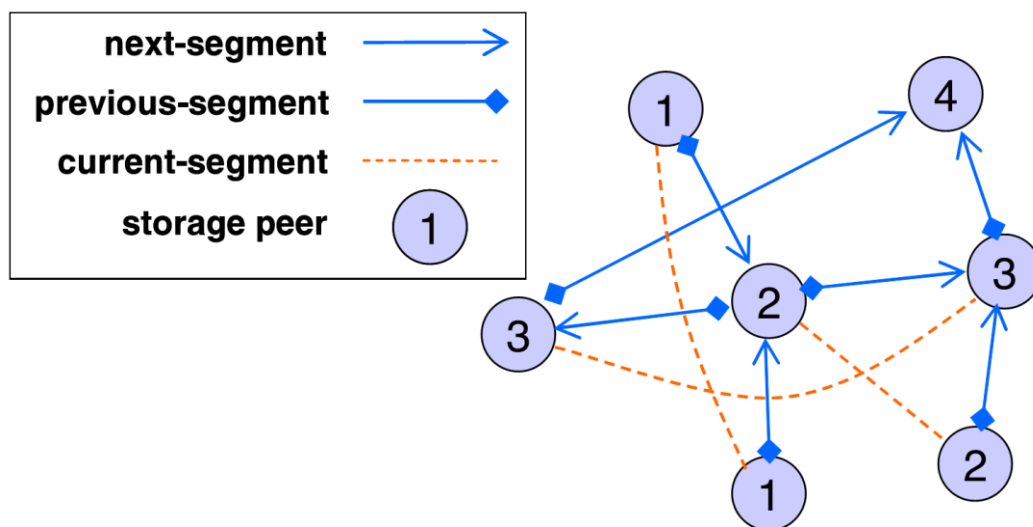
Figure 3.4: VMesh segment pointer structure [80]

In addition, the authors proposed a popularity-based segment storage in which the peers store segments in order of popularity to increase serving capability of the more frequently accessed segments. A distributed consensus is first introduced to estimate the distribution of all segments' popularity in a distributed manner by periodic

communications between peers. An adaptive segment caching mechanism is then presented to enable caching of segments according to their popularity.

Simulation results show that VMesh can reduce server stress, continuity of playback, start-up and jump latency. However, VMesh is not efficient in case the seeking point is far from the current playing point. Besides, the feedback-based maintenance is not efficient since it does not allow newly joined peers to contribute to the download as well as guarantee consistency in the previous/current/next segment lists across the peers. Moreover, it is hard to maintain the consistency of the previous/current/next segment lists when the number of peers in the network is large.

C. Xu et al. proposed a *QoE driven User-centric solution for VoD services (QUVoD)* [81] in urban vehicular network environments. QUVoD architecture is composed of two wireless networks, a lower layer VANET via vehicle-to-vehicle communication WAVE interfaces [82] for data transfer and an upper layer on top of cellular network via 4G interfaces for maintaining a Chord P2P overlay. The authors argue that a cellular connection is used because in comparison with the vehicle-to-vehicle connections, cellular connections are more stable and hence suitable for maintaining the Chord overlay even when the vehicles are moving with high dynamicity. This innovative architecture enables a high lookup success rate and good data delivery at the same time. The authors then proposed a distributed grouping-based video segments storage in which all vehicles playing the same video will be assigned the same prefix in Chord ID (video ID) and hence those vehicles form a Chord sub-circle. This sub-circle is further sub-divided into multiple groups according to the number of video segments. The nodes in the same group will store several consecutive segments starting with the same segment index. The first node in the group acts as the group scheduler. The group scheduler distributes downloading sessions to members in the group on a round robin basis to ensure load balancing among the members in the group. In addition, a speculation-based pre-fetching strategy is proposed to estimate video segment playback order by analyzing users' playback logs obtained by users' interactive viewing behaviours while playing the video. Based on this estimation, pre-fetching of the expected segments is employed to smooth the video playback. However, the proposed QUVoD does not give recommedations on which peer to choose to download the video segment from. The employed round robin approach, which aims to guarantee load

balancing, cannot ensure the best retrieved video quality as the source and destination peers are possibly geographically far from each other.

D. Wang et al. proposed a ***superchunk-based fast search network (SURFNET)*** [83]-[84] to provide reliable and fast search in P2P VoD systems. In SURFNet, each video is divided into chunks, and then several chunks are grouped into a superchunk. Based on which super chunk the peers hold, SURFNet two-layer structure network is formed as shown in Figure 3.5. This structured network consists of two layers: the Adelson-Velskii and Landis (AVL) tree [85] layer and the holder-chain layer. For stability, the AVL tree layer is constructed using superchunk ID and formed by stable peers which are supposed to be online for a long time. At holder-chain layer, each holder-chain is a linked list which groups all peers holding the chunks belonging to the same superchunk. This holder-chain is attached to a stable peer in the AVL tree (a chain head).
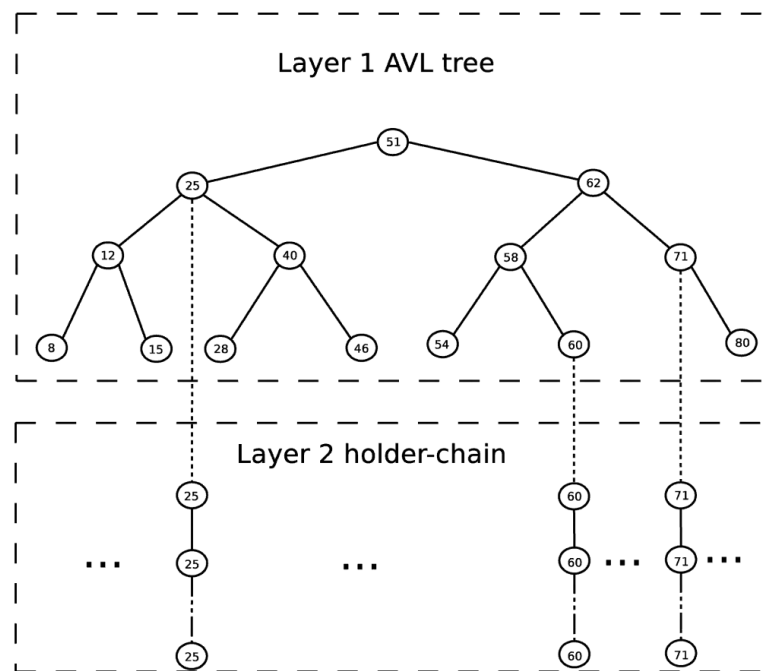
Figure 3.5: The two-layer SURFNet search network. [84]

Using this search network, content discovery in SURFNet involves two steps: chunk search and superchunk search. In the chunk search, the requesting peer sends query messages to its neighbours in the local holder-chain, requesting the required chunk. If no neighbour holds the required chunk, a superchunk search will take place. In the superchunk search, the query message traverses the AVL tree to the chain head of the superchunk which will search its holder-chain to find the requested chunk. The provided analysis shows that the superchunk search path length is bounded by $O(\log N_s)$ (N_s is the total number of superchunks). The simulation results show that by using superchunks, SURFNet can significantly reduce the search hops, search latency and search failure for jumps. However, the tree-based structure is not flat like DHT and failure of peers higher in the hierarchy such as the root peer would severely affect the overlay performance. In addition, the search cost analysis stops at the superchunk level which does not reveal the complete search complexity up to the chunk level. Finally, the search network cannot give a reference on which peer holding the chunk is the best peer to get the video chunk from in order to improve the video retrieval quality.

3.2.3 Discussions

A summary of the advantages and disadvantages of methods to improve P2P overlay content delivery over wireless multihop networks is illustrated in Table 3.2.

In wireless multi-hop scenarios, if an overlay network is constructed independently from the physical network, an overlay peer has no reference on which peer is better for getting the content from when the content is available at multiple peers across the network. For instance, if a peer selects a content provider which is far from itself in terms of hop count rather than a closer peer, the download path spans a longer route which make it more vulnerable to interference, and bandwidth contention with other traffic. A bad selection of peer would result in a poor achievable bandwidth, higher delay and a degraded quality experienced by users. This is especially true for bandwidth-hungry applications such as multimedia. As a result, in order to improve overlay content retrieval over wireless multi-hop, it is essential that the overlay network be aware of the underlying physical topology.

70

Table 3.2: Summary of advantages and disadvantages of methods to improve P2P overlay content delivery over wireless multihop networks.

Category	Scheme	Advantages	Disadvantages
Link Quality-aware methods	Wi-Share [74]	Uses hopcount, battery levels and traffic load to select the best peer	It is not clear how to determine the weight for each metric Uses broadcast based request which is not efficient
	P2PMesh [75]	Shares wireless links, minimizing the route coupling	Computationally expensive
	Sub-flow admission and path provisioning [76]	Uses SINR for sub-flow admission control.	It is hard to have accurate SINR values of all the nodes along the path available to do the optimization
	Optimize P2P video transfer using lower layer parameters [77]	Uses parameters from different layers to optimize flow admission	Computationally expensive It is hard to have all the accurate information from all the intermediate nodes for optimization
Improving VoD Seek and Jump Operations	VMesh [80]	Each peer keeps a list of the peers who have the previous and next segments to reduce the jump delay	It is hard to maintain the consistency of the previous/current/next segment list when the number of peers is large
	QUVoD [81]	Groups peers with the same video into a Chord sub-circle and then uses round robin to enable load balancing	Does not give the references on which is the best peer to download the segment from
	SURFNET [83]-[84]	Uses AVL tree and holder chain to arrange peers and to speed up segment search	Sensitive to peer failure

Among the proposed approaches in the literature, hop count which is used in [74]-[75] is the most commonly used metric. Other metrics used to find the best peer to download the content from include the battery level, traffic load of intermediate nodes [74], or route coupling [75]. Ideally, a combination of these metrics would be one of the best solutions, but it is very hard to find the right weight to balance these metrics in a single combined metric as they reflect different network characteristics and are topology

dependent. Moreover, most of the above studies use reactive route discovery processes to resolve the metrics for peer selection. Since these reactive solutions are based on network flooding, they can cause broadcast storms in the network and easily reduce the available bandwidth when the request rate increases. Besides, these processes are usually done only once before the peer selection, are susceptible to noise and may not accurately reflect the actual network conditions between the source and the destination peers.

Following the above discussions, it can be concluded that a close match between the overlay network and the physical topology is key to improve overlay content delivery in wireless multi-hop network. In WMN, since the MRs are generally stationary, a location-aware content retrieval promises to greatly improve the overlay services without incurring much overhead traffic. In this thesis, *a location-aware video segment seeking algorithm* is proposed in order to improve the video content retrieval. Moreover, throughout this study, traffic load is shown to have a significant impact on the content retrieval quality. As a result, in this study, *a link aware peer selection for video delivery* is also proposed to enable overlay peer selection based on underlying traffic load and to mitigate from bad selections such as provider peer with bottleneck link or with high loaded background traffic path.

3.3 Chapter Summary

This chapter has presented related works in the area of overlay construction schemes over different wireless scenarios and methods for improving overlay content retrieval over wireless multi-hop networks. The overlay construction schemes over wireless networks are categorized into unstructured and structured schemes. A discussion was provided to show the pros and cons of each method and has concluded that a structured overlay is more scalable and more suitable in WMN. The methods for improving overlay content retrieval over wireless multi-hop networks are classified into link quality aware methods and solutions for improving interactive operation in VoD applications. A discussion is also provided and it has identified the need for an overlay network that is aware of the underlying network topology and the link conditions in order to make high quality overlay content retrieval feasible.

CHAPTER 4: System Architecture

Abstract

This chapter describes the proposed system architecture for both the location-aware overlay construction and the peer-to-peer video streaming application. The basic operational principles of the proposed architecture are also presented. This system architecture will be used throughout this thesis and serves as the basis of the proposed location-aware overlay and the video segment seeking algorithms.

4.1 Introduction

Since its first introduction and commercialization in 1997, Wireless Fidelity (Wi-Fi) has made a huge leap forward to become the most widely used wireless data access network solution today. While the number of Wi-Fi hotspots is increasing on a daily basis, from a user's perspective, they appear to be just a collection of isolated "data oases". In order to become a ubiquitous coverage access network, these oases need to be connected together. This idea is one of the motivating factors behind the development of Wireless Mesh Network (WMN) technology. In a WMN network, Mesh Routers (MR) connect to each other to form a wireless backbone in order to provide data connectivity and services to the Mesh Clients (MCs) which are user devices which consume data.

However, the usage of WMN technology is not limited to a metropolitan wireless access network. When used in conjunction with Peer-to-Peer (P2P) data transfer solutions, the potential of WMN is widely open for the implementation of many innovative applications such as distributed data storage, resource sharing, and P2P Video on Demand (VoD) delivery. In particular, in a P2P VoD application, since many users may watch the same video at the same time, the same video segment may be simultaneously available at several peers across the network. If the P2P VoD application is integrated with an intelligent overlay mechanism, the huge community of peers that already had the segment can assist the playback of a peer. This mechanism can significantly improve the video quality retrieval for the user, reduce the server load and can enhance the traffic load balance across the network.

Nevertheless, this integration of overlay network over WMN is not straightforward. First, the current overlay protocols are designed for resource-rich wired networks with a high volume of maintenance traffic and behave poorly in a wireless multi-hop scenario with limited bandwidth and high channel variations. Second, in wireless multi-hop network, since the achievable bandwidth and packet loss performance degrade sharply with many factors such as the hop length of the path and the traffic load, selecting from which peer segments are retrieved is a key factor in improving the quality of service.

In this context, this thesis presents three major contributions: 1) **Wireless Location-aware Chord-based Overlay mechanism for WMN** (WILCO) – a location-aware overlay with integrated physical topology to improve overlay efficiency; 2) **WILCO-based novel geographical location-aware video segment seeking mechanism** – a video segment seeking mechanism with underlay topology awareness in order to enable locating and retrieving video segments from the closest peer; 3) **Cross-layer Wireless Link Quality-aware Overlay peer selection mechanism (WLO)** – a cross-layer video segment seeking mechanism with link quality awareness to enable locating and retrieving video segments from the peer with the best path link quality. In this chapter, the system architecture upon which the three contributions are built is described. The detailed descriptions and analysis of each contribution are presented in the following chapters.

4.2 Proposed System Architecture

4.2.1 System Architecture
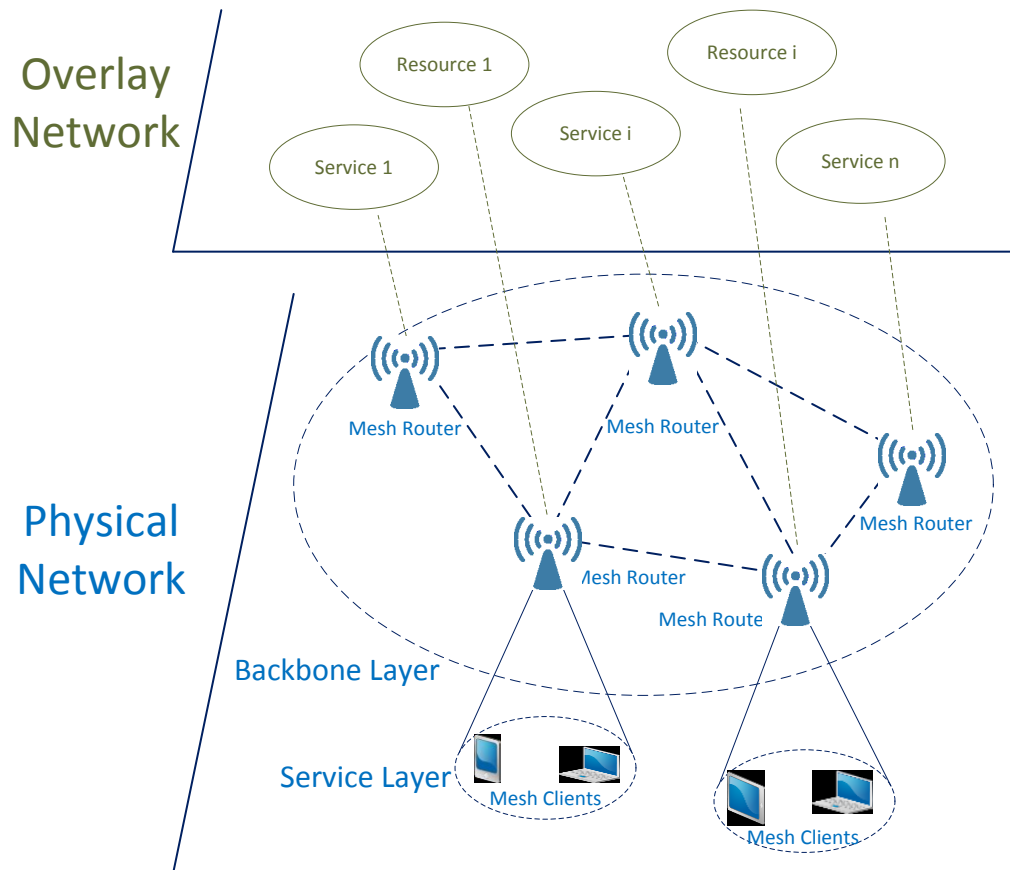
Figure 4.1: Proposed system architecture.

To accommodate resource sharing on WMN, a two-layer architecture composed of service and backbone layers is employed as illustrated in the Physical Network part in Figure 4.1. The service layer includes MCs as end user devices, which share services and resources and use those shared by others. The backbone layer includes stationary, power-unlimited MRs, with some of the MRs having wired Internet connectivity. These MRs run WILCO, the proposed Chord-based location-aware protocol to build up an overlay network for locating resources and services within the WMN to serve the MCs as illustrated in the Overlay Network part in Figure 4.1. An overview of the operations of the Chord protocol, is included in chapter 2 and further details can be found in [35].

WILCO uses a location-aware overlay with multi-level ID mapping and an improved finger table is proposed to improve the overlay communication efficiency. Details of WILCO will be presented in chapter 5. Moreover, in order to improve the overlay video delivery, WILCO-based and WLO video segment selection mechanisms are proposed. The WILCO-based location-aware video segment seeking mechanisms use WILCO location-aware ID mapping to select the best peer in terms of hop count distance for video content retrieval. The details regarding WILCO-based location-aware video segment seeking mechanisms are to be presented in chapter 6. Different from WILCO-based video segment seeking mechanism, WLO selects the best peers based on the link quality using a novel Multiplication Metric Selector (MMS) and a cross-layer selection mechanism. The details regarding WLO are to be presented in chapter 7.

4.2.2 Block-level Architecture
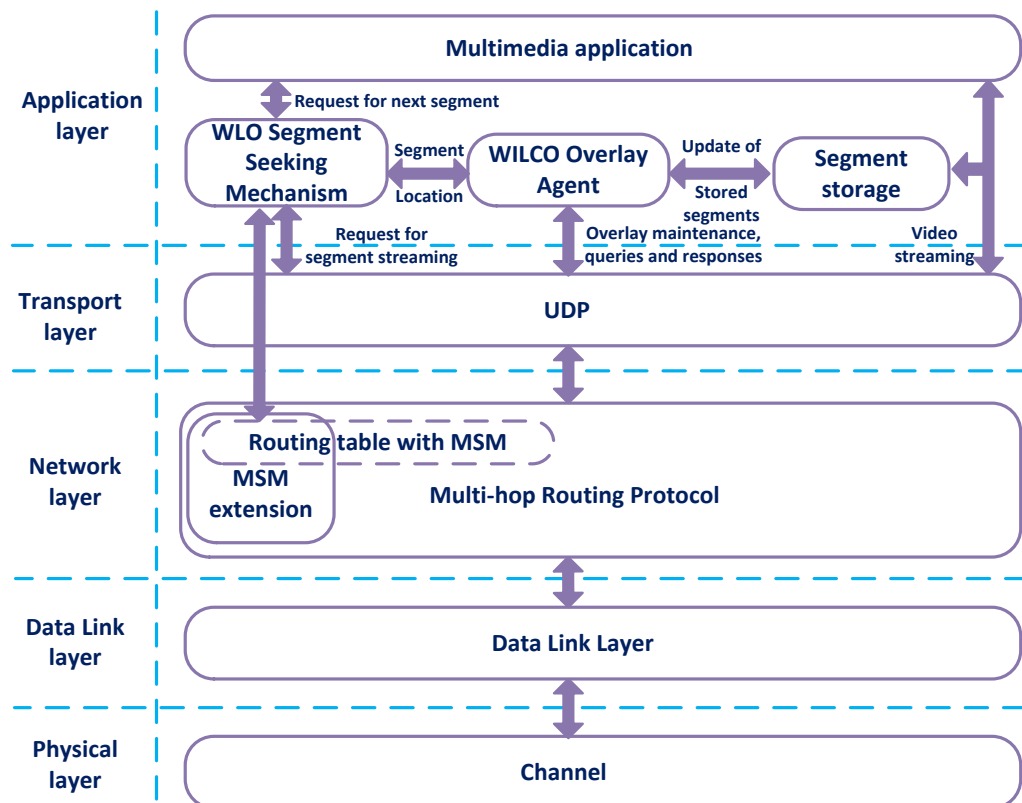
Figure 4.2: Block-level structure of the mesh router system with integrated video overlay.

76

Since a typical wireless mesh network is very large in terms of number of nodes, in order to simplify the implementation and also to reduce the simulation run time, the functionalities of the mesh clients are also integrated into the mesh routers. In comparison to a real implementation of a WMN, this simplification removes the service layer with the mesh clients; however, since the MRs normally have different wireless interfaces for connecting to the mesh backbone and for serving the mesh clients, this simplification just removes a constant delay for this last hop connection from the results. Since all the comparisons between different schemes throughout this thesis are based on this simplification model, the comparisons are fair and valid.

Figure 4.2 illustrates the block-level architecture of the mesh routers with the proposed video sharing peer-to-peer overlay with respect to the TCP/IP protocol stack. In this protocol stack, at the application layer, as well as the multimedia application, the video segment storage, the proposed WILCO Overlay Agent and the proposed Segment Seeking Mechanism block are implemented to realize the peer-to-peer VoD application.

The WILCO overlay agent which implements the proposed WILCO location-aware overlay is the heart of the application. This agent is responsible for the *overlay communications* among the overlay peers. The overlay communications include overlay maintenance and processing of queries and responses according to the Chord protocol [35] which were described in chapter 2. Additionally, the agent provides the Segment Storage block which stores the requested segment for peer selection.

The Segment Seeking Mechanism block chooses the best peer from all the peers that stored the requested segment and request this best peer to stream the segment to the requested peer. Upon receiving the requested segment, this segment is forwarded to the multimedia application for playing and is also stored in the segment storage for further sharing purpose.

4.2.3 Overlay Video Distribution Mechanism

For P2P video distribution, each shared video will be assigned a unique key and is managed by a MR according to the Chord protocol [35]. To efficiently support video delivery on a peer-to-peer overlay, the server divides each video into equal size segments

and assigns consecutive segment sequence numbers to them in the order of playback. During the distribution process, many segments of the video become available in several places within the WMN. These segments are registered and periodically updated to the MR which manages the video and are stored in a database in the structure of

$$[ID_i, S_i, L_i]$$

Where:

ID_i is the ID of the MR which stores the video segments.

S_i is the start segment sequence.

L_i is the number of segments the node stores.

It is noted that a MR can have multiple contiguous/noncontiguous segments; in this case the MR segments are represented using multiple entries. In order to protect the system from single node failures, the successor of the MR with respect to the Chord ring which manages the key also stores and updates a copy of this database.

When a peer requests the segment S_j, the MR searches its database for the set of peers that have this segment, i.e., $S_j \in [S_i, S_i + L_i]$, and replies to the requesting peer with this set of peers. Based on the ID of the requesting and destination peers, the proposed WILCO-based or the WLO segment seeking mechanism is performed to select the best destination peer to retrieve the segment.
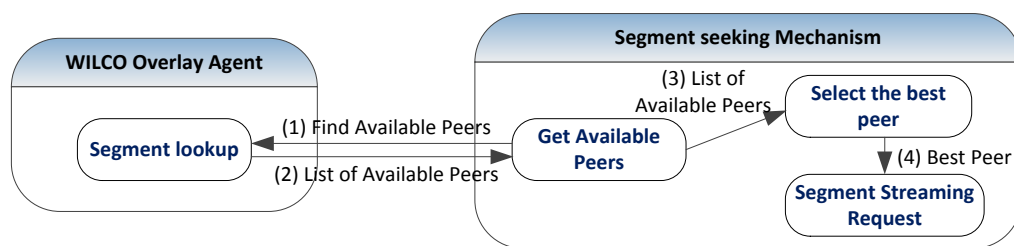
Figure 4.3: Overlay Video segment seeking procedure.

The video segment seeking procedure is illustrated in Figure 4.3 and the message flow for overlay video distribution is illustrated in Figure 4.4. When the next video segment is needed, the Segment seeking mechanism requests the list of available peers

which store this segment from the WILCO Overlay Agent. The WILCO Overlay Agent requests this peer list from the peer which manages the video and returns this list to the Segment Seeking Mechanism.

Upon receiving the list of all potential serving peers, the Segment Seeking Mechanism performs the peer selection to select the best peer from which to retrieve the segment. In this thesis, two WILCO-based location-aware peer selection algorithms are proposed to enable enable location and retrieval of the video segments from the closest peer in terms of hop count. In addition, WLO - a cross-layer video segment seeking algorithm with link quality awareness is proposed to enable location and retrieval of the video segments from the peer with the best path link quality. In WLO, a Multiplication Selector Metric (MSM) extension is integrated into the underlay routing protocol (as shown in Figure 4.2) to enable link quality awareness across the peers. This MSM extension calculates the MSM metric for each of the path in the MR routing table. Moreover, a cross-layer connection is constructed between the MSM extension and the Segment Seeking Mechanism block to enable overlay peer selection with underlay link quality awareness. Details about the peer selection mechanisms are to be presented in chapter 6 and chapter 7.
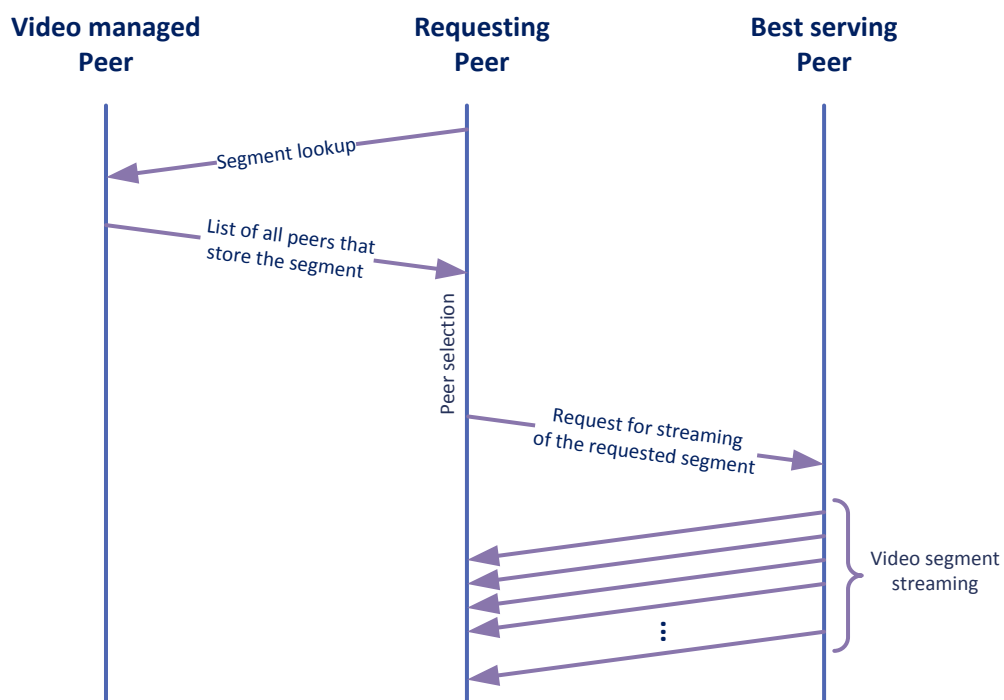
Figure 4.4: Overlay video distribution message flow.

After selecting the best peer for retrieving the video segment, the requested peer will send a request to this best peer and the streaming of the video segment will be started from the best peer to the requested peer.

4.3 Chapter Summary

This chapter presents the architecture on which the proposed solutions rely, including WILCO, WILCO-based location-aware segment seeking algorithms and the WLO link-aware segment seeking algorithm. The placement and the principle of each contribution with respect to the TCP/IP protocol stack are described. Details of each contribution and numerical results will be described in the following chapters.

CHAPTER 5: WILCO – Wireless Location-aware Chord-based Overlay for WMN

Abstract

In this Chapter, the proposed **Wireless Location-aware Chord-based Overlay mechanism for WMN** (WILCO) is described. The location-awareness of the proposed mechanism is realized through a novel geographical multi-level Chord-ID assignment to the MRs on grid WMNs. An improved finger table is proposed to make use of the geographical multi-level ID assignment to minimize the underlay hop count of overlay messages. An analytical framework is developed to analyze the lookup efficiency of the proposed scheme. This study proves that in comparison with the original Chord, WILCO can reduce the maximum number of lookup messages by half, and has symmetric lookup behaviour in both forward and backward directions of the Chord ring. The analytical framework also shows that the proposed scheme has a stretch factor of $O(1)$, which implies that the constructed overlay closely matches the physical topology. Simulation results show that in comparison with Chord and MeshChord, WILCO significantly improves lookup efficiency in terms of the average number of lookup messages, the number of hops a lookup travels on the physical network, lookup time and stretch factor. Additionally, simulation results also show that the proposed scheme greatly reduces

messaging overhead and provides more overhead balance among the MRs, which indicates that WILCO is able to scale to large WMNs.

5.1 Introduction

Recently, innovative applications such as distributed storage, resource sharing, and peer-to-peer Video on Demand, have become more and more popular. These applications rely on peer-to-peer overlay structures which offer many benefits that the traditional client–server paradigm lacks. These benefits include *self-scaling*, i.e., the capacity of the overlay increases as more users participate in the overlay; *self-organization*, i.e., the overlay network is composed of overlay peers which require no dedicated infrastructure and *self-healing* the overlays update their structure after the joining and leaving of peers. With these advantages, by using the peer-to-peer overlays, these and other innovative applications promise to greatly enhance the user experience. However, when deploying peer-to-peer overlay networks over wireless multi-hop networks such as WMNs, many challenges arise mainly due to issues such as bandwidth constraints of the WMN, high maintenance overhead of the overlay network and routing stretch. The latter refers to the overlay routing inefficiency due to the independence between the overlay network and the physical topology which actually does the packet-level routing. A literature review of the existing methods of enhancing overlay efficiency over wireless multi-hop network has been presented in Chapter 2. Most of the solutions proposed in the literature use network flooding to enable overlay communications which introduces significant overhead and can result into broadcast storm, greatly degrading the performance of the network.

This chapter proposes WILCO, a location aware Chord-based overlay over WMNs. WILCO makes use of MR locations to integrate the physical topology into the overlay network through a **multi-level location-aware ID mapping**. In order to further improve the overlay communication and achieve a better stretch factor over WMN, an **improved finger table** is proposed. The detailed WILCO mechanisms, overlay efficiency analysis and simulation results are introduced in the following sections of this chapter.

5.2 WILCO Multi-level Location-aware ID Mapping

5.2.1 Assumptions

The principle behind the mechanism of the proposed multi-level location-aware ID mapping is to make use of the locations of the MRs and integrate them into the ID space of the Chord Ring (described in chapter 2). This interaction aims to have MRs which are close together in the underlay topology also be identified as close together in the overlay network. This location-awareness is very important in reducing the overlay overhead, stretch factor and in increasing the overlay communication efficiency as overlay messaging is restricted to some physical boundary instead of traversing across the actual WMN many times to reach another overlay peer.

There are two assumptions for the proposed location-aware ID mapping mechanism. Firstly, the WILCO location-aware ID mapping assumes that MRs are stationary, i.e., the positions of the MRs do not change over time. This assumption is essentially the basic assumption for most of the two-layer architecture wireless multi-hop networks including WMN. Secondly, for ease of explanation, it is assumed that MRs are laid out in a grid network, almost equally distanced between each other. However this is not strictly needed as explained later on in this thesis (end of section 5.2.2).. This grid-like WMN is used since it is shown in [86] that a random topology is unsuitable for large-scale mesh deployment and the grid topology provides the best balance between MR density, backbone connectivity and network capacity.

5.2.2 WILCO Multi-level Location-aware ID Mapping Mechanism
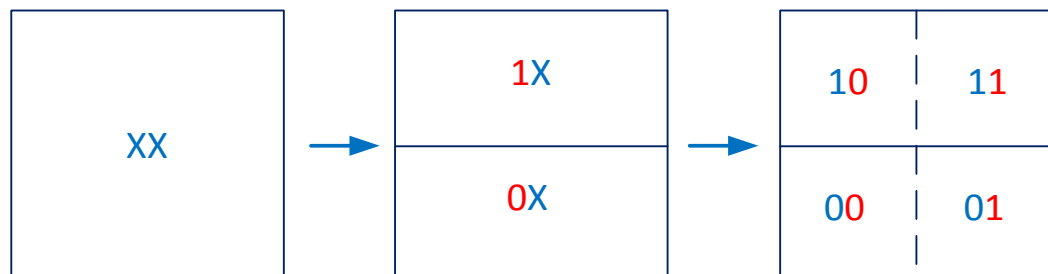
Figure 5.1: The first step division in WILCO ID allocation.

Consider a planned WMN deployment over an approximately square area with $N = 2^m$ stationary MRs laid out in a grid manner: i.e., MRs are almost equally distanced between each other.
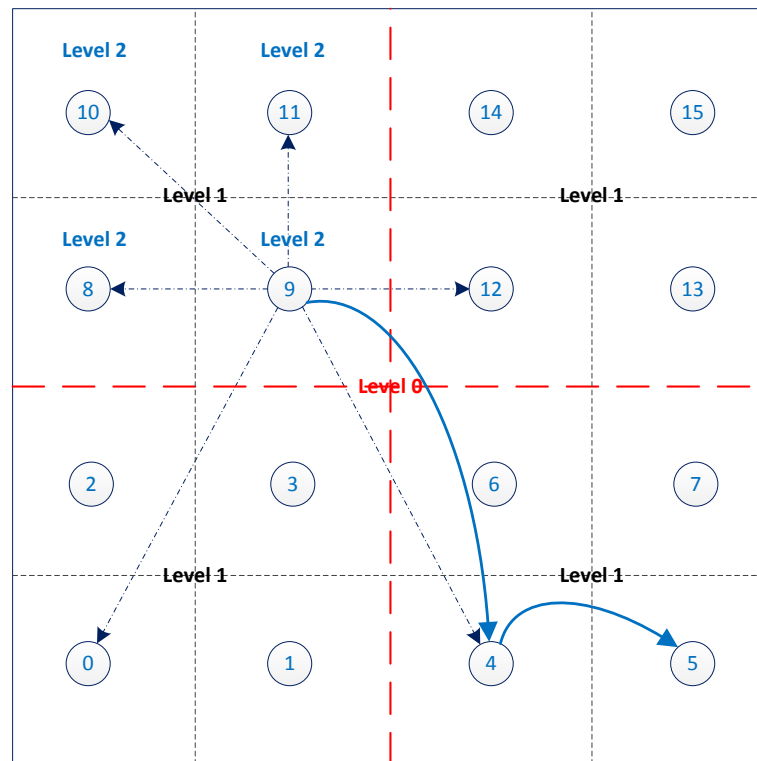
Figure 5.2: WILCO location-aware ID mapping for *m*=4.

An m-bit binary addressing scheme is used. In the WILCO location-aware ID mapping, the location of the MR is encoded as follows. It is first assumed that m is even (the topology represents a square grid). The deployment area is divided into 2^m equal areas each containing a single MR in $\log_4 N$ steps. Each step subdivides the deployment area into 4 subareas, divided along the vertical axis (y axis) and the horizontal axis (x axis). The two bits of the ID space are assigned to the MRs according to this division as follows and recursively use the subdivisions to assign a unique m-bit address to each MR. In the first step (Figure 5.1), the division on the y axis separates the deployment area into two halves and all the MRs residing on the upper half have the most significant bit set to 1. Likewise, all of the MRs residing on the lower half have the most significant

bit set to 0. Next, the division on the x axis partitions each of these two halves into two areas: MRs on the left side get their second significant bit set to 0 and the MRs on the right side have their second significant bit set to 1. In the subsequent steps, each of the four areas from the previous step will be partitioned further into four smaller areas following the same mechanism as in the first step. After $\log_4 2^m$ steps, the deployment network is divided into 2^m areas, each containing one MR with a unique ID, expressed in binary form.

Let define the areas produced after step i division as level i areas. Following this definition, the area at level 0 is the whole WMN deployment area containing all the MRs and the level $\log_4 N$ areas contain a single MR each. Figure 5.2 illustrates WILCO location-aware ID mapping for 16 MRs ($m = 4$) and the resulting areas at level 0, 1 and 2.

Let N_i be the number of MRs at a level i area. An intuitive interpretation of a WILCO ID is that at level i, the most significant $(m - \log_2 N_i)$ bits represent a unique identification of the level i area in which the MR resides in among the other level i areas and the least significant $\log_2 N_i$ bits represent a unique identification of a MR within the given area. Note that in each step, each of the areas in the previous step is divided into 4 equal-sized areas, and hence, the number of MRs in an area at level i is $N_i = 4^{\frac{m}{2}-i}$. Furthermore, since the most significant $(m - \log_2 N_i)$ bits represent a unique identification of the level i area in which the MR resides in among the other level i areas, two MRs with IDs p and k share the same area at level i if:

$$\left\lfloor \frac{p}{N_i} \right\rfloor = \left\lfloor \frac{k}{N_i} \right\rfloor \qquad (5.1)$$

It is remarked that after the $(\log_4 2^m - 1)$-th step, there are only 4 MRs in each area and all but the last two ID bits are determined. Since the last 2 bits are decided in the next step, those MRs have consecutive IDs. This ensures that MRs that are close together in the physical topology stay also close to each other in the overlay. Assuming that the communication range of each MR covers the distance from itself to the nearest MR in diagonal direction (i.e., in Figure 5.2, MR 0 can connect MR 3 directly), then all four MRs with consecutive IDs can directly communicate with each other. It is noted that there are peers with consecutive IDs but are not placed next together; this issue will be

addressed and resolved by using WILCO's improved finger table which will be introduced in the next section. The last, but not least important remark is that each area at level i contains a quarter of the number of MRs as an area at level $(i - 1)$, and hence, the maximum number of physical hops between two MRs residing in the same area at level i is half of that between two MRs residing in the same area at level $(i - 1)$. This remark plays a central role in our location-aware ID mapping in terms of reducing the underlay hop count and in the proof related to the stretch factor to be presented.

It is noted that m is not necessarily even. It is easy to see that the proposed location-aware ID mapping also holds when m is odd. In this case, in the first step one division is performed and the most significant bit is allocated only; all subsequent bit allocation steps remain unchanged, as already described. It is also noted that the location of each MR can be determined easily with a location-based solution such as using GPS or WiFi localization [87] for example; and that since the MRs are assumed stationary, the mapping of IDs needs to be done once only at the planning stage and remains unchanged thereafter.

Figure 5.3: A streetlight mounted MR (Image source:
http://computer.howstuffworks.com/how-wireless-mesh-networks-work.htm).

5.2.3 WILCO Multi-level Location-aware ID Mapping Mechanism

It is noted that for the deployment of real WMNs, the MRs do not need to be strictly equally separated for the location-awareness of WILCO to be feasible. From Figure 5.2, it can be seen that WILCO location-aware ID mapping only requires each MR to reside in its lowest level area (level 2 in this case) so that each MR has a unique ID. For a real network deployment, assuming the separation between the MRs is designed to be 100m, the size of each lowest level area is 10,000m^2. Finding a suitable place to install a MR in such a large area is not a very big issue, especially since MRs nowadays are so versatile that they can be easily mounted on streetlights[14] as shown in Figure 5.3.

5.3 WILCO Finger Table

The WILCO location-aware ID mapping maps a two-dimensional position of a MR into a one-dimensional ID space of the Chord Ring and makes the MRs which are close together in the physical topology close together in the overlay Chord Ring. However, overlay communications are enabled through finger table lookup in which the overlay message is sent to the closest peer in the finger table with respect to the Chord Ring. As a result, if the overlay finger table is also location-aware, overlay communication efficiency can be further improved.

In order to speed up the lookup process and make use of the proposed multi-level location-aware ID mapping, a new Chord finger table of $3 \times \log_4 N$ entries is proposed. Starting from the highest level ($\log_4 N - 1$), at every level i area, each MR maintains three entries (fingers) pointing to MRs with the lowest ID in each of the other areas at level i with which it shares the same level ($i - 1$) area. For example, the finger table of MR 9 in Figure 5.2 (shown as dash-dot arrows) is as follows:

- Level 1 fingers: ID 8, 10, 11.
- Level 0 fingers: ID 0, 4, 12.

---

[14] Motorola Mesh Wide Area Network products –
http://www.motorola.com/Business/US-EN/Business+Product+and+Services/Wireless+Broadband+Networks/Mesh+Networks

In general, the finger table of MR with ID p at level i ($0 \le i < m/2$) is expressed as described next:

$$\text{Let } ID = N_{i-1}k + \left\lfloor \frac{p}{N_{i-1}} \right\rfloor N_{i-1}, \qquad k = 1, 2, 3 \tag{5.2}$$

Then:

$$Finger_{i,k} = \begin{cases} ID & , if \; \left\lfloor \frac{ID}{N_i} \right\rfloor = \left\lfloor \frac{p}{N_i} \right\rfloor \\ \left\{ \left\lfloor \frac{p}{N_i} \right\rfloor + 1 \right\} N_i - ID + \left\{ \left\lfloor \frac{p}{N_{i-1}} \right\rfloor - 1 \right\} N_{i-1}, if \; \left\lfloor \frac{ID}{N_i} \right\rfloor \ne \left\lfloor \frac{p}{N_i} \right\rfloor \end{cases} \tag{5.3}$$

where $N_i = 4^{\frac{m}{2}-i}$ is the number of MRs in an area at level i.

The operation and usage of the updated finger table is the same as in the original Chord. For instance, for MR 9 to locate key 5, MR 9 searches its finger table for a finger with the greatest ID less than or equal to 5 (MR 4) and sends a lookup message to this peer. When MR 4 receives the lookup message, it searches its finger table and finds MR 5 as its level 1 finger entry. It then forwards the lookup message to MR 5 to complete the lookup process. As depicted in Figure 5.2 (curved lines), this example further illustrates that the proposed ID indexing and finger table is location-aware. It is illustrated from this figure that, by using WILCO finger table, the lookup message gradually descends from the geographically larger areas to smaller areas. In our example, the lookup goes from MR 9 $\rightarrow$ MR 4 on level 1 and then from MR 4 $\rightarrow$ MR 5 on level 2. Hence, the search is geographically limited on a step by step basis.

Similar to a Chord finger table, a WILCO finger table provides higher resolution information at lower level areas (large i) giving more location information about MRs in the immediate vicinity than at higher level areas. Another important remark is that since three level 0 fingers of any MRs point to the three MRs with the lowest IDs in three areas at level 1 (except the level 1 area where the MR resides), in the lookup for key k at MR p, the proposed finger table provides at least one finger f that shares the same area at level 1 with k. In other words, if p and k share the same area at level ($i < \log_4 N$), the proposed finger table of p provides at least one finger f that shares the same area at level ($i + 1$) with k. Compared to the finger table of Chord, with $\log_2 N$ entries, WILCO

finger table has $3 \times \frac{\log_4 N}{\log_2 N} = 1.5$ times more entries. This overhead of the new WILCO finger table is just a scale factor from that of Chord [35], i.e., $O(\log N)$; hence, with the increase in network size WILCO finger table is as scalable as that of Chord.

5.4 Lookup Efficiency Analysis

To investigate the lookup efficiency of WILCO, an analysis framework is developed. Lemma 1 and Theorem 1 provide an upper bound on the number of overlay messages needed to resolve a lookup from any node. Lemma 2 proves the symmetric lookup characteristic of WILCO. Last but not least, by using the *stretch factor* (as defined in [64]-[67]), Theorem 2 proves that WILCO overlay is location-aware with a stretch factor of $O(1)$.

5.4.1 Number of overlay messages per lookup
<u>Lemma 1</u>:

> *Suppose MR p wishes to resolve a query for key k. If p and k share the same area at level i, $(0 \le i \le \log_4 N - 1)$ then $(\log_4 N - i)$ lookup messages are required for p to resolve the lookup.*

Proof: Induction is used to prove the lemma.

It is first show that the Lemma holds when p and k share the two lowest levels $(i = \log_4 N - 1$ and $i = \log_4 N - 2)$:

- For $i = \log_4 N - 1$: Since the area at level i includes only 4 directly connected MRs and according to the definition of the improved finger table, level i finger table of p has already included all of these fingers, including k. Hence, p can reach MR k with only one lookup message.
- For $i = \log_4 N - 2$: Since the finger table of p at level i includes three fingers for each area at level $(i + 1)$ that share the same area at level i, p sends lookup request to finger f with greatest ID less than k. Since f is the MR with lowest ID in this area, f and k share the same area at level $(i + 1)$. When f receives the lookup request, it forwards this request to k as in the

case of $i = \log_4 N - 1$. Hence, $\log_4 N - i = 2$ lookup messages are required for p to reach MR k.

Suppose this lemma holds until level i ($i > 0$), the lemma is proved that it also holds for level $(i - 1)$:

- Since p and k share the same area at level $(i - 1)$ and p holds a level i finger f that shares the same area at level i with k (according to the definition of our improved finger table); p needs one lookup message to reach f. Since f and k share the same area at level i, another $(\log_4 N - i)$ lookup messages are needed to get to k. Hence, in total, there are $\left(\log_4 N - (i - 1)\right)$ lookup messages. This concludes the proof.∎

Theorem 1:

With the proposed finger table, a lookup for any key k from any MR p requires at most $\log_4 N$ lookup messages.

Proof: Suppose MR p wishes to lookup key k, the number of lookup messages needed to reach MR k is analyzed.

Let i be the lowest level for which p and k share an area. According to Lemma 1, $(\log_4 N - i)$ lookup messages are required to find k. Since $i \geq 0$, the maximum lookup messages required is $\log_4 N$.∎

5.4.2 Symmetric lookup
Lemma 2:

The proposed finger table gives symmetric lookup on both directions of the Chord Ring.

Proof: Suppose MR p wants to resolve lookups for key k and k'. Assume that level i is the lowest level where k and k' share the same area. Further assume that $p < k$ and $p > k'$. It is show that using the proposed finger table, p can find k and k' with the same number of lookup messages.

According to Lemma 1, since p, k and k' share the same area at level i, it requires $(\log_4 N - i)$ lookup messages to resolve for k as well as $(\log_4 N - i)$ lookup messages to resolve for k' ■.

To evaluate the location-awareness of the proposed scheme, the definition of stretch factor in [64]-[67] is adopted.

5.4.3 Location awareness

Definition: Stretch factor of network A is defined as

$$stretch(A) = \frac{l(P(k))}{l(k)} \tag{5.4}$$

Where:

$P(k)$ is the shortest path traversed by the lookup for key k in the overlay network.

$l(P(k))$ is the shortest hop length of $P(k)$ in the physical network.

$l(k)$ is the hop length in the physical network between the MR at which the lookup is invoked and the MR that manages the key range to which k belongs.

Theorem 2:

The stretch factor of the proposed location-aware ID mapping and modified finger table is $O(1)$.

Proof: From the proposed location-aware ID mapping, each area at level i contains a quarter the number of MRs as at level $(i - 1)$; hence, the maximum number of physical hops between two MRs residing in the same level i area is only half of that between two MRs residing in the same area at level $(i - 1)$.

From Lemma 1, every time a MR forwards a lookup message on the overlay, it forwards the message to its finger which shares the same area with the key, but at one level lower than itself. As a result, for each finger lookup on the overlay, the searching

area shrinks by a quarter and the maximum number of physical hops from the next finger shrinks to half. It is noted that the maximum number of hops a lookup message needs to travel in the physical topology at level 0 area is $\sqrt{N}$. From Theorem 1, the proposed scheme requires the maximum of $\log_4 N$ lookups; hence, the maximum number of hops a lookup traverses in the physical topology is:

$$\max_k\{l(P(k))\} = \sqrt{N} + \frac{\sqrt{N}}{2} + \cdots + \frac{\sqrt{N}}{2^{\log_4 N}} = \sqrt{N} \sum_{j=0}^{\log_4 N} \frac{1}{2^i} \qquad (5.5)$$

Since $\lim_{m\to\infty} \sum_{i=0}^{m} \frac{1}{2^i} = 2$, for large topologies ($m \to \infty$), it is shown that $l(P(k)) \le 2\sqrt{N}$.

For the considered grid topology, the hop distance in physical network between two MRs is $l(k) = O(\sqrt{N})$. Hence, the stretch factor can be calculated as follows:

$$stretch(A) = \frac{l(P(k))}{l(k)} = O\left(\frac{2\sqrt{N}}{\sqrt{N}}\right) = O(1) \ \blacksquare \qquad (5.6)$$

5.4.4 Comparison with MeshChord

Table 5.1: Overlay communication efficiency comparison.

	Overlay Communication Efficiency		
	Maximum overlay steps	**Symmetric Lookup**	**Stretch factor**
MeshChord	$\log_2 N$	No	$O(\sqrt{N}\log N)$
WILCO	$\log_4 N$	Yes	$O(1)$

Remark 1: In comparison with Chord [35] and MeshChord [66]-[68] which require at most $\log_2 N$ overlay lookup steps, by utilizing the improved finger table, WILCO reduces this number by 50% $\left(\frac{\log_4 N}{\log_2 N} = 0.5\right)$. This improvement significantly reduces the overlay messaging overhead and also enables faster overlay lookup.

Moreover, in comparison to the Chord mechanism, WILCO lookup is symmetric on both directions of the Chord Ring which further reduces the overlay steps required to resolve a lookup and hence, reduces the lookup response time.

Remark 2: In comparison with MeshChord with a stretch factor of $O(\sqrt{N\log N})$ [67], WILCO location-aware scheme with a stretch factor of $O(1)$ significantly reduces the stretch factor.

$$\frac{stretch_{MeshChord}(A)}{stretch_{WILCO}(A)} = O(\sqrt{N\log N}) > O(\sqrt{\log N \log N}) = O(\log N) \qquad (5.7)$$

Since $O(N) > O(\log N)$, as shown in equation (5.7), this reduction of stretch factor is by at least a magnitude order. This reduction in the stretch factor proves that WILCO has a better location-awareness and a better overlay-underlay integration in comparison to MeshChord. A stretch factor of $O(1)$ shows that WILCO overlay communications efficiency is bounded by a constant scale factor in comparison to the direct underlay network communications. In addition, since WILCO overlay communications are closely matched to the underlay direct communications, it promises a significant reduction in the overlay overhead and a significant reduction in the overlay lookup time.

5.5 Simulation-based Testing and Result Analysis

5.5.1 Simulation Overview

The performance of WILCO, the proposed location-aware scheme is evaluated through detailed, packet-level simulations using Network Simulator NS-3 [88], a discrete event-based simulator which is widely used in networking research. The simulated topology follows the descriptions from Section 5.2, consisting of N MRs arranged in a grid topology. The distance between two adjacent MRs is set to 100m (a common network scenario for WMN simulations, i.e., [64]-[69]). In the simulations, all MRs are equipped with IEEE 802.11b radios (the physical and data link details are described in Table 5.2) and OLSR is used as the underlay routing protocol. For the purpose of comparison, the original Chord with IDs of MRs randomly assigned from the ID space with no overlap and a finger table as in [35] and MeshChord [67] with geographical ID mapping, but not the MAC cross-layer support, are also considered on the same topology and with the same settings. The cross layer support of MeshChord was not implemented since there is little difference in the overlay performance between MeshChord with and

without the cross layer mechanism as shown in paper [67]. In each of the simulation scenarios, 5000 lookups are generated; each from a MR to a random key following a uniform distribution and the results are averaged.

Table 5.2: NS-3 wireless simulation parameters

Radio Technology	802.11b (Ad-hoc)
Peak Data Rate	11Mbps
Rate control algorithm	AARF-CD
Channels Sharing	CSMA/CA
Slot time	9μs
SIFS	16 μs
CTS Timeout	75 μs
ACK Timeout	75 μs
Antenna Type	Omni Antenna
Wireless transmission range	150m

The performance of WILCO is compared with that of the original Chord and MeshChord in terms of both lookup efficiency and message overhead efficiency. In particular, the *lookup time*, *number of lookup messages* for lookup and *message overhead* are monitored. These are important parameters for evaluating the overlay performance and are commonly used in the literature. In addition, the *underlay hop count* and *stretch factor* are also investigated to show the location-awareness of the proposed scheme in comparison to the two alternative schemes. The descriptions of the performance measurement parameters are as follows.

- *Underlay hop count*: average number of hops a lookup traverses in the physical topology.
- *Lookup time*: average amount of time for a lookup request to be resolved.
- *Number of lookup messages for each lookup*: average number of fingers a lookup traverses to reach its destination.
- *Stretch factor*: the ratio between the hop count the lookup traverses on the overlay (through intermediate fingers) and the actual physical hop count between the MR source and destination. This metric evaluates the location-awareness of the proposed scheme and is adopted from [64]-[67].
- *Message overhead*: is the packet rate received at each MR to maintain the overlay and to resolve the lookups.

5.5.2 Lookup Efficiency
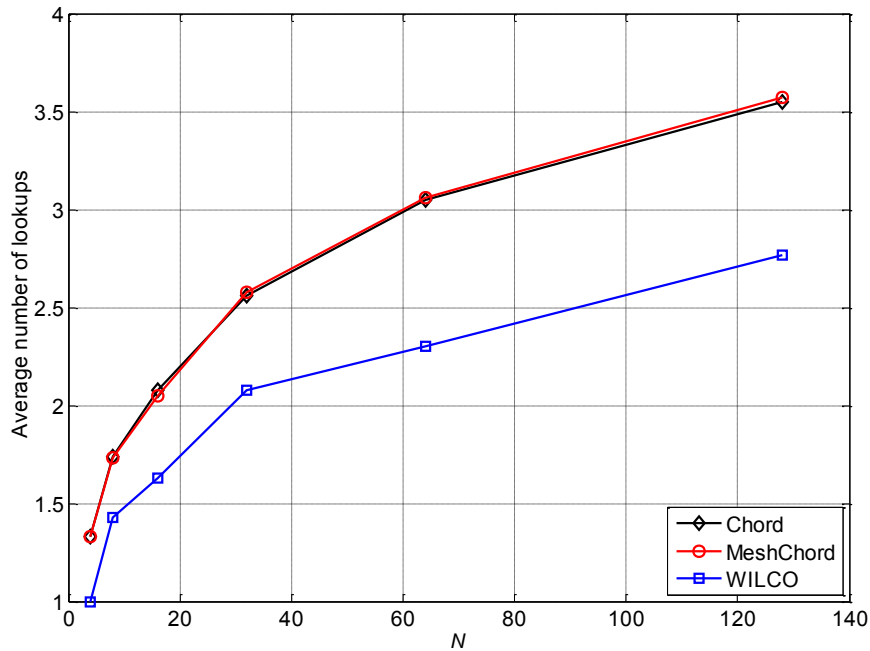
Figure 5.4: Average number of lookup messages versus the number of MRs (*N*)

The lookup efficiency of WILCO is first examined. Figure 5.4 shows the average number of lookup messages for each lookup with increasing number of MRs, when WILCO and the two compared schemes are employed, respectively. It is observed that both Chord and MeshChord require the same number of lookup messages on average to resolve a lookup. This is due to the fact that both of the two mentioned schemes use the Chord finger table, and as a result, the finger lookup behaviours are identical to each other.

Figure 5.4 also illustrates that WILCO, with the improved finger table, requires the least number of lookups among the three compared solutions and although this number increases logarithmically for all compared schemes, the rate of increase is the slowest for WILCO. According to the numerical result in Figure 5.4, it is shown that the proposed scheme consistently saves up to 22% of the number of lookup messages in comparison with Chord and MeshChord for all of the testing scenarios. This trend is similar with that resulted from theoretical analysis. In Section 5.4, it is shown that the maximum number of lookup messages to resolve a lookup when using WILCO with its

modified finger table is $\log_4(N)$; hence, the average number of lookup messages should increase with $\log_4(N)$. In contrast, the number of lookup messages exchanged by Chord should increase with $\log_2(N)$, following the same argument.
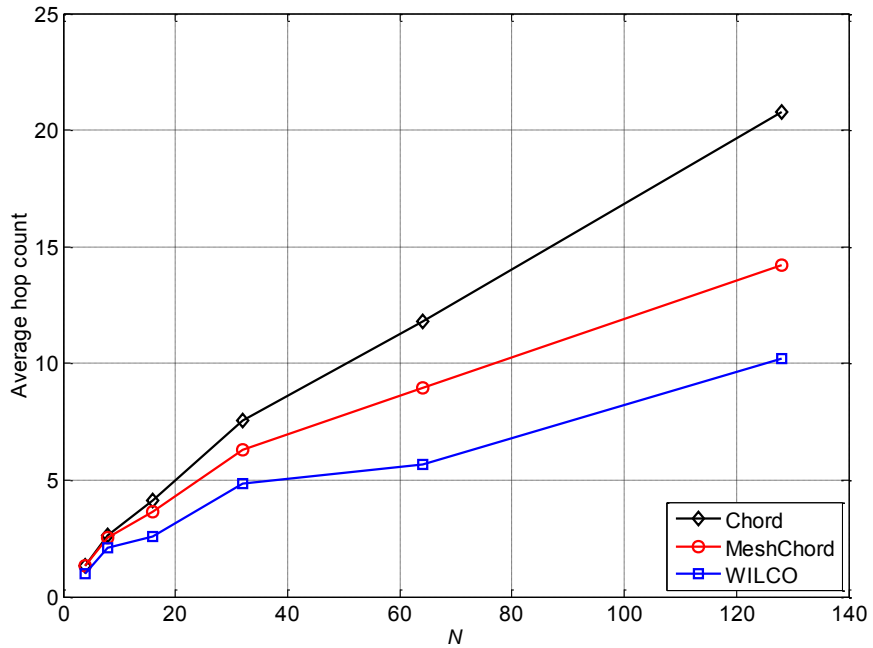
Figure 5.5: Average hop count versus the number of MRs (N)
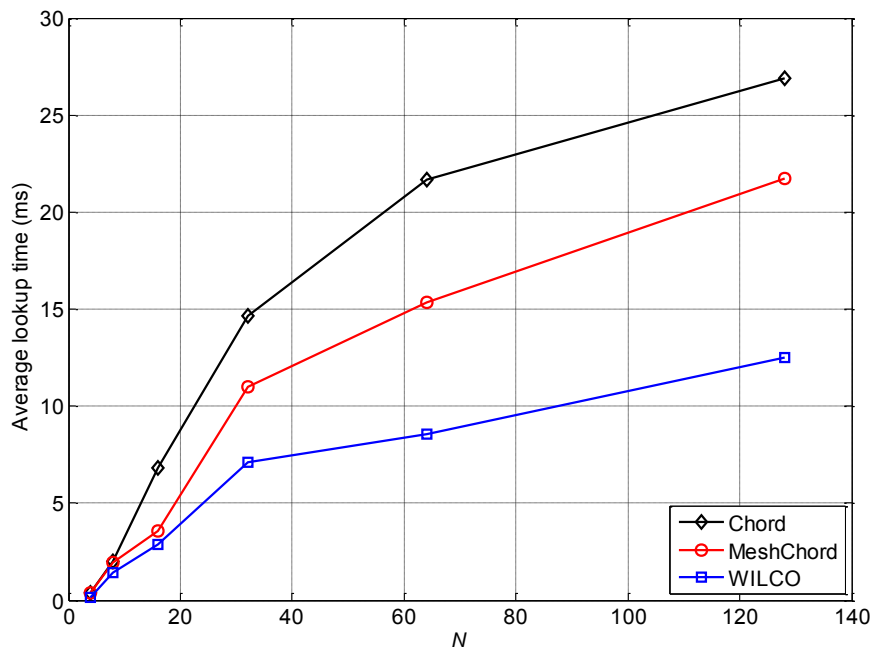
Figure 5.6: Average lookup time versus the number of MRs (N)

Table 5.3: Numerical comparison of Chord, MeshChord and WILCO for *N*=128.

		WILCO	MeshChord	Chord
Lookup efficiency	**Number of Lookup messages**	2.77	3.57	3.55
	Improvement of WILCO	-	22.31%	21.90%
	Hop count	10.19	14.23	20.80
	Improvement of WILCO	-	28.40%	51.01%
	Lookup time (ms)	12.50	21.76	26.89
	Improvement of WILCO	-	42.57%	53.51%
	Stretch factor	1.96	3.52	5.21
	Improvement of WILCO	-	44.42%	62.41%
Message overheads	**Average overhead (pk/s)**	30.01	35.98	63.52
	Improvement of WILCO	-	16.58%	52.74%
	90-percentile overhead (pk/s)	51.16	52.56	94.87
	Improvement of WILCO	-	2.66%	46.07%

Figure 5.5 compares the average undelay hop count of Chord, MeshChord and WILCO. It is observed that for all network sizes, both the average hop count and its rate of increase are the highest for Chord, MeshChord comes second and the proposed WILCO is the most efficient scheme in this category. In particular, whenever *N* is doubled, the underlay hop count of Chord increases approximately 2 times, while that of MeshChord increases approximately 1.5 times. The underlay hopcount for WILCO only doubles every time *N* increases by 4. Since both MeshChord and WILCO are location-aware, this figure implies that geographical ID assignment plays a central role in reducing the number of underlay hops and hence, improves the lookup efficiency. However, since WILCO requires a lower number of hops to resolve a lookup, this result suggests that its multi-level location-aware ID mapping is better than the geographical ID mapping of MeshChord, especially for large WMNs. Figure 5.5 illustrates that WILCO can reduce by 50% the number of underlay hops as compared to Chord and roughly by 30% as compared to MeshChord. This result is confirmed by Figure 5.6 where WILCO outperforms Chord by approximately 50% and MeshChord by approximately 40% respectively in terms of lookup time.

Figure 5.7 compares the stretch factor of the three schemes with the increase in *N*.

The graph has $\log(N)$ on the x axis. This figure illustrates that the stretch factor of Chord increases linearly with $\log(N)$, showing that the number of hops a lookup traverses on the underlay increases with the network size. Hence, on a large WMN, communication over the overlay is very inefficient and introduces a significant overhead. The stretch factor for MeshChord also increases linearly with $\log(N)$, confirming the result of the proof presented in [67] with the stretch factor of $O\left(\sqrt{N \log N}\right)$. However, the increase rate of the stretch factor of MeshChord is noticeably lower than that of Chord, which confirms the analysis presented previously that location ID assignment can significantly improve overlay communications.
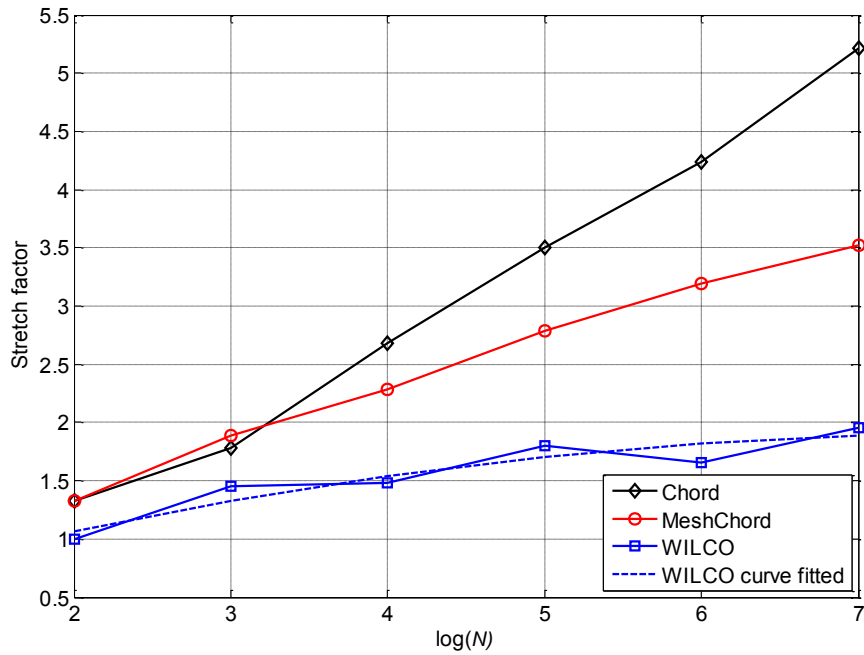
Figure 5.7: Stretch factor versus log(*N*)

Following MeshChord geographical ID assignment which zigzags across the network row by row as shown in section 3.1.2, it is easy to see that lookup messages also zigzag the network towards theirs destinations making the stretch factor increase with the size of the network and hence not being very efficient. Table 5.3 shows that the stretch factor of WILCO is significantly lower than the two schemes it is compared against with only 1.96 for a network size of 128 MRs (roughly 60% lower than Chord and 40% lower

than MeshChord). Moreover, the curve fitted representation in this figure illustrates the trend of the WILCO stretch factor towards saturation. This result confirms the $O(1)$ stretch factor which is proved earlier in Theorem 2. This efficient stretch factor of WILCO comes from the proposed multi-level ID assignment and the use of the modified finger table which narrows down the search to a quarter of the network for each intermediate lookup. These results illustrate that the proposed location-aware ID assignment and modified finger table reflect the physical topology accurately, i.e., communications on the overlay should be as efficient as the communication between the same MRs on the physical topology.

5.5.3 Overhead Efficiency

The overall overhead efficiency of the three schemes considered is studied first by measuring the average message overhead, illustrated in Figure 5.8. It is observed that WILCO introduces the lowest message overhead, significantly lower than Chord and noticeably lower than MeshChord. This result shows that the random ID assignment of Chord is not efficient since overlay maintenance and lookup messages have to travel across the entire network to reach its successor, predecessor or finger peers. This results in a massive message exchange and the situation gets substantially worse with the increase in network size. On the other hand, a systematic planned ID assignment such as that of MeshChord and especially WILCO restricts geographically overlay messaging and hence, significantly reduces the network overhead. For a reasonably large WMN of 128 MRs as shown in Table 5.3, the message overhead of WILCO is approximately 50% and 20% lower than those of Chord and MeshChord, respectively. Consequently, among the three schemes, WILCO is the most scalable, especially for large-scale WMN.

The 90-percentile messaging overhead is examined next in Figure 5.9, in order to evaluate the load balance of the three schemes. The Chord value is almost two times higher than those of WILCO and MeshChord. This result illustrates that in the worst-case scenario, 90% of the MRs in Chord must withstand a double message overhead in comparison with MeshChord and WILCO, and hence, Chord provides not only the highest overhead, but also the poorest load balance. A highly unbalanced network overhead results in more chance of collisions and congestions which make the network

unstable. Compared to MeshChord, the 90-percentile of WILCO is always lower, but not by a large margin. For a WMN of 128 MRs as shown in Table 5.3, the improvement is roughly 3%. Perhaps MeshChord already provides good load balancing and the multi-level ID assignment of WILCO can further improve this by a small amount only.
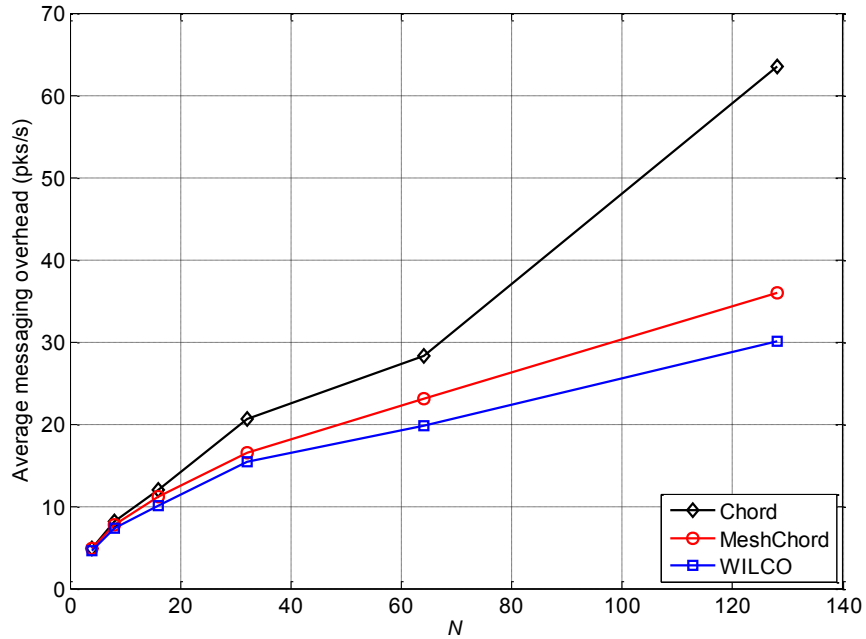
Figure 5.8: Message overhead versus the number of MRs (*N*)
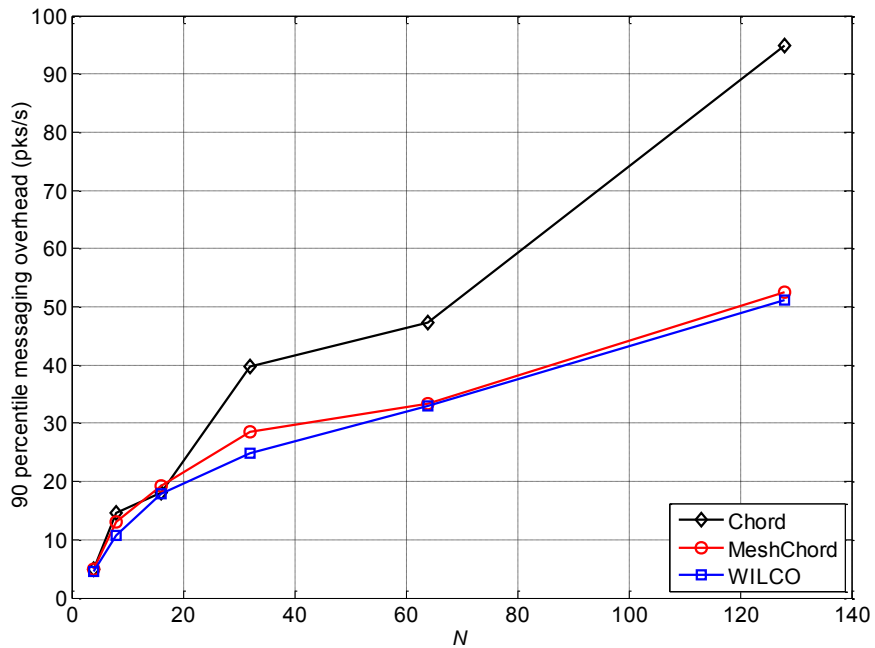
Figure 5.9: 90-percentile overhead versus the number of MRs (*N*)

5.6 Discussion
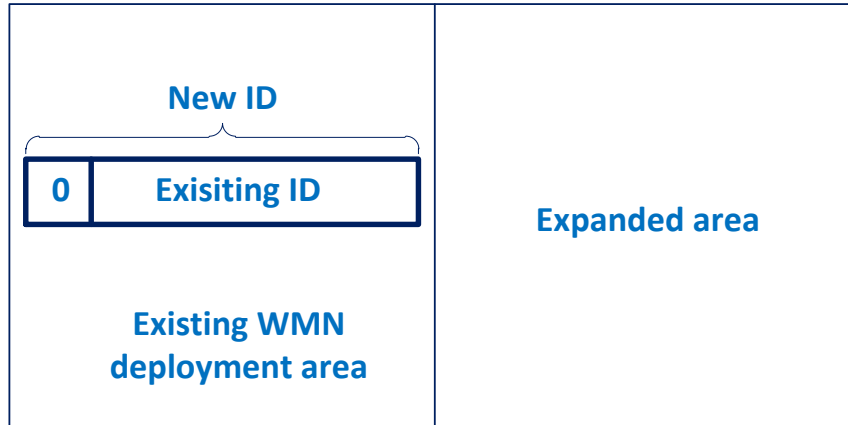
Figure 5.10: WILCO deployment area expanding

The analytical and simulation results show how a location-aware ID assignment improves the overlay lookup efficiency in terms of average hop count on the underlay and lookup time. Depending on the location-aware indexing scheme, the overlay routing (finger table) has to be tweaked accordingly and an appropriate enhancement of the finger table could greatly improve the overlay communication. For example, in the case of WILCO, a stretch factor of $O(1)$ can be obtained. Furthermore, an appropriate location-aware overlay is also the key to a lightweight peer-to-peer protocol on WMN that can support many services without greatly affecting the overall network performance.

It is observed that the hierarchical addressing scheme used in WILCO presents advantages over MeshChord in terms of rescaling of existing networks. A geographical ID assignment like that of MeshChord is based on a predetermined fixed size of the deployment area. Consequently, such a scheme is not flexible, especially when the network needs to be expanded beyond the previous planned boundary (which may happen quite often in reality). In such case, the whole network has to be re-planned and all MRs have to be reassigned with new IDs. As the network gets bigger, the task is more and more complicated which makes it impractical. On the other hand, the proposed multi-level ID assignment of WILCO is modular as the allocation of two areas at the same level only differs from each other in their prefixes. Figure 5.10 shows an illustrative example when the network size is doubled.

In this case, the existing MRs only need to add a prefix bit to their current IDs without the need of redo the ID mapping procedure. This demonstrates how the proposed multi-level location-aware ID assignment is scalable and is suitable for real WMN deployment.

5.7 Chapter Summary

This chapter proposed WILCO, a location-aware ID mapping scheme and an improved finger table for building a Chord-based overlay on grid-like WMNs. The proposed scheme exploits the location information of MRs to build up an overlay in which neighbouring MRs in the physical topology are also closely located in the overlay. The simulation results show how WILCO significantly improves lookup efficiency in terms of lookup time, number of lookup messages and stretch factor (up to 50% and 40% in comparison with Chord and MeshChord respectively). It also noticeably reduces the overlay overhead (up to 50% and 20% in comparison with Chord and MeshChord, respectively). With a location-aware overlay scheme that is well-suited for WMN, the next chapters will focus on proposing algorithms to efficiently make use of location-awareness to improve service quality, especially for P2P VoD services.

CHAPTER 6: WILCO Location-aware Video Segment Seeking Algorithms

Abstract

When using WMN in conjunction with peer-to-peer data transfer solutions, many innovative applications and services such as distributed storage, resource sharing and live video delivery can be deployed without any centralized administration. However, in order to achieve a good quality of service in wireless multi-hop environments, it is important that the associated peer-to-peer overlay is not only aware of the availability, but also of the location, of its peers and services. Focusing on the quality of video delivery, in this chapter, a WILCO-based novel video segment seeking algorithm is proposed to make use of WILCO multi-level area ID assignment to locate and retrieve requested video segments from the nearest peers in order to improve video quality. An improvement of WILCO segment seeking algorithm, WILCO+ is also proposed to mitigate WILCO suboptimal selections by using a coordinate-based segment seeking algorithm. An analysis framework is proposed to show the superiority of WILCO and WILCO+ in terms of content retrieval efficiency. Simulation results show how the proposed WILCO and WILCO+ outperform existing state-of-the-art solutions in terms of video quality in different network scenarios, background loads and number of segment replicas.

6.1 Introduction

One of the important characteristics of an overlay network is that they are constructed independently from the underlay network topology. This is not a serious problem when deploying over wired networks with rich bandwidth and reliable connections. However, when the overlay network is implemented on top of a wireless multi-hop network, this independence becomes a significant disadvantage. In particular, in wireless multi-hop networks, a large number of intermediate hops between two peers could greatly reduce the content retrieval quality. As a result, how to select the best overlay peer to get the content from in order to improve the content delivery is an important question to be researched.

As discussed in chapter 4, in P2P VoD, there may be many users watching the same video at the same time, but at different points in the video stream. Hence, the same segment of the video may be simultaneously available at several places in the network. In this context, downloading the video segment from the geographically closest peer (in terms of hop count) promising to greatly improve quality of the retrieved video. This observation is especially true for wireless multi-hop networks such as WMN since it is well-known that the achievable bandwidth degrades sharply with an increasing number of hops between the source and destination peers. Motivated by this observation, a WILCO-based novel geographical location-aware video segment seeking algorithm is proposed for peers to get requested segments from the geographically closest peer for improved video quality retrieval. In addition, WILCO+, an improvement of WILCO location-aware video segment seeking algorithm is proposed to improve WILCO location-awareness by mitigating WILCO suboptimal geographical selections. A data retrieval efficiency analysis and comparison is provided to illustrate the benefit of WILCO algorithms. The simulation results in different scenarios also confirm that WILCO location-aware algorithms significantly improve the video retrieval quality in terms of PSNR and packet loss in comparison with an existing state-of-the-art distributed approach and a centralized server-based solution.

6.2 WILCO Geographical Location-aware Video Segment Seeking Algorithm

The aim of WILCO location-aware video segment seeking algorithm is to improve the overlay video retrieval quality by enabling overlay peers to select the best peer in terms of hop count from which to retrieve the requested video segment.

Let r be the ID of the requesting peer and $D = \{d_j, j = 1, ..., k\}$ be the set of destination peers that store the requested video segment, where d_j is the ID of the destination peer j. The principle behind WILCO segment seeking algorithm is based on its multi-level location-aware ID assignment. WILCO location-aware segment seeking algorithm includes three steps to select the closest peer in terms of hop count.

Step 1 – Coarse selection
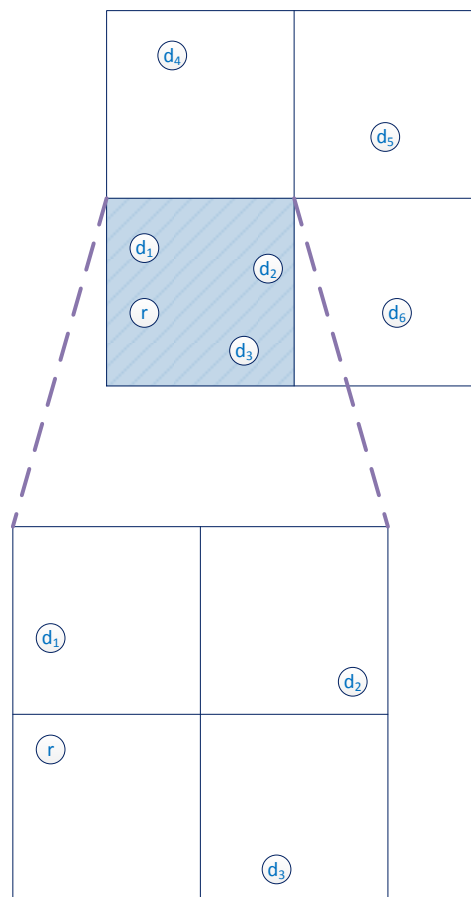
Figure 6.1: Step 1 of WILCO segment seeking algorithm - Coarse selection.

The goal of the first step is to refine the set of destination peers D to a smaller set, namely the coarse destination set, D_{coarse}. Using the WILCO multi-level ID assignment, the requesting peer selects all of the destination peers which share with it the same lowest level area. According to Chapter 5, two MRs with IDs p and k share the same area at level i if equation (6.1) is satisfied:

$$\left\lfloor \frac{p}{N_i} \right\rfloor = \left\lfloor \frac{k}{N_i} \right\rfloor \tag{6.1}$$

Where $N_i = 4^{\frac{m}{2}-i}$ is the number of MRs in the level i area (m is the number of bits used for the WILCO ID assignment).

Algorithm 6.1: Coarse selection step

Compute $i_{max} = \max \left\{ i: \left\lfloor \frac{d_j}{N_i} \right\rfloor = \left\lfloor \frac{r}{N_i} \right\rfloor, j = 1, ..., k \right\}$

$D_{coarse} = \{\emptyset\}$

$N_{i_{max}} = 4^{\frac{m}{2}-i_{max}}$

for $j = 1$ to k

    if $\left(\left\lfloor \frac{d_j}{N_{i_{max}}} \right\rfloor == \left\lfloor \frac{r}{N_{i_{max}}} \right\rfloor \right)$

        $D_{coarse} = D_{coarse}.\text{append}\{d_j\}$

    end if

end for

By using equation (6.1), WILCO IDs of all destination peers in D are checked to find all of the destination peers which share the lowest level area i_{max} with the requesting peer r. Algorithm 6.1 presents in details the pseudo-code of this coarse selection step.

Figure 6.1 illustrates an instantiation of the application of this coarse selection step. As illustrated in this figure, there are six destination peers $D = \{d_1, d_2, ..., d_6\}$ available in the network with the requested video segment. Using the WILCO multi-level area division, it is shown that among the six destination peers, only d_1, d_2, d_3 share the lowest level area (smallest area) with the requesting peer r. The coarse destination peer set in this case is $D_{coarse} = \{d_1, d_2, d_3\}$.

Step 2 – Fine selection

The goal of this second step is to further reduce the coarse destination set D_{coarse} into a smaller set, namely fine destination set, D_{fine}. Different from step 1, in this step, the selection is between the destination peers that share the same lowest level area. After the completion first step described above, if there is only one destination peer left in D_{coarse}, r chooses this peer to retrieve the video segment from, otherwise the algorithm continues with the second step. In the second step, the requesting peer assigns costs to all destination peers in the coarse destination set, D_{coarse}. These costs are calculated based on the relative distance between the area at level $(i_{max} + 1)$ which contains the requesting peer and each of the destination peers.

This step consists of $(m/2 - i_{max} - 1)$ iterations. In each iteration, the area at level t ($t \in [i_{max} + 1, m/2 - 1]$), in which destination d_j resides is divided into two regions. These two regions are anotated as the "*near*" and the "*far*" regions. The *near* and *far* regions are named with respect to the position of the area at level $(i_{max} + 1)$ in which r resides. Figure 6.2 illustrates the first division step following the example in Figure 6.1. If a destination peer d_j in d_{coarse} is in the far region, a cost of $2^{\frac{m}{2}-t}$ is added to the cost associated with d_j.
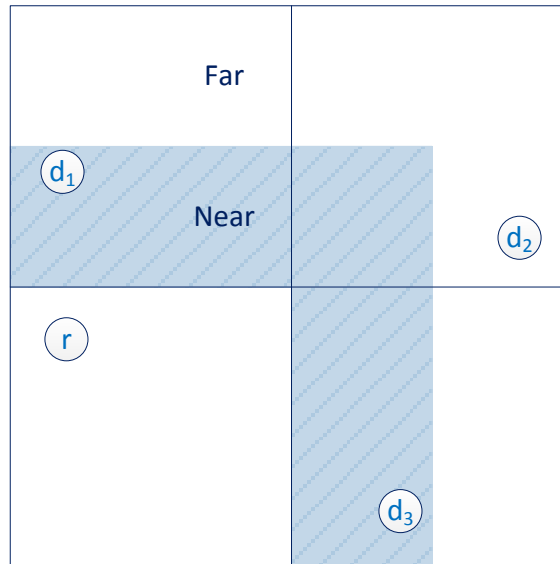
Figure 6.2: Step 2 of WILCO segment seeking algorithm - Fine selection

The cost of $2^{\frac{m}{2}-t}$ is used in each step so that the early divisions contribute more to the accumulated cost than latter division. This cost calculation comes from the observation that the early divisions cover more physical area than the later divisions. As a result, a destination peer which resides in the *far* region in the first division is farther from the requesting peer than the furthest destination peer in the *near* region and hence, it should have a higher cost.

Based on the resulting accumulated costs, r selects the destination peers with the lowest accumulated costs. These destination peers are kept in the fine destination set D_{fine}. This fine destination set forms a collar of minimum distance around the level $(i_{max} + 1)$ area containing r similar to the illustration in Figure 6.3. Algorithm 6.2 describes the fine selection step in details with three main parts: calculating the cost associated with each peers in D_{coarse}, finding the lowest cost and adding all peers with the lowest cost into D_{fine}.

An illustrative example is shown in Figure 6.2 and Figure 6.3 which follows Figure 6.1. In this figure, destination peer d_1 and d_3 have the lowest cost and therefore, are retained in the fine destination set d_{fine}.

Algorithm 6.2: Fine selection step
// Calculate the cost associated with each $d_j \in D_{coarse}$
for each $d_j \in D_{coarse}$
for $t = i_{max} + 1$ to $m/2 - 1$
divide level t area containing d_j into near and far regions with respect to level i_{max} containing r
if $d_j \in$ far region
$cost_{d_j} = cost_{d_j} + 2^{\frac{m}{2}-t}$
end if
end for
end for
// Find the lowest cost
Compute $cost_{min} = \min\left\{cost_{d_j}, d_j \in D_{coarse}\right\}$
// Select all peers with cost $==$ lowest cost into D_{fine}
$D_{fine} = \{\emptyset\}$
for each $d_j \in d_{coarse}$
if $cost_{d_j} == cost_{min}$
$D_{fine} = D_{fine}.\text{append}\{d_j\}$
end if
end for

Step 3: Tie break

The goal of this step is to finalize the selection to a single destination peer to retrieve the requested video segment from.

If there are more than one destination peers in d_{fine}, the algorithm continues with the tie break step.

In this step, the $(i_{max} + 1)$ level area containing r is divided into 4 equal level $(i_{max} + 2)$ subareas and depending on which area r resides in, r prefers to select the destination peer which is adjacent to the requesting peer's subarea as illustrated by the arrows in Figure 6.3. If there is more than one peer after this selection, the requesting peer will select the destination peer closest to it in the ID space. WILCO's tie break step is described in details in Algorithm 6.3 including the selection based on adjacent area and the selection based on closest peer in the ID space.

Figure 6.3 also shows an illustrative example, which follows Figure 6.1 and Figure 6.2, of this final step selection in the WILCO segment seeking algorithm where destination peer d_1 is chosen to download the video segment from, since its area is adjacent to the requesting peer sub-area.
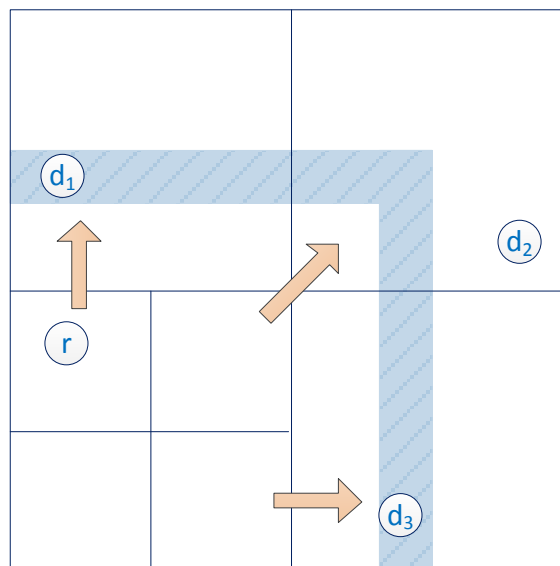
Figure 6.3: Step 3 of WILCO segment seeking algorithm - Tie break.

Algorithm 6.3: Tie break step

// Select base on adjacent area

if $\left(\left\lfloor\dfrac{r}{N_{i_{max}+1}}\right\rfloor \bmod 4\right) \neq \left(\left\lfloor\dfrac{r}{N_{i_{max}+2}}\right\rfloor \bmod 4\right)$

$\quad D_{tb} = \left\{d_j \in D_{fine}: \left(\left\lfloor\dfrac{d_j}{N_{i_{max}+1}}\right\rfloor \bmod 4\right) = \left(\left\lfloor\dfrac{r}{N_{i_{max}+2}}\right\rfloor \bmod 4\right)\right\}$

else

$\quad D_{tb} = D_{fine}$

end if

// Select base on closest peer in the ID space

if $size(D_{tb}) > 1$

$\quad destination\ peer = \left\{d_j \in D_{tb}: \left|r - d_j\right| = \min_j\{\left|r - d_j\right|\}\right\}$

else

$\quad destination\ peer = D_{tb}$

end if

6.3 WILCO+ Coordinate-based Location-aware Video Segment Seeking Algorithm

6.3.1 WILCO Suboptimal Selections
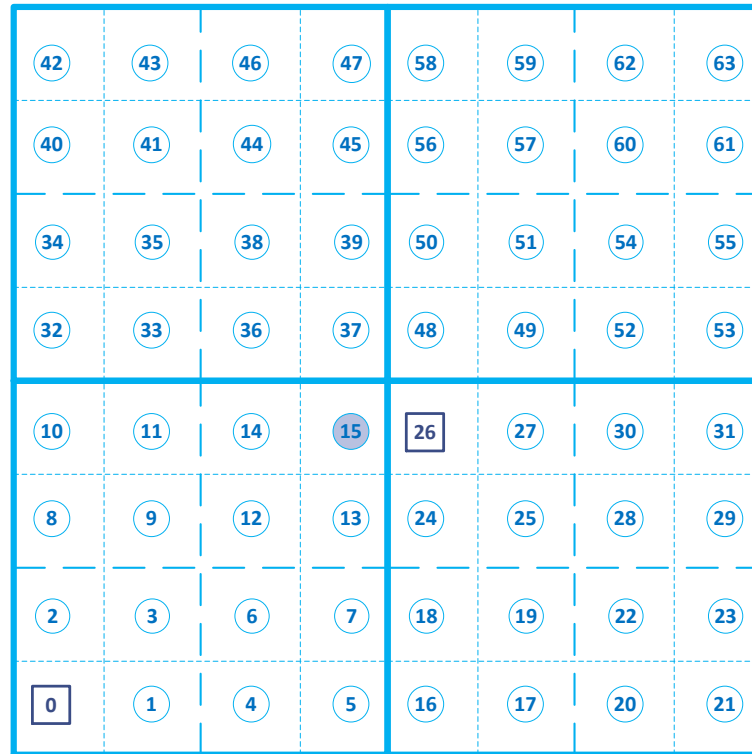
Figure 6.4: WILCO location-aware segment seeking suboptimal scenario.

Figure 6.4 illustrates a WILCO location-aware indexing for a topology of 64 MRs. Since WILCO location-aware segment seeking algorithm is based on the WILCO multi-level area border, as formulated by equation (6.1), suboptimal selection may happen. For instance, consider a network layout as in Figure 6.4, the requesting peer r is located at node 15 (the shaded node) and the two destination peers reside at node 0 and node 26 (the square nodes). In this scenario, using the WILCO segment seeking algorithm, the requesting peer would select node 0 as its best peer to download the video segment since node 15 and 0 share the same lower level area (as with step 1 of 6.3). This selection is suboptimal as it is clear from Figure 6.4 that node 26 is actually the closest peer in terms of hop count to r. This suboptimal selection results from the WILCO area border selection in WILCO step 1 using equation (6.1) and may be severe if the network size is large or when the segments are randomly distributed. For instance, in the example in Figure 6.4, instead of getting the content from the adjacent peer, the requesting peer selects the peer four physical hops away which would significantly reduce the retrieval quality. This suboptimal selection could also greatly affect other network traffic as the video streaming traffic is carried across the network via a longer path, competing for network resources with other network flows.

WILCO+ is proposed to overcome WILCO border area effect using a different approach based on WILCO location-aware ID mapping scheme. By extracting the location coordinate information from the MRs' ID, the requesting peer can calculate the distance in terms of hop count using Euclidean distance. Upon comparing this distance, the closest destination peer can be accurately determined regardless of whether they reside in the same level area or not.

6.3.2 WILCO+ Coordinate-based Location-aware Video Seeking Algorithm

In contrast to the WILCO location-aware segment seeking algorithm, the WILCO+ segment seeking algorithm first extracts the coordinate information of the requesting and the destination peer based on WILCO location-aware ID assignment by using the peer overlay IDs.

111

Recall the WILCO location-aware ID mapping introduced in Chapter 5. In the WILCO ID mapping, each step consecutively assigns two bits to the MRs IDs. The division on y axis decides the first bit and the division on the x axis decides the second bit. As a result, the odd bits from the WILCO ID represent the y coordinate while the even bits represent the x coordinate of the MR in the network topology. In order to determine the Euclidean distance between the requesting peer r and a destination peer j, the Pythagorean Theorem can be applied using these coordinate information as in equation (6.2)

$$distance^2 = \left(x_r - x_j\right)^2 + \left(y_r - y_j\right)^2 \qquad (6.2)$$

Where x_r, x_j and y_r, y_j are the x and y coordinates extracted from the IDs of the two MRs.

In the WILCO ID assignment, since each lowest level area contains only one MR, this distance indicates the number of hops between the two peers. As a result, using only the WILCO overlay IDs, the requesting peer can easily find the closest destination peer to get the video segment from by performing a new algorithm denoted as WILCO+ segment seeking algorithm. This WILCO+ segment seeking algorithm is described in Algorithm 6.4.

Algorithm 6.4: WILCO+ coordinate-based location-aware video segment seeking

x_r = even bits extracting from the ID of the requesting peer.
y_r = odd bits extracting from the ID of the requesting peer.
x_j = even bits extracting from the ID of each of the destination peers, $j = 1, \dots, k$.
y_j = odd bits extracting from the ID of each of the destination peers, $j = 1, \dots, k$.
for each d_j
$\qquad distance_j = sqrt\left(\left(x_r - x_j\right)^2 + \left(y_r - y_j\right)^2\right)$
end for
$d_{min} = \{d_j : distance_j = \min\{distance_j, j = 1, \dots, k\}\}$

In comparison with the three-step WILCO segment seeking algorithm, WILCO+ uses only one step to determine the best destination peer and therefore is simpler. In addition, WILCO+ is also more accurate. As described earlier, the multi-level area border effect can affect the WILCO segment seeking resulting in suboptimal selection by

referring the destination peer to a node in the same area instead of choosing the closest destination peer which may reside in a different area. On the other hand, the WILCO+ segment seeking algorithm is based on coordination extraction from the IDs of MRs which resolves the suboptimal problem in WILCO segment seeking and promises a better retrieval video performance.

6.4 Overlay Content Retrieval Efficiency

Consider a WMN of N MRs using WILCO location-aware ID mapping. Assume that the number of replicas of a video segment is n and these replicas are uniformly distributed over the network.

This section analyses and compares the overlay content retrieval efficiency of a non-location-aware approach, of the WILCO location-aware segment seeking algorithm and of the WILCO+ coordinate-based location-aware seeking algorithm.

6.4.1 Non-location-aware Peer Selection Approach.

In this approach, since the requesting peer has no reference on which peer is better, it can randomly choose any destination peer to retrieve the video segment from or select the destination peer in a round-robin fashion in order to evenly distribute the traffic load across the serving peers as in QUVoD [81].

Since the network size is N nodes, the network diameter is $\sqrt{N}$ hops. As the destination peer is picked randomly, the average distance between the requesting and destination peer is

$$d_{NLA} = O(\sqrt{N}) \tag{6.3}$$

It can be seen from this result that the number of segment replicas does not play a role in equation (6.3). As a result, even when number of replicas is high, i.e., there are more peers which store the requested video segment, the hop distance between the source and the destination peer is unlikely to reduce and hence, the data retrieval performance is unlikely to improve. Another important remark from studying equation (6.3) is that since

the number of segment replicas does not contribute to d_{NLA}, a non-location-aware overlay segment retrieval strategy should perform no better than the single server strategy where a single server is used.

6.4.2 WILCO Segment Seeking Location-awareness

Recall from chapter 5 that when using the WILCO location-aware ID assignment, the number of MRs in a level i area is $N_i = 4^{\frac{m}{2}-i}$ and the area diameter is $\sqrt{N_i} = 4^{\frac{1}{2}\left(\frac{m}{2}-i\right)}$ hops. The probability that there is at least one destination peer which has the requested segment residing in the same level i area with the requesting peer is expressed as in equation (6.4).

$$\Pr_i = 1 - (1 - P_s)^n = 1 - \left(1 - \frac{N_i}{N}\right)^n \tag{6.4}$$

where $P_s = \frac{N_i}{N}$ is the probability that the destination peer which has the requested segment resides in the same level i area with the requesting peer if there is only one segment available in the network.

Let X_i's be the areas at level i's that both the destination peer and the requesting peer reside in and x_i's are the corresponding area diameters. Since WILCO segment seeking algorithm prefers the destination peer which share the lowest level area with the requesting peer, the hop distance between the requesting peer and the destination peer according to the WILCO algorithm is presented in equation (6.5)

$$d_{WILCO} = \min\{x_i\} \tag{6.5}$$

As illustrated in equation (6.4), when the number of segment replicas increases, the probability that both the destination peer and the requesting peer resides in the same level i area increases. By applying Bernoulli's inequality to the left side of equation (6.4), an upper bound of this probability is achieved, as shown in equation (6.6):

Since

$$\left(1 - \frac{N_i}{N}\right)^n \geq 1 - \frac{nN_i}{N}$$

Hence,

$$\text{Pr}_i = 1 - \left(1 - \frac{N_i}{N}\right)^n \leq 1 - \left(1 - \frac{nN_i}{N}\right) = \frac{nN_i}{N} \tag{6.6}$$

As illustrated in equation (6.6), since $\left(1 - \frac{N_i}{N}\right)^n$ decreases with the increase of n, the probability Pr_i increases with the increase in the number of replicas. The Bernoulli's upper bound shows that the increase rate of this probability could be as good as linear relative to the number of segment replicas. As a result, WILCO is not only capable of finding the closest peer to retrieve the segment from, but also can make use of the segment replica number to improve its data retrieval efficiency.

6.4.3 WILCO+ Segment Seeking Location-awareness

Since the location-awareness of WILCO is affected by the WILCO multi-level area border effect, suboptimal selections may happen as discussed before. WILCO+ is designed to overcome this limitation. By extracting the location coordinate information from the MR IDs, the accurate distance in terms of hop count can be determined as in equation (6.2). When considering this distance, the closest destination peer can be accurately determined.

Let $distance_j$ ($k = 1, ..., n$) be the hop distance from the requesting peer to each of the destination peers. Using WILCO+, the hop distance between the requesting peer and the selected peer is expressed as in equation (6.7)

$$d_{WILCO+} = \min\{distance_j, j = 1, ..., n\} \tag{6.7}$$

The comparisons of WILCO+, WILCO and the non-location-aware approaches in terms of data retrieval efficiency are summarized in Table 6.1. It is shown from this table that both WILCO and WILCO+ have superior data retrieval efficiency in terms of hop count in comparison with a non-location-aware approach. Moreover, while the number of segment replicas n does not play any role in non-location-aware approach, the data retrieval efficiency of WILCO and WILCO+ improves with the increase of this number, effectively exploiting the benefits of a peer-to-peer approach.

Table 6.1: Overlay content retrieval efficiency comparison between WILCO+, WILCO and non-location-aware approaches.

	Data retrieval efficiency
	Hop distance between requesting and destination peer
WILCO+	Nearest destination peer: $d_{WILCO+} = \min\{distance_j, i = 1, \ldots, n\}$
WILCO	$d_{WILCO} = 4^{\frac{1}{2}\left(\frac{m}{2}-i\right)}$ hops with probability $\Pr_i = 1 - \left(1 - \frac{N_i}{N}\right)^n$ where: $2^m = N$, $N_i = 4^{\frac{m}{2}-i}$
Non-location-aware (e.g. QUVoD)	$d_{NLA} = O\left(\sqrt{N}\right)$ hops

6.5 Simulation Results

The performance of WILCO and WILCO+, the two proposed location-aware schemes is evaluated through detailed, packet-level simulations using Network Simulator NS-3 [88]. The simulated network topology follows the descriptions from Chapter 5, and consists of $N = 64$ MRs arranged in an 8x8 grid, with the distance between two adjacent MRs set to 100m. In the simulations, the detail wireless settings are the same as described in chapter 5, all MRs are equipped with IEEE 802.11b radios and OLSR is chosen as the routing protocol. The simulation scenario is illustrated in Figure 6.6.

In our simulations, real video trace files are used to simulate the retrieval of three video segments ($S = \{S_1, S_2, S_3\}$) by each of the overlay peers. The trace file is obtained from the MPEG-4 video clip *Akiyo* [89] with video bit rate of 341Kbps; is 10 seconds long and about 0.44MB in size. The video trace file includes details at the level of packet transmissions with streaming deadline. Figure 6.5 illustrates a video trace file after this conversion. In a trace file, each row denotes the information required to transmit a video frame. The first and second columns are the video frame number and frame type accordingly. The third and fourth columns are the number of bytes and the number of

packets needed for transmitting a video frame. The last column is the relative timing deadline from the streaming session starting time that the frame has to be transmitted in seconds, for instance, in Figure 6.5, the second frame has to be transmitted after 33ms from the starting time of the streaming session.

```
1      H      9717     10      0.008
2      P      4488     5       0.033
3      P      1719     2       0.066
4      P      1221     2       0.099
5      P      1249     2       0.132
6      P      1203     2       0.166
7      P      1058     2       0.199
8      P      1209     2       0.231
9      P      1254     2       0.267
10     P      1306     2       0.299
11     P      1177     2       0.330
12     P      1311     2       0.364
13     H      16192    16      0.396
14     P      1456     2       0.429
15     P      2131     3       0.462
16     P      1308     2       0.495
17     P      1926     2       0.529
18     P      2185     3       0.567
19     P      1424     2       0.595
20     P      1626     2       0.628
21     P      1470     2       0.661
```

Figure 6.5: A video trace file.

In order to simulate video streaming, an implementation of the EvalVid video streaming model [90] on NS-3 is used. In particular, whenever the streaming deadline of a frame is met (according to the last column), a number of User Datagram Protocol(UDP) packets as specified in the fourth column with the total number of bytes as specified in the third column are sent to the requested node. Since the size of a video frame may be large, the frame content can be divided into many packets. The size of each packet is restricted to 1000 bytes in order to accommodate the headers at network and data link layers without being further fragmented. Since each frame has a deadline when it should be transmitted, UDP is used and hence, dropped packets will not be resent. At the receiver, a receive trace file is built based on the received packets. Using the video trace file and the receive trace file, the quality of the streaming video is

117

calculated in terms of PSNR for each segment using equation (6.8) [47], which translates the effect of bit rate and packet loss to user perceived quality.

$$PSNR = 20 \log_{10} \left(\frac{Bitrate}{\sqrt{(EXP_{Thr} - CRT_{Thr})^2}} \right) \quad (6.8)$$

Where:

- $Bitrate$ is the average bit rate of the data stream transmitted.

- EXP_Thr is the average throughput expected to be obtained.

- CRT_Thr is the actual average measured throughput.

It is noticed that in the case where there are very good channel conditions and the video is streamed between very close peers (in terms of hop count), CRT_{Thr} is close or even equal to EXP_{Thr}. As a result, the calculated $PSNR$ is very high as the denominator of equation (6.8) is very close to 0. Instead of leaving the resulting $PSNR$ value very high for this case, this PSNR value is capped at 50dB. The reason for this is that when there is no packet loss and the packets arrived at the destination peer on time for video playback, there is no significant difference between the received video and the original one and a very high quality of the received video is used.

The video server is located at MR 51 (diamond node in Figure 6.6) and contains all the three video segments. Throughout our simulations, unless otherwise stated, the number of replicas for each video segment is three. Regarding the placement of the replica segments, two scenarios are considered. Each simulation is repeated 10 times and the results are averaged.

Scenario 1 represents content replication by a network operator. In this case, replicator servers are spread evenly throughout the network. For this scenario, video segments are partly available at MR 12 ($\{S_1, S_2\}$), 25 ($\{S_2, S_3\}$) and 38 ($\{S_3, S_1\}$) (square nodes in Figure 6.6). It is important to note that not all video segments are available at these positions.

Scenario 2 represents P2P content sharing via an overlay network where video segments are only stored in the user's storage. In this scenario, the placements of the segment replicas are randomly distributed across the network.
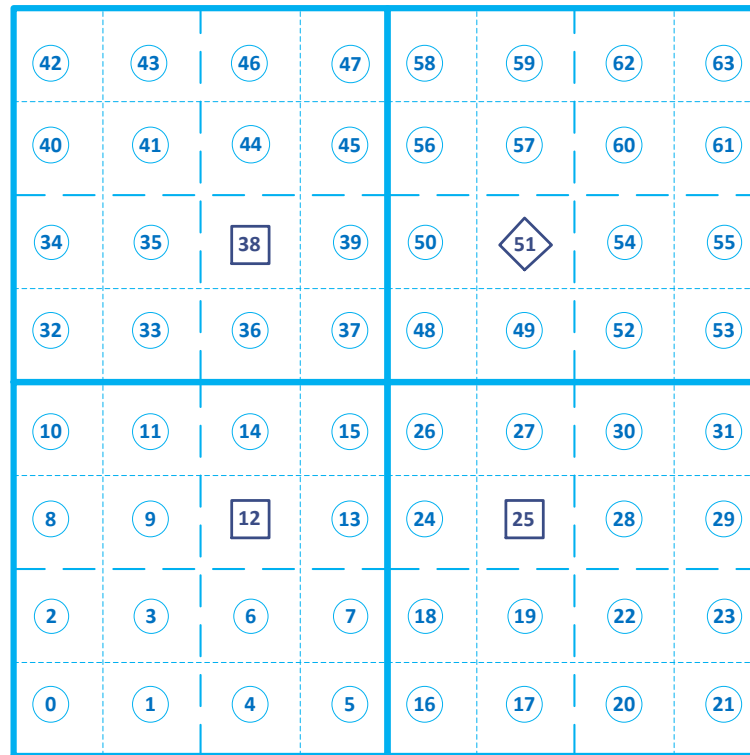
Figure 6.6: Simulation scenario

Video quality retrieval performance is then analyzed to show the benefit of the proposed location-aware video segment seeking schemes in terms of Peak Signal-to-Noise Ratio (PSNR), Mean Opinion Score (MOS) and packet loss. WILCO and WILCO+ will be compared against a server only solution (*Server*) in which the video segments are obtained from the server only; and the state of the art *QUVoD* [81] algorithm which obtains the video segments from the peers in a round robin manner and does not consider the location information of peers. Peak Signal-to-noise Ratio (PSNR), Mean Opinion Score (MOS) and packet loss of the four schemes are compared in the two segment placement scenarios (as mentioned above) with different background load and replication rates to show their overlay data retrieval performance and benefits.

6.5.1 Video Retrieval Performance with No Background Load

The performance of WILCO and WILCO+ is first analyzed with the segment placement as in Scenario 1 and with no background traffic.

Table 6.2: PSNR and packet loss comparisons

	PSNR (dB)		Average packet Loss(%)
	Average PSNR	**PSNR Variance**	
WILCO+	39.72 (+75%)	12.23 (-27%)	2.17 (-82%)
WILCO	39.22 (+72.78%)	13.15 (-21.07%)	2.38 (-79.85%)
QUVoD	25.64 (+12.95%)	17.31 (+3.9%)	8.38 (-29.04%)
Server	22.70	16.66	11.81

Table 6.3: PSNR to MOS mapping [48]

PSNR	MOS (Mean Opinion Score)	Value
>37	5 (excellent)	Imperceptible
31-37	4 (good)	Perceptible but not annoying
25-31	3 (fair)	Slightly annoying
20-25	2 (poor)	Annoying
<20	1 (bad)	Very Annoying

Table 6.2 shows the average PSNR and packet loss results when WILCO, WILCO+ and the other two schemes are employed in turn. Using *Server* as the baseline for comparison, the numbers in brackets show the improvement of the mentioned scheme from the baseline.

It is observed that WILCO and WILCO+ outperform both the two other schemes by a significant margin of more than 14dB in terms of average PSNR (72% improvement). Moreover, the PSNR variances of WILCO and WILCO+ are also the lowest among the four compared schemes with roughly 4dB difference (21% improvement). These results illustrate that the video quality delivered by WILCO and WILCO+ is not only the highest, but also the most consistent across the peers.

When applying pair-wise comparison between WILCO and WILCO+ results and those of the two other schemes based on a t-test, it can be said that there is a statistically significant difference in favor of WILCO and WILCO+ with confidence level of 99% in terms of PSNR. This improvement is achieved due to their ability to intelligently choose

the nearest peer to get the video segment from, greatly improving the throughput and reducing the packet loss, positively affecting user perceived quality.

Table 6.2 also shows that packet loss is the lowest in the case of WILCO and WILCO+, more than 5 times lower than the baseline and 3 times lower than that of QUVoD. As packet loss is one of the key factors that decide the received video quality level, this result confirms the PSNR-based evaluation and gives another view on the effectiveness of the proposed WILCO algorithms.
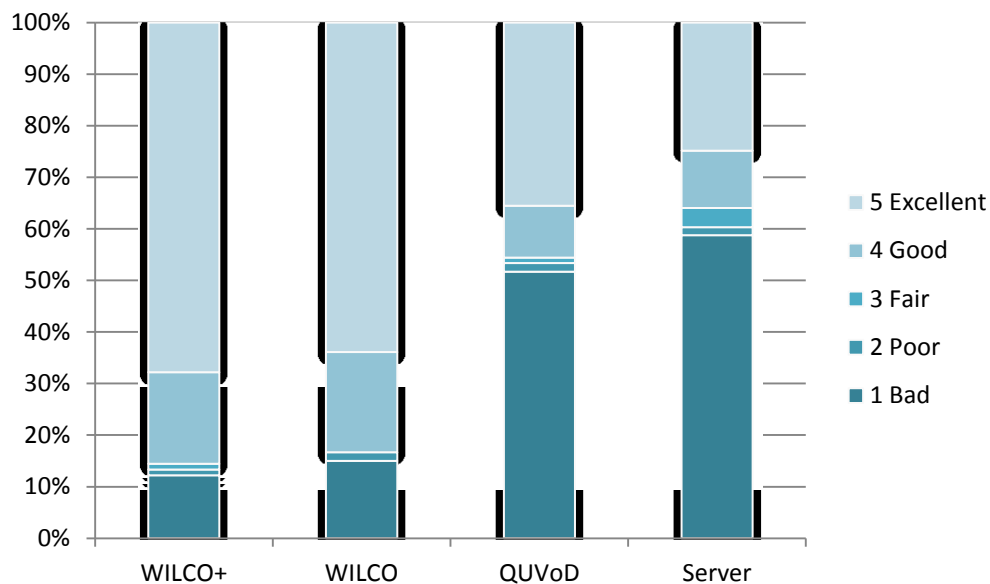
Figure 6.7: MOS distribution of WILCO and the two compared schemes.

The MOS distribution of the video streams of the four schemes is investigated to show the distribution of perceived video quality across different MOS levels. Perceived video quality levels are mapped from the PSNR results according to Table 6.3 which is recommended in [48]. Figure 6.7 demonstrates that the user perceived video quality level is the best when WILCO and WILCO+ are employed. This figure shows that 64% and 68% of the streaming sessions of WILCO and WILCO+ are of excellent quality, outperforming the two compared schemes by roughly 30%. In addition, while in the case of WILCO and WILCO+ only 15% and 12% of streaming sessions suffer from "bad" videos, this figure is more than 50% for the other two compared schemes. These numbers

clearly illustrate the inconsistency in video quality retrieval of the compared schemes versus WILCO and WILCO+.

In comparison to WILCO, as illustrated in Table 6.2, WILCO+ improves the video quality and packet loss by only a small margin. This small improvement is explained by the fact that in this scenario, the video segments are placed evenly across the network topology and it is rare to have a suboptimal selection of the overlay peer to retrieve the segment from. As a result, the video retrieval performance of both WILCO and WILCO+ are very similar. This difference is more pronounced in Scenario 2 in which the segment replica placements are randomly distributed across the network topology.

6.5.2 Video Retrieval Performance with Background Load

This section presents the performance evaluation of WILCO algorithms with different background traffic loads in both Scenario 1 and 2. Again, the video retrieval performance of WILCO and WILCO+ are compared against *QUVoD* and *Server*. In order to simulate background load, in each simulation, $n/4$ constant bit rate (CBR) UDP streams are generated between $n/2$ source and destination peers. The peers which generate the background traffic are randomly selected. The load of the background streams are varied from 0 (no load) to 50Kbps.

Figure 6.8 illustrates the PSNR performance of the four schemes. It is observed that throughout all the background load levels, WILCO+ and WILCO outperform the two compared schemes by a significant gap of at least 50%. This improvement is most pronounced when the background load is low to moderate ($\leq$30Kbps) where WILCO+ and WILCO improve the received video quality levels significantly with more than 10dB. According to Table 2.4, this difference in PSNR translates into two video quality levels on the MOS scale. When the background traffic is heavy, the PSNR performance of all schemes reduces rapidly and the video quality becomes very bad.
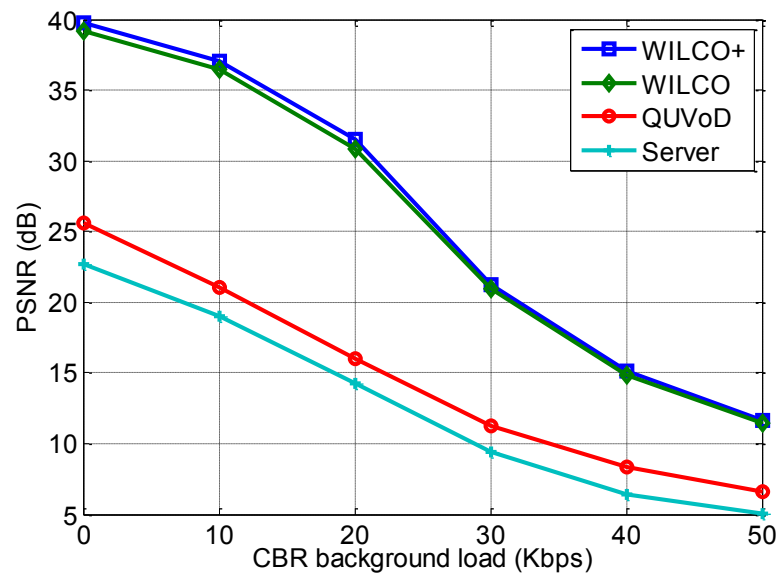
Figure 6.8: PSNR comparisons in Scenario 1 with different background loads
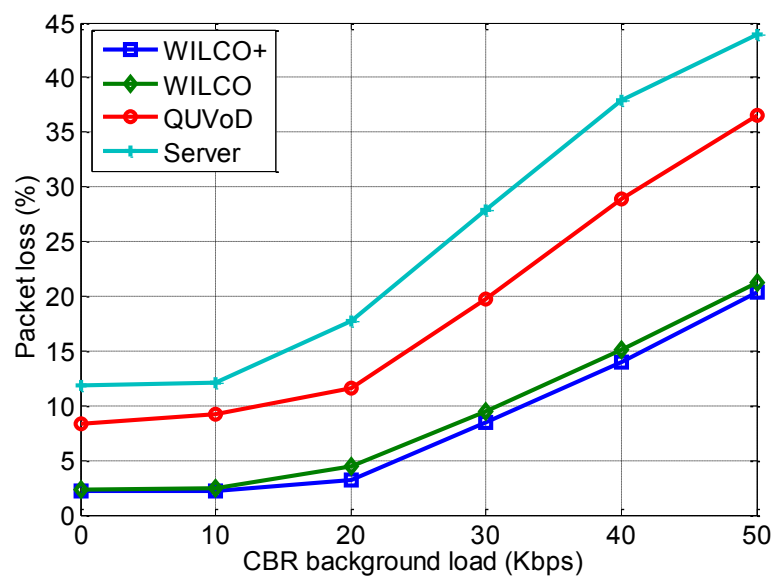
Figure 6.9: Packet loss comparisons in Scenario 1 with different background loads.

It is interesting to see that the difference between the QUVoD and *Server* approaches is not very substantial across all the background load levels. This remark clearly shows that an overlay over a wireless multi-hop network, cannot greatly improve the video delivery quality without the consideration of the underlay network topology such as location information. Figure 6.9 confirms this result, showing that WILCO significantly reduces the packet loss by at least 50% compared to the two other schemes.

In comparison with WILCO, WILCO+ is always better, but only by a very small margin of about 0.5dB in terms of PSNR. This is because with the regular segment placement as in Scenario 1, video segments are almost uniformly distributed geographically across the network and the multi-level area border suboptimal issue is not pronounced.

Table 6.4: PSNR comparison at 20Kbps background load.

	Scenario 1		Scenario 2	
	PSNR (dB)	**Improvement**	**PSNR (dB)**	**Improvement**
WILCO+	31.51	54.82%	25.23	42.72%
WILCO	30.82	53.81%	23.62	38.81%
QUVoD	15.96	10.83%	12.59	-6.34%
Server	14.23	N/A	14.45	N/A

The PSNR performance changes drastically when the video segments are distributed randomly (Scenario 2), as illustrated in Figure 6.10 and in Table 6.4. It is observed that the retrieved video quality reduces significantly for all the peer-to-peer schemes due to the suboptimal segment placement. However, WILCO+ and WILCO are able to retain a very high PSNR of over 30dB, greatly outperforming the other two schemes. The random segment placement clearly reveals the superiority of WILCO+ in comparison to WILCO, as it outperforms WILCO by roughly 2dB throughout the background loads. This is because the multi-level area border effect affecting WILCO's segment seeking which tends to prefer a more distant destination peer that resides in the same area to a closer peer but in a different area, as described in Section 6.4.1.

It is interesting to observe that according to Figure 6.10, QUVoD is inferior to *Server* when the video segments are randomly placed with light background load. When the background load is high, QUVoD becomes better than *Server*, but the achievable PSNR is already very low anyway. This result agrees with our data retrieval efficiency analysis performed in section 6.5 on wireless multi-hop network scenarios, which state that deploying P2P services "as is" without considering the physical topology is not better than using single server solution for all overlay peers.
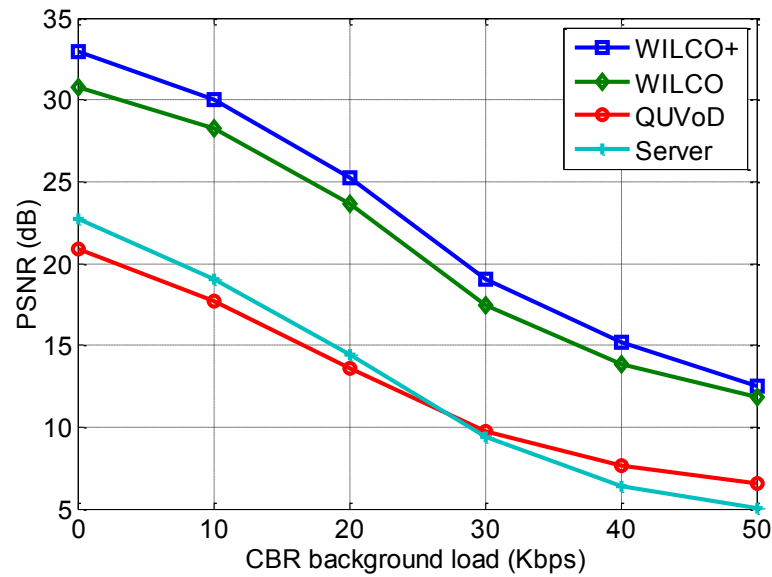
Figure 6.10: PSNR comparison in Scenario 2 with random segment placement at different background loads
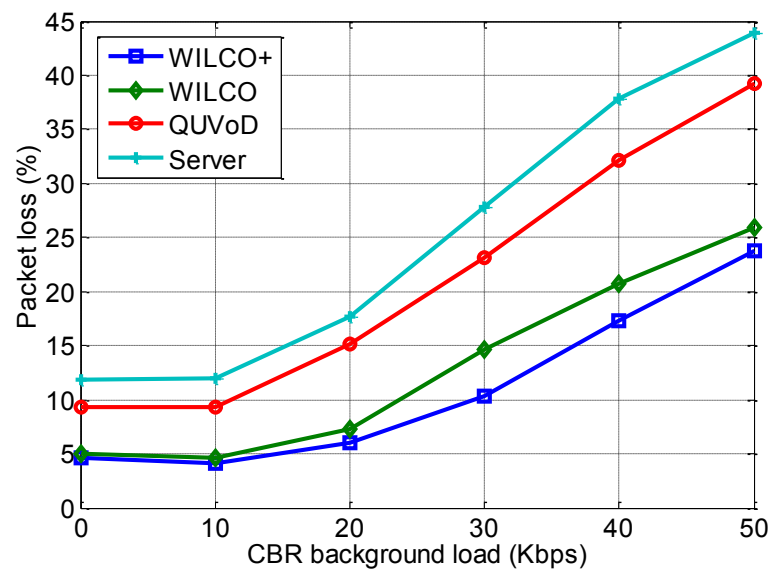
Figure 6.11: Packet loss comparison in Scenario 2 with random segment placement at different background loads.

The better packet loss figure of QUVoD in Figure 6.11 can be explained by the fact that in the *Server* scheme, all the peers get video segments from the server, hence, the peers which are close to the server can get high quality videos with very little packet loss while the peers far away basically get very low quality video with high loss. As a result, on average, the PSNR quality of Server is better than that of QUVoD, but its

packet loss performance is worse. On the other hand, the round-robin peer selection of QUVoD makes the quality and packet loss variation among the peers less pronounced.

In addition, the average hop distance between the requesting and destination peer of WILCO and WILCO+ was also calculated in the simulation to further demonstrate the superiority of WILCO+. Our results indicate that this figure of WILCO is 2.4 hops on average while that of WILCO+ is 2.2 hops on average. These figures show an approximately 10% reduction in terms of hop length between requesting and destination peer with WILCO+. This reduction in hop count is the result of the very good location-awareness in video segment seeking algorithm.

6.5.3 Video Retrieval Performance with Different Number of Segment Replicas

Furthermore, an investigation of the effect of the number of segment replicas to the achievable PSNR of the four considered schemes is conducted. In this simulation, the random segment placement as in Scenario 2 is considered for its generality with the background load of 10Kbps. The number of segment replicas varies from 2 to 7 (10% replication rate). It is remarked that in this scenario, the replication rate does not affect the performance of the *Server* scheme since the overlay peers get all the segments from the server anyway.

As shown in Figure 6.12, when the number of segment replicas increases, the PSNR performance of all P2P schemes also increases. Among all the schemes, WILCO+ does not only perform the best, but its rate of increase in terms of PSNR is also the most pronounced. This improvement is more than 10dB (37% improvement) as the number of replicas increases from 2 to 7. The PSNR gap between WILCO+ and WILCO increases from roughly 1dB to 3dB with the growth of the number of segment replicas. This growing performance gap between the two schemes illustrates that WILCO+ can make a better use of location information than WILCO by mitigating the suboptimal selections in WILCO to shorten the transfer path.

126
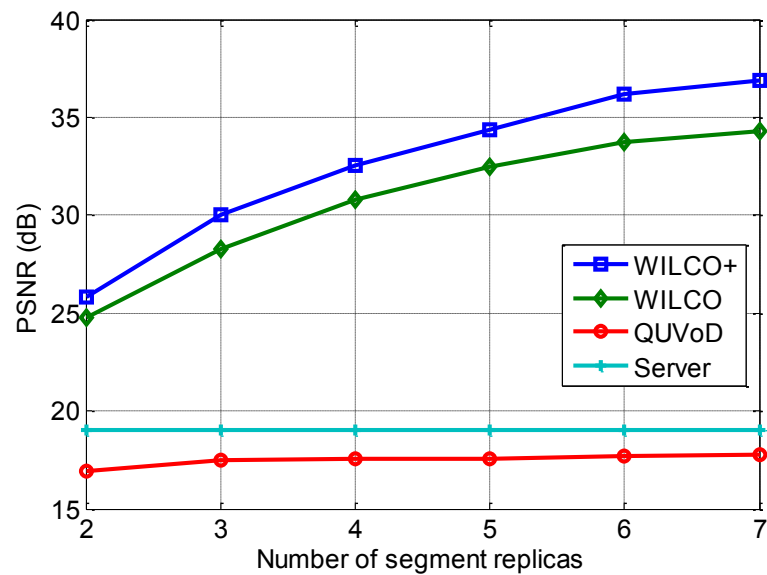
Figure 6.12: PSNR comparison with different number of segment replicas.

Analyzing Figure 6.12, it is interesting to remark that the PSNR performance of QUVoD does not noticeably increase with the number of segment replicas and is even worse than that of the *Server* scheme even when there are seven segment replicas in the network. This can be explained by its round-robin based peer selection which does not consider the physical network information such as the locations of peers. As a result, peers may end up seeking content from a distant destination peer even when the replication rate is high. This result also agrees with our data retrieval efficiency analysis performed in Section 6.5 which already indicated that a non-location-aware scheme cannot make use of the high number of content replicas in the network in order to improve the content retrieval efficiency.

6.6 Chapter Summary

This chapter proposed a WILCO-based novel location aware video segment seeking algorithm for video distribution overlays over WMN. The WILCO segment seeking algorithm uses an innovative WILCO multi-level area ID assignment to locate and retrieve the requested video segments from the nearest peers in order to improve

video quality. In addition, WILCO+, an improvement of WILCO segment seeking algorithm is proposed to provide a better location-awareness by mitigating WILCO border area effect and avoid potential suboptimal selections. A content retrieval efficiency analysis is provided to analyse the content retrieval efficiency of WILCO and WILCO+, and compare with that of a non-location-aware overlay peer selection mechanism. The analysis shows that WILCO and WILCO+ are not only more efficient in content retrieval by utilizing a shorter path, but also can productively make use of the number of segment replicas in the network to improve this efficiency. Additionally, simulations were performed and the results show that WILCO and WILCO+ significantly improve the video delivery quality up to 50% in comparison with other solutions in terms of PSNR and have lower packet loss at different background loads and replication rates.

CHAPTER 7: WLO - Wireless Link-aware Overlay for Video Delivery over WMN

Abstract

In the previous chapter, a location-aware video segment seeking algorithm is proposed to make use of the MR locations to select the closest peer in term of physical (or underlay) hop count to retrieve the video segments with improved quality. However, on a WMN, many other factors beside the hop count distance contribute to the end-to-end video delivery quality such as the background traffic load or the link quality. As a result, selecting the peer with the best link quality to retrieve the video segment from, could further improve the video retrieval quality. In this chapter, a Multiplication Selector Metric (MSM) for overlay peer selection is proposed. The proposed multiplicative metric selector resolves the two major drawbacks of the traditional summation-based metric approaches for overlay peer selection, i.e., the bottleneck link identification and the hop count behaviour. MSM can employ any link-aware metric without any additional networking overhead. Then, a cross-layer Wireless Link quality-aware Overlay peer selection mechanism (WLO) is proposed, using MSM to identify the best peer to retrieve the video content from. Simulation-based testing using OLSR-ETX shows how the proposed peer-to-peer solution for WMN outperforms the existing state-of-the-art solutions in terms of video quality. Finally, real-life emulation test-beds and

experiments are deployed to confirm the simulation results. Subjective video quality assessment tests are also conducted to show the significant impact of overlay peer selection on the user perceived video quality.

7.1 Introduction

When an overlay network is deployed over a wireless multi-hop network such as a WMN, the wireless link quality between the peers in the network plays a significant role in the delivery quality of the overlay content. For instance, it is well-known that the achievable bandwidth of wireless multi-hop network degrades quickly with the number of hops between the source and the destination node. With this observation in mind, an intuitive solution should be selecting the closest peer in terms of hop count for content retrieval. Indeed it was shown in chapter 6 that one such algorithm, namely WILCO greatly enhance the delivery quality of overlay videos. However, although this intermediate hop minimizing approach is effective over a non-location-aware approach, wireless hop count is not the only factor that contributes to the quality of service and overlay content retrieval can still be enhanced.

Picking up the closest peer in terms of hop count does not always guarantee the best choice among the overlay peers. For instance, if the path to the closest peer is highly loaded, the resulting video retrieval quality may not be as good as retrieving the video from a further peer, but on a load-free path. The same argument can be generalized to the link quality in general. If the path to the closest peer is very bad in terms of link quality, excessive packet loss, delay or jitter may occur which greatly degrade the quality of the content retrieval process, especially in the case of video streaming service. In this case, it could be better to select a peer on a longer path in terms of hop count, but with a better link quality. The objective of this chapter is to provide a better way of selecting peers based on wireless link quality.

Motivated by this observation, a Multiplication Selector Metric (MSM) for overlay peer selection is first proposed. The proposed selector metric is shown to be superior to the traditional summation-based metric when it is used to select among multiple peers on different paths by overcoming the two major limitations of the

traditional summation-based metric: bottleneck link identification and hop count minimization behaviour. The proposed MSM can be implemented with any existing routing protocol without any additional networking overhead by using an existing link-aware metric. A Wireless Link quality-aware overlay (WLO) peer selection mechanism is then proposed. Using a cross-layer approach, WLO selects for retrieval the peer with the best path quality in terms of MSM among all the peers that possess the requested video content. Simulation results with different background loads and different degrees of topology incompleteness show how WLO improves the quality of video retrieval in WMN in terms of average PSNR and packet loss.

Furthermore, a real-life emulation test-bed was setup and real-life video streaming tests were performed in order to confirm the similarity between the results of simulations and real-life emulation experiments. Besides, subjective video assessment tests are conducted on several video sequences in several real-life emulation-based test cases to show the importance of overlay peer selection on the user perceived video quality.

7.2 Multiplication Selector Metric for Overlay Peer Selection

The proposed Wireless Link Quality – Aware Overlay (WLO) solution aims at improving the overlay video retrieval by selecting from among peers storing the content the one to which the requesting peer has the best quality path. In terms of peer selection metric, it is first shown that the basic summation metric does not work well in a large WMN network. A novel Metric Selector Multiplication (MSM) is then proposed to overcome the drawbacks of the traditional summation-based metric for overlay peer selection.

In order to achieve link level awareness on the overlay for peer selection, it is natural and straightforward to use a link quality aware routing protocol and then employ a cross-layer mechanism to get and compare the path metrics of all the destination peers to select the best peer. However, the following analysis shows that this simple mechanism is not efficient for overlay peer selection due to the nature of the summation-based metric.

According to [91], in spite of the metric diversity, in most recent routing protocols, the path metric is computed as a summation of all the link metrics along the path as in equation (7.1)

$$M = \sum_{i=1}^{k-1} m_{n_i,n_{i+1}} \tag{7.1}$$

In equation (7.1), M is the path metric along a route of k nodes $(n_1, n_2, \dots, n_k)$ and $m_{n_i,n_{i+1}}$ is the link metric between node n_i and node n_{i+1}.

In comparison to other operators such as multiplication, this additive way of computing the path metric is well-suited for route selection to a single destination due to its ability to prevent small variations in one link along the path from significantly changing the whole accumulated metric as well as changing the whole route. As a result, the use of a summation–ased metric increases the route stability by reducing the flipping between routes, especially when a link-aware metric is used which may vary quickly with time. However, when evaluating the path quality to different destinations on different routes such as is the case of selecting the best peer from multiple overlay peers, this approach is not suitable for the two major reasons which will be discussed next. It is noted that these discussions apply to the case of selecting the best destination among multiple different destinations and not in the case of selecting the best path from multiple different paths to the same destination.

First, the summation metric calculation **fails to identify the bottleneck** along the path. If a link quality – aware metric is used, one bad link along the path will severely affect the overall end-to-end service. However, the link metric of this bad link contributes only a small part to the summation-based path metric. As a result, this bottleneck can be easily buried by small fluctuations in metric calculation of the other links along the path. This weakness in bottleneck identification can be severe when selecting among multiple different destination peers as destinations with very different end-to-end path characteristics could have very similar metric values.

Second, the summation of link metrics, in fact, **imitates the hop-count behaviour**. Since the path metric increases after each traversed link, the accumulated metric can be recognized of the summation of hops along with the link-aware metrics as

the weights. This hop-count behaviour tends to prefer the destination with the least-hop-path although of its path quality on the component links could be worse than that of a longer path. For example, if the Expected Transmission Count (ETX) metric [92] is used, a link metric of 1 implies a perfect link while a link metric of 2 implies that the packet loss on this link could be as high as 50%. As a result, a destination on a one-hop path with a 50% loss link would be preferred over a three-hop path with little or no loss.

7.2.1 The Proposed MSM

Motivated by these observations, a novel Multiplication Selector Metric (MSM) is proposed. MSM is used as the metric for peer selection on the overlay and is calculated as a product of all component link metrics as in equation (7.2).

$$MSM = \prod_{i=1}^{k-1} m_{n_i, n_{i+1}} \qquad (7.2)$$

In equation (7.2), MSM is the Multiplication Selector Metric along a route of k nodes $(n_1, n_2, \dots, n_k)$ and $m_{n_i, n_{i+1}}$ is the link metric between node n_i and node n_{i+1}.

Since the link metrics are multiplied together, a bottleneck with a significantly higher link metric will boost the resulting MSM by a few times and cannot be hidden by small fluctuations in metric calculation of the other links. In addition, the multiplicative way of calculating MSM mitigates the hop-count behaviour of the traditional additive metric by emphasizing the quality of the links along the path rather than the path-length. As a result, a peer on a longer path with very good link quality will be preferred over the one on a shorter path but with bad link quality.

It is noted here that the use of a multiplicative metric for underlay routing has already been proposed in the literature (e.g. [93]). However, since the aim of underlay routing is to choose the best path among multiple different paths to a single destination, multiplying small changes in link metrics could change the whole route virtually with every routing update. If a link-aware metric is in used, the link metric could change constantly with time causing route flipping, making routing unstable. Moreover, the objective of this research is different, i.e., choosing the best overlay peer for content retrieval among different destination overlay peers. For this purpose, the proposed study

suggests the use of multiplicative metric for overlay peer selection, but still uses an additive metric, as is, for underlay routing. The simulation results in section 5 of this chapter illustrate that the proposed approach is well suited to overlay peer selection. Moreover, since the proposed solution uses MSM for selecting the best overlay peer and use the underlay routing protocol as is with the traditional (summation-based) metric that came along with the routing protocol, the proposed solution does not have to tie to any link-aware routing protocol or metric.

7.2.2 MSM Computational Complexity

In comparison with other approaches which either introduce additional networking overhead, are incompatible with the existing standard routing protocols, or are very computationally intensive, the computational processing of MSM is negligible. In order to get the MSM metric values, as well as the traditional additive metric, MSM multiplication metric is also calculated by multiplying the component path metric values whenever a new node is added into the path in the routing table construction process.

In particular, let l be the number of links in the route, the exact number of additional multiplication operators needed for calculating MSM is $(l - 1)$ operators. In general, since the diameter of a network of N nodes is $\sqrt{N}$, the additional multiplication operations of each path is only $O(\sqrt{N})$, depending on the number of links in the route. Since MSM is calculated along during the routing table construction process, which is a distributed process, the MSM calculation is also distributed and does not require any centralized administration.

7.2.3 MSM Networking Overhead Requirements

In comparison with other approaches to evaluating path quality which usually require the exchange of probing packets for link quality estimation, MSM is calculated using the existing link-aware metric which is already built-in with any existing routing protocol. As a result, no extra networking overhead is required for MSM calculation. This advantage makes MSM easy to implement and integrate into any existing WMNs as

an MSM extension is required only and there is no need to modify the whole network layer or build an additional block for overlay path quality-awareness.

7.3 WLO Cross-Layer Overlay Peer Selection Mechanism
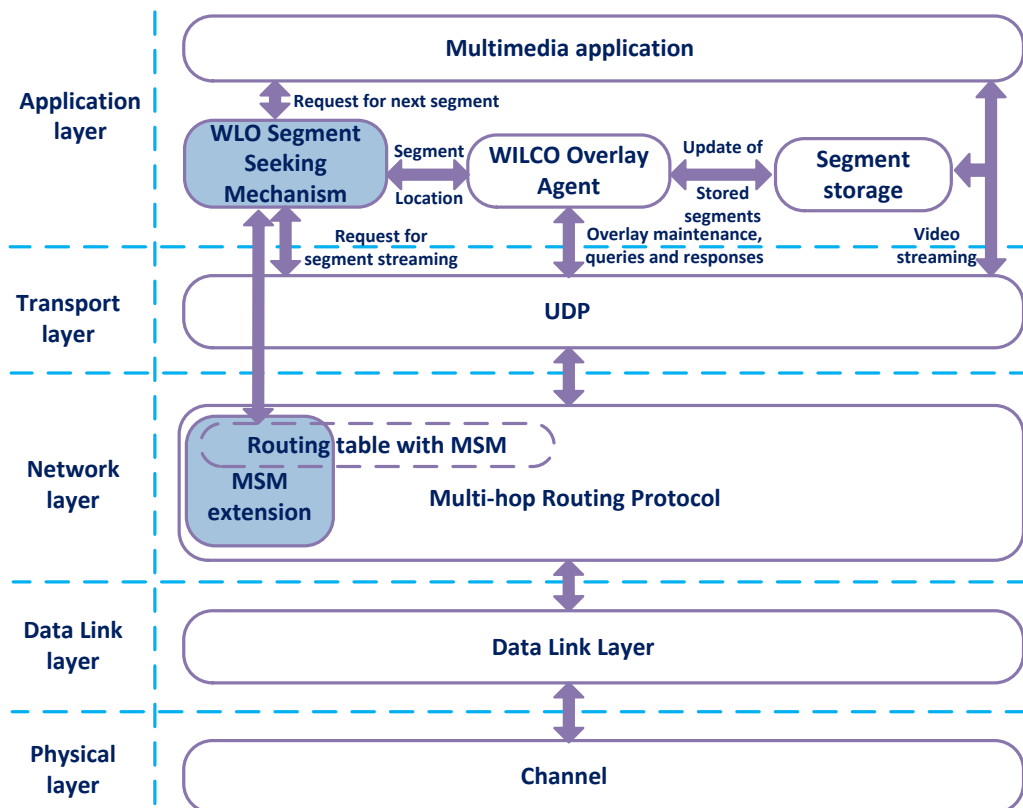
Figure 7.1: WLO Cross-layer architecture.

In order to enable link quality - aware overlay peer selection using MSM, the MSM calculation is integrated into the WMN routing protocol by adding a MSM extension ash shown in Figure 7.1. During the construction of the routing table, this MSM extension of the routing protocol calculates MSM values for the best route to each of the underlay peer. This MSM values are inserted into the routing table with the corresponding route for overlay peer selection use later on. As discussed in the previous section, the integration of MSM extension requires a negligible additional computation complexity ($l-1$ additional multiplication operators, where l is the number of links in the path or $O(\sqrt{N})$ multiplication operators in general, where N is the number of nodes

in the network), requires no additional networking overhead and can be easily implemented to the existing Network Layer without any significant change in the existing routing protocols and metrics.

7.3.1 WLO Algorithm

Algorithm 7.1: WLO overlay peer selection mechanism using MSM

---

for each requested segment S_j

    Get the addresses of all overlay peers $\{d_1, d_2, ..., d_k\}$ which store the requesting video segment S_j.

    for each overlay peer $d_i \in \{d_1, d_2, ..., d_k\}$

        Perform cross-layer lookup for MSM_i in local routing table

    end for

    $MMS_{min} = \min\{MMS_i, i = 1, ..., k\}$

    Select overlay peer d_{min} with MSM_{min} to retrieve S_j.

end for

As detailed in Algorithm 7.1, when the overlay application wants to select the best peer to get the video segment from, WLO performs a cross-layer lookup to the Network Layer routing table with MSM. Using the IP address of the overlay peers which store the requested video segment, WLO retrieves all the MSM values of all those destination peers from the local routing table. Based on the acquired MSM values of the overlay peers, WLO selects the peer with the lowest MSM as the best peer to retrieve the video content from.

7.3.2 Computational Complexity of WLO

Let k be the number of replicas of a segment in the network. The WLO has to loop through all of the MSM of the k peers to find the best peer with a minimum MSM. As a result, the computational complexity of WLO is linearly with k, or $O(k)$. Although this computational complexity would increase linearly with the number of replicas in the network, this number of replicas is generally small so the computational complexity of WLO cross-layer lookup is negligible in practice.

7.3.3 Expected Transmission Count (ETX) Metric

The link-aware metric that will be used along with MSM in this chapter is the Expected Transmission Count (ETX) metric. ETX metric is chosen due to its simplicity in implementation and yet is an effective link-aware metric.

The Expected Transmission Count (ETX) metric was proposed by Douglas S. J de Couto et al. in [92]. In a wireless multi-hop environment, ETX aims at finding a path with the fewest expected number of transmissions (including the number of retransmissions) required to deliver a packet all the way to its destination. ETX metric predicts the number of transmission required by using the link-by-link measurement of packet loss ratios in both directions of each wireless link. As a result, using ETX metric, the best path is the path to the destination with the highest throughput, despite the packet losses.

The ETX of a link is calculated using the forward and reverse delivery ratios of the link. Let d_f and d_r be the forward and reverse delivery ratios of a link respectively. The forward deliver ratio, d_f, is the measured probability that a data packet successfully arrives at the recipient. The reverse delivery ratio, d_r, is the probability that a ACK packet travels in a reverse direction can be received successfully. The expected probability that a transmission is successfully received and acknowledgement is $d_f \times d_r$. If either the data packet transmission or the acknowledgement fails, a retransmission is required. Since the transmissions are independent, the expected number of transmissions required is expressed in equation (7.3)

$$ETX = \frac{1}{d_f \times d_r} \tag{7.3}$$

Since there is no implementation of ETX on NS-3, an OLSR – ETX model based on the OLSR – ETX model on NS-2[94] was implemented on NS-3. The delivery ratios d_f and d_r are measured using dedicated link probing packets. Each node broadcasts a link probing packet at an average period τ. To avoid the synchronization problem when neighbouring nodes broadcast probing packets at the same time, a random jitter of 0.1τ is added to the probing broadcast period. By counting the number of probing packets a node received from a neighbour during a measured window of w seconds, the reverse delivery ratio can be calculated using equation (7.4)

$$d_r = \frac{count(w)}{w/\tau} \tag{7.4}$$

In equation (7.4), $count(w)$ is the number of probes received from the neighbour during the window w, and w/τ is the number of probes that should have been received.

By using this method, the reverse delivery ratio d_r can be obtained at all the communication nodes. Consider a link between node X and Y, it is clear that the reverse delivery ratio calculated at X is the forward delivery ratio d_f of Y on the link. In order to let Y know its forward delivery ratio, d_f, each probing packet sent by X contains the number of probing packets received by X from each of its neighbours during the last window time w. Using this embedded information, each node in the network can also calculate its forward delivery ratio, d_f, with a neighbour.

7.4 Simulation-Based Testing

The performance of the proposed WLO is evaluated using Network Simulator 3 [88]. The simulated topology consists of $N = 64$ MRs arranged in an 8x8 grid, as illustrated in Figure 7.2. The distance between two adjacent MRs is set to 100m. In the simulations, all the wireless settings for MRs are the same as in Table 5.2 in chapter 5, and the OLSR-ETX routing protocol is used to perform underlay routing and enable data transfer. Each simulation is repeated 10 times and the results are averaged.

First, some simple scenarios are investigated to illustrate the effectiveness of MSM over the traditional summation-based metric. Then, more thorough simulation results are presented to show WLO's benefits in general scenarios. Throughout the simulations, video retrieval quality is evaluated using the same MPEG-4 video clip Akiyo [83] and the calculations of the Peak Signal-to-Noise Ratio (PSNR) and packet loss are the same as described in chapter 6. The video quality retrieval performance of WLO is compared to that of WILCO+, WILCO, QUVoD [81] and a server-only solution (*Server*).

7.4.1 Illustration of MSM Effectiveness in Simple Scenarios

First, the effectiveness of MSM over the traditional summation metric (ETX) for overlay peer selection is illustrated in four simple scenarios. In these simple scenarios, MR A is the requesting peer; MRs D and E and F in Figure 7.2 are the three serving peers storing the requested video segment. Background traffic load, if it exists, is from B to C. The video retrieval from F to A is on a load free path and is used as a baseline for comparison. The four scenarios include video streaming at different path lengths and background loads along with the traditional summation metric and MSM obtained from MR A's routing table. The PSNR results and packet loss of the four simulation scenarios are summarized in Table 7.1. The video performance is evaluated by simulating streaming of one real video segment using the same trace file that was used in Chapter 6. The video used for streaming is the same as in chapter 6 with a bit rate of 341Kpbs, is 10 seconds long and is about 0.44MB in size.
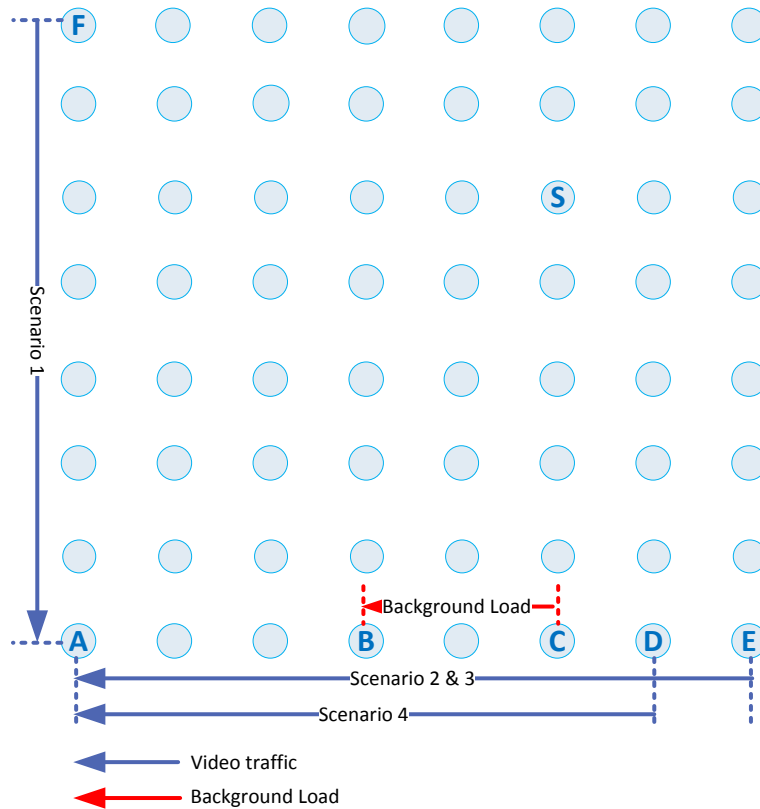

Figure 7.2: Simulation topology

In Table 7.1, scenario 1 is used as a baseline for comparison with the other scenarios. Scenario 2 and 3 present PSNR and packet loss performance of the same network path length as with the baseline scenario, from A to E, but under different background loads. It is observed that in comparison to scenario 1, both the PSNR and packet loss become worse in scenario 2 and 3 due to the increase of background load levels. However, it is important to remark that the ETX metrics vary very little in the second and the third scenario in comparison with the baseline scenario. The ETX's and packet loss figures in Table 7.1 illustrate that while the packet loss is very high in scenario 3, when the background load in the intermediate nodes is high, the ETX metric in this scenario is less than 10% higher than that of scenario 1 with a load-free path. If there were some small variations in metric measurement on scenario 1, this insignificant difference in the ETX summation-based metric could be easily buried and a peer selection using an underlay summation-based could be a bad choice. As a result, an overlay peer selection using a summation metric directly from the routing table could select the peer with the bad link quality for content retrieval due to the bottleneck and the hop-count behaviour which were described earlier in this chapter. On the other hand, it can be seen from Table 7.1 that the MSM metric reflects very well the path quality in each of the first three scenarios, having a significant higher MSM in scenario 3 in comparison with scenarios 1 and 2.

Table 7.1: Illustration of MSM effectiveness in four simple scenarios.

	Scenario 1	Scenario 2	Scenario 3	Scenario 4
Requesting Peer	A	A	A	A
Serving Peer	F	E	E	D
Background Load	No Load	50 Kbps	1 Mbps	1 Mbps
PSNR	29.49 dB	28.46 dB	5.68 dB	6.70 dB
Packet loss	4.77%	5.87%	49.59%	30.80%
ETX	11.00	11.20	11.81	10.23
MSM	29.26	30.38	46.41	42.36

Furthermore, in scenario 4, both the traditional summation ETX metric and MSM are investigated when the serving peer is on a path with one hop less than the other scenarios, but with a very high background traffic load on the intermediate nodes along

the path. It is important to see from Table 7.1 that while the PSNR and packet loss performance is very bad in this scenario due to the high load of background traffic on the intermediate nodes, the ETX is lower than that of all the other three scenarios. This is due to the hop count behaviour mentioned earlier that the traditional summation metric imitates the hop count metric and increases after each hop along the path. As a result, a longer but much better path is not preferred over a shorter, but heavily loaded one. On the other hand, in this scenario, the MSM metric continues to reflect the path quality very well, having a significantly higher value than in both scenarios 1 and 2.

These four simple but typical scenarios confirm our claim on the effectiveness of MSM in choosing the best overlay peer to retrieve the content from. As a result, a multiplication metric is a better indication of the goodness of multiple overlay peers on different paths and was preferred when proposing MSM.

7.4.2 Video Retrieval Performance of WLO in Different Levels of Background Load
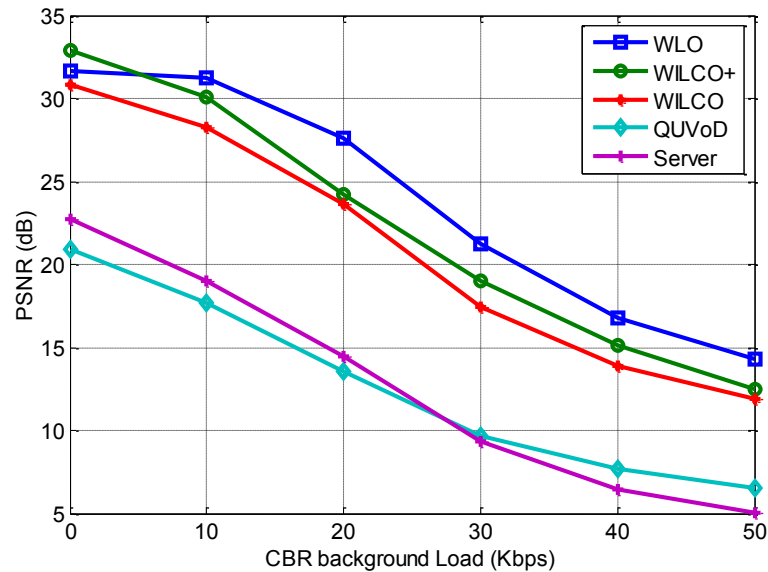

Figure 7.3: PSNR comparisons with different background loads

In this section, the performance of the proposed overlay peer selection (WLO) is evaluated with different background traffic loads. The video retrieval performance of WLO is compared against that of WILCO, WILCO+ QUVoD and Server. The

simulation topology and wireless settings are the same as in 7.5.1. To simulate background load, $N/4$ constant bit rate (CBR) UDP streams are generated between $N/2$ randomly selected source and destination peers. The load of each of the background traffic streams is varied from 0 (no load) to 50Kbps.
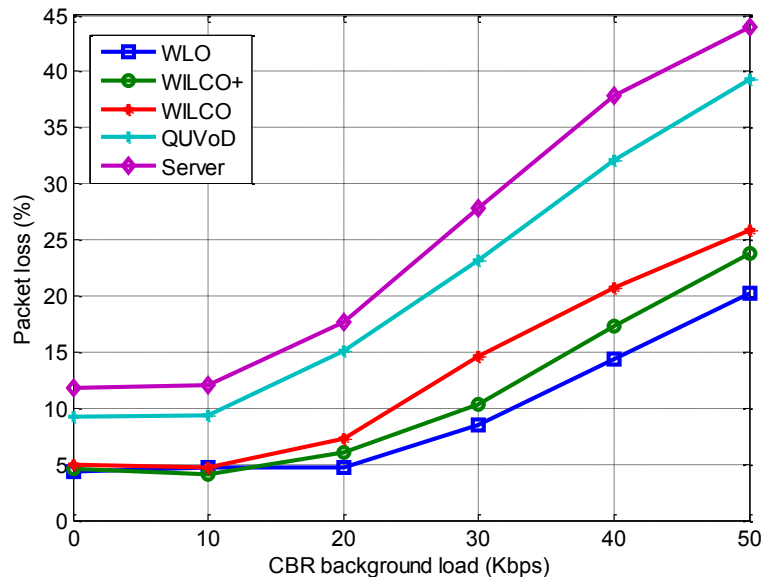
Figure 7.4: Packet loss comparisons with different background loads

In these simulations, real video trace files are used to simulate the retrieval of three video segments ($S = \{S_1, S_2, S_3\}$) on each of the overlay peers. The video descriptions are the same as in chapter 6 and in section 7.4.1. The number of replicas for each video segment is three. The video server is denoted by S in Figure 7.2 and contains all the three video segments. The other segment replicas are randomly distributed across the network.

Figure 7.3 illustrates the video retrieval PSNR performance of the five schemes. This figure shows that for all the background load levels, the PSNR values achieved by WLO, WILCO+ and WILCO are very high (around 30dB) when the background load is low and are about 10dB higher than those of the other two schemes. It is important to note that the difference in PSNR of QUVoD and Server is negligible across all the observed background loads. This fact clearly shows that on a wireless multi-hop network scenario, deploying P2P services without considering the physical topology conditions is not better than using a single server in terms of the quality of content retrieval. Figure 7.4

confirm this result, showing that WLO and WILCO can significantly reduce the packet loss by at least 50% in comparison to QUVoD and Server schemes.

In comparison with the location-aware schemes, i.e., WILCO and WILCO+, with no background load, the PSNR values of WLO, WILCO+ and WILCO are similar. The slightly lower PSNR of WLO at 0 background load could be due to the fact that even at zero load, channel variations could affect the ETX measurement. However, when the background load increases, the PSNR of the location-aware schemes decrease quickly, while WLO retains a very high PSNR with a slower rate of decrease. It is observed that throughout all the background loads, WLO outperforms WILCO by a good 4dB and outperforms WILCO+ by about 2dB in terms of PSNR. This result illustrates the ability of WLO to intelligently select the best peer with the lightest load or in general, the better link condition path even if the selected peer is on a longer path. On the other hand, the location-awareness of WILCO and WILCO+ schemes concentrate only on the physically nearest peer and do not care about the link-level conditions of the path such as the link contention due to the traffic load along the path. Figure 7.4 further confirms this result. While the packet loss of WILCO and WILCO+ generally increases with the background load, WLO packet loss remains under 5% up to 20Kbps. At higher background loads, by using MSM, the link quality aware overlay peer selection mechanism of WLO enables it to select the peer with a better path and hence, be able to keep the packet loss lower than the location-awareness of WILCO and WILCO+ which only rely on the shortest path in terms of hop count for overlay peer selection.

7.4.3 Video Retrieval Performance in Incomplete Topologies

In real-life deployments, it is ideal to have a complete grid topology as in Figure 7.2. However, this complete topology may be hard to achieve due to factors such as cost, obstacles or difficulties in installation. In this section, video retrieval performance of WLO, WILCO+, WILCO, QUVoD and Server are compared in incomplete topologies by turning off some of the MRs. The MRs which are turned off are uniformly randomly distributed across the physical topology. The degree of incompleteness is 5%, 10% and 20% which correspond to three, six and thirteen MRs in a 64 MR topology as illustrated in Figure 7.2 accordingly. It is observed in the simulation that anything larger than 20%

would partition the original topology into disconnected parts. In each case, ten different topologies are generated and tested against and the results are averaged. The background traffic load is 10Kbps and all the other simulation assumptions are kept the same as described in Section 7.4.1.

Figure 7.5: PSNR comparisons in incomplete topologies

Figure 7.5 shows the PSNR comparisons of the five schemes in incomplete topologies with the x axis representing the degree of topology incompleteness at 0% (complete topology as in Section 7.4.1 and section 7.4.2), 5%, 10% and 20%, respectively. It is illustrated that the retrieved video quality degrades with the incompleteness of the topology due to suboptimal paths. However, while WLO retains a very high PSNR even when 20% of the MRs are off, PSNR values for the other four schemes decrease sharply. In comparison to the PSNR in a complete topology, WLO performance in a 20% incompleteness topology decreases by only roughly 5% with about 2dB, while that of the other four schemes degrade by roughly 20% in similar situations, even with the location-awareness of WILCO and WILCO+.

From Figure 7.5, it is interesting to see that the PSNR performance of WILCO+ and WILCO are the most sensitive to the topology incompleteness. This can be explained

by the fact that the WILCO and WILCO+ location-aware segment seeking algorithms assume a complete topology. As a result, the peer selection could be worse even in terms of hop count in incomplete topology scenarios.

7.4.4 Video Retrieval Performance with Mobility
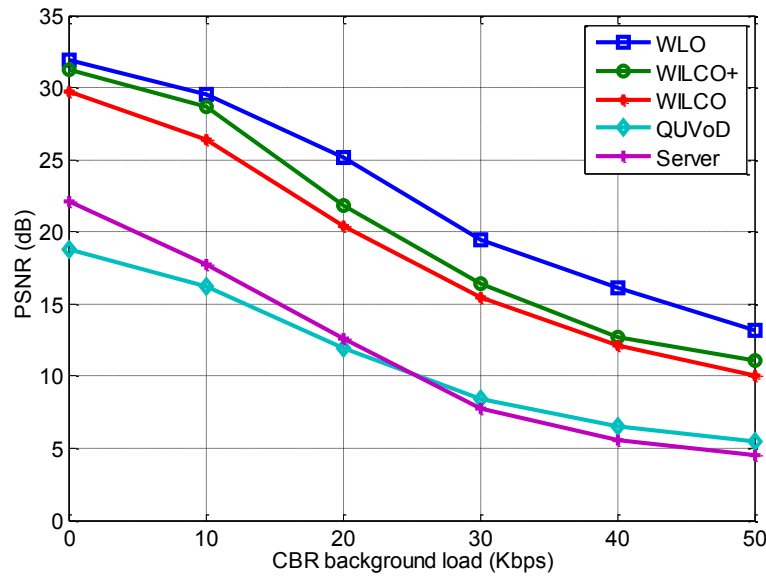
Figure 7.6: PSNR comparison with mobility

In real-life scenarios, users are moving around even as they are accessing data content or watching videos. In this section, the video retrieval performance of WLO, WILCO+, WILCO, QUVoD and Server are compared in the case of user mobility. The users can move from one WILCO lowest level area to one of the four adjacent areas with equal probability. In this test, the data handover is not considered so the users are assumed to watch an entire video segment, moving to an adjacent area and then proceed with the next video segment. The video segment seeking is done for every requested segment. The background traffic load varies from 10Kbps to 50Kbps and all the other simulation assumptions are kept the same as described in section 7.4.1
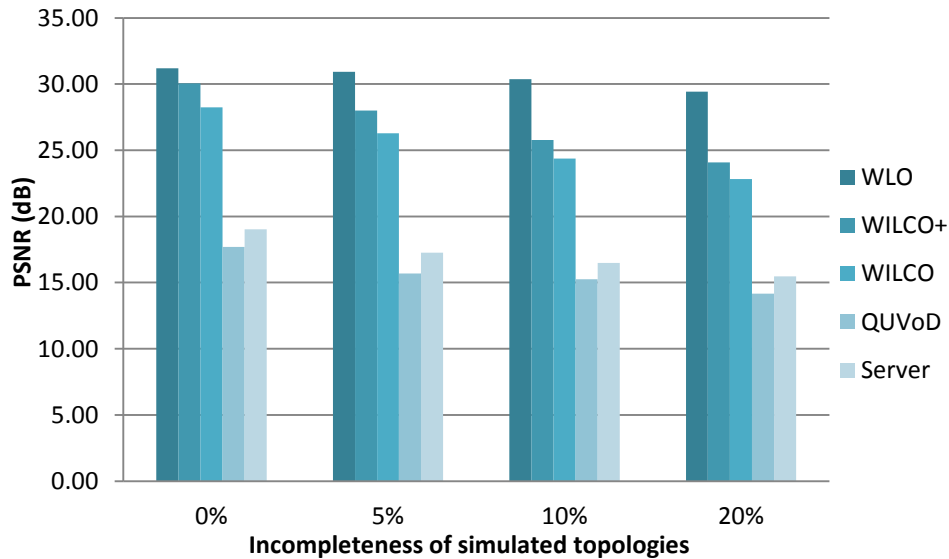
Figure 7.6 presents the PSNR comparison among the five schemes with user mobility; the x axis shows the background load level in the scenario. It is shown that the

received video PSNR with mobility reduces in comparison with that resulted in section 7.4.2. However, there is a significant gap of about 8dB between the WILCO, WILCO+ and WLO in comparison with the QUVoD and Server schemes throughout the graph. It is illustrated in this figure that WLO upper bounds WILCO+ and WILCO with approximately 3dB (more than 10%) difference, except for the low traffic load. It is also shown in Figure 7.6 that the reduction rate of WLO is much slower than that of WILCO and WILCO+, which is the result of WLO's ability of selecting the peer with the best link quality to retrieve the video segment from.

7.5 Emulation Tests based on Streaming of Real Videos

So far, in this chapter, simulation-based tests were used to quantify the video retrieval performance in various scenarios using video quality metrics such as PSNR. In this section, quality evaluations based on actual measurements and perceptual evaluations are performed to confirm the simulation results and to show the effectiveness of the proposed mechanisms. Using a real-life emulation-based test-bed, real videos are streamed between real hosts (desktops) through an emulated WMN and the video quality is evaluated through both objective and subjective-based evaluations.

7.5.1 Emulation Concept and Architecture

Network emulation enables the creation of network scenarios on a physical machine and allows the other physical machines with real applications and real traffic to interact with each other through the emulated network by connecting to the network-emulated machine. The network emulation is usually accomplished in software using simulation programs such as NS-3 [88], NS-2 [94], etc. With the flexibility in changing the emulated network at will, the main advantage of using an emulation-based test-bed is that it reduces the time and the cost of testing solutions when real applications are required without the need of purchasing and deploying of real networks.

In this section, the network emulation scenarios are conducted using the NS-3 Tap Bridge mechanism [95]. The NS-3 Tap Bridge emulation architecture is shown in Figure 7.7. In NS-3 emulation, the networking environment and network nodes are built and simulated normally in a separated machine (*Simulation Host* as illustrated in Figure 7.7) using NS-3 except for nodes that are to be replaced by the real hosts. For nodes in NS-3 simulation that are to be replaced by the real hosts (the *NS-3 Client Nodes* in Figure 7.7), only the node container and the net device are created, the NS-3 IP stack and upper layer applications are replaced by the external host. The communication between the NS-3 simulation environment and the simulation host is done through sockets. The simulation host binds these sockets to its real network devices which are then connected to the real hosts (*Video Server Host* and *Client Host* as illustrated in Figure 7.7) for communication purpose. These communication links between the real host and the communication hosts enable real traffic to flow between real hosts while being transferred through a complex NS-3 simulated topology in real time.
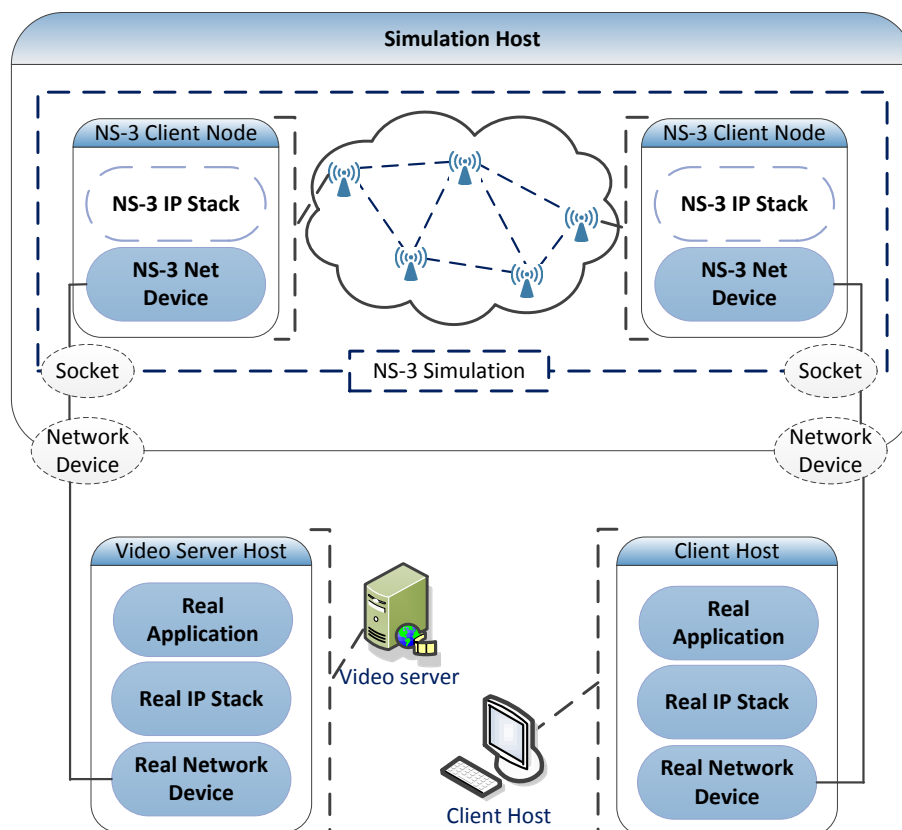
Figure 7.7: NS-3 emulation architecture.

7.5.2 Emulation Test-bed Hardware and Software Configuration

Figure 7.8 shows the actual test-bed deployment with three PCs playing the roles of the media server, media client and the NS-3 simulation host. The hardware equipment involved in the tests is listed below:

- *Media server host*: a desktop with Ubuntu 12.04, Intel Core i7-3770 at 3.48GHz and NetXtreme BCM5722 Gigabit Ethernet PC Card.
- *Media client host*: a desktop with Ubuntu 12.04, Intel Core i7-3770 at 3.48GHz and NetXtreme BCM5722 Gigabit Ethernet PC Card.
- *NS*-3 *simulation host*: a desktop with Ubuntu 12.04, Intel Core i7-3770 at 3.48GHz and two Ethernet cards:
  - o NetXtreme BCM5722 Gigabit Ethernet PC.
  - o 82579LM Gigabit Network Connection.
- Two KRONE PremisNET CATEGORY 5e Ethernet cables are used for the connection between the media server and the simulation host, and between the media client and the simulation host.

Figure 7.8: Test-bed Deployment.

The software used in the tests is listed below:

- *Video LAN Client (VLC)[15]*: an open-source video player supporting multiple operating systems and most of the existing codecs. VLC also supports video

---

[15] Video LAN Client - http://www.videolan.org/vlc

streaming with both the role of video streaming server and client. VLC is deployed at both the media server host and the client host for streaming and receiving of videos.

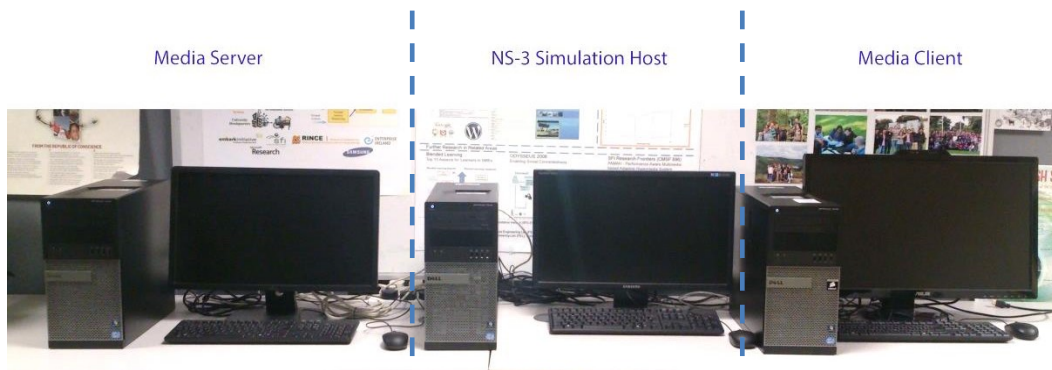- *Moscow State University (MSU) Video Quality Measurement Tool* [96]: an objective video quality assessment software which supports comparing the original video and the impaired video to evaluate the quality of the impaired video. MSU supports many objective quality assessment metrics such as PSNR, MSE, etc.

- *MSU Perceptual Video Quality Tool* [97]: a subjective video quality assessment software which automates the perceptual video tests. MSU Perceptual Video Quality Tool support many types of subjective tests, including Double Stimulus Impairment Scale (DSIS) [42], SCACJ (Stimulus Comparison Adjectival Categorical Judgement) [98], etc.

7.5.3 Video Sequences

Three video sequences were used for emulation tests. The properties of the video sequences are shown as in Table 7.2. The first sequence is the *Akiyo* sequence [89] that was used for simulations throughout the thesis and is used in the emulation to confirm the simulation results. The second and the third sequences are taken from the *Big Buck Bunny* animation movie [99] and are used for the extended emulation scenarios with different video complexities. The second sequence presents a high spatial and temporal complexity sequence with fast changing scenes and complex backgrounds. The third sequence presents a low spatial and temporal complexity sequence with a bird slowly glides across the screen on an empty sky. Figure 7.9 illustrates the frames belonging to the three sequences respectively.

Table 7.2: Properties of video sequences used for the emulation tests

Video Sequence Number	Duration (seconds)	Encoding Codec	Overall Bit Rate (Kbps)	Resolution (pixels×pixels)	Frame rate (fps)	Color Space
1	10	MPEG-4	341	352×288	30	YUV
2	20	MPEG-4	988	512×288	25	YUV
3	15	MPEG-4	984	512×288	25	YUV

Video Sequence 1

Video Sequence 2   **Video Sequence 3**
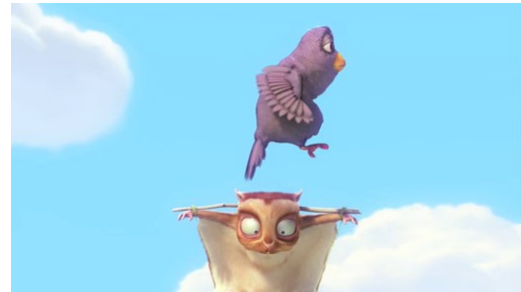
Figure 7.9: Video sequences used for emulation tests

7.6.4 Experimental Scenarios

The video delivery performance of the three sequences in Table 7.2 is evaluated in real-life emulation-based tests. In the simulation-based tests earlier in this chapter, since each of the data points in the previous simulation tests was averaged over more than 1800 simulation runs, it is impossible to manually emulate each and every simulation run. As a result, only the four simple scenarios described in section 7.4.1 are replicated in the emulation-based tests to confirm the simulation results. Furthermore, the effectiveness of WILCO location-aware segment seeking algorithm and WLO are demonstrated in various test cases on emulation test-bed along with user perceptual tests. The experimental scenarios are detailed as follows:

- **Simulation results confirmation**. In this test, the four simple simulation scenarios in section 7.4.1 are replicated in emulation tests in order to confirm the simulation results. In these emulation-based tests, video sequence 1,

which was also used in the simulations, is used for evaluating the video retrieval performance. In these tests, the source and the destination peers are replaced by the real desktops which run VLC applications for streaming of the video sequence. The corresponding NS-3 WMN and background load are deployed and emulated on the NS-3 emulation host. The received videos are evaluated in terms of PSNR using MSU and compared with the simulation results.

- **Extended emulation scenarios on the effectiveness of peer selection**. In this test, video sequences 2 and 3 are streamed across a WMN in various hop count and background traffic load scenarios. The three backhaul WMN scenarios are as follows: a four-hop link with 200Kbps background load, a two-hop link with 200Kbps background load and a two-hop link with no background load. The received videos are evaluated using perceptual tests to show the effectiveness of peer selection in these scenarios.

7.5.5 Experimental Scenarios

7.5.5.1 Simulation Results Confirmation

Table 7.3: Emulation test-bed versus simulation result comparison.

		Scenario 1	Scenario 2	Scenario 3	Scenario 4
Setup	**Hop count (hops)**	7	7	7	6
	Background Load	No Load	50Kbps	1Mbps	1Mbps
Test-bed	**PSNR (dB)**	30.31	28.38	12.78	14.07
Simulation	**PSNR (dB)**	29.49	28.46	5.68	6.7

The video retrieval qualities of the four simple scenarios described in section 7.5.1 are replicated in the emulation test-bed. The PSNR, obtained from the emulated tests and computed by the MSU application, is used as the objective video quality assessment metric for evaluating the received videos. The PSNR results from the emulation test-bed are then compared with the simulation results in order to confirm that they share the same trends. It is argued that the other simulation results in this thesis would share similar tendencies when applied to real-life scenarios.

Table 7.3 shows the comparison between the emulation test-bed results and the simulation results for the four tested scenarios. In general, the test-bed results and the simulation results share the same tendency, i.e., the video quality degrades when the background load increases. In scenarios 1 and 2, the PSNR results of the test-bed and the simulation closely match each other. In scenarios 3 and 4, the PSNR results from the test-bed are a bit higher than those from the simulations. This difference can be explained by the fact that the PSNR value obtained from the simulation was calculated from the PSNR estimation in [47] which is very sensitive to high packet loss. As a result, when the packet loss is high, i.e., in scenarios 3 and 4, the PSNR estimation in the simulation gives a lower value than the actual comparison and evaluation using the original video and the impaired video. Using t-test with the confidence level of 99%, it can be said that there is no significantly statistical difference between the simulation result and the emulation-based test-bed. The t-test result confirms that the simulation results are statistically similar to the real-life emulation test-bed results.

7.5.5.2 Extended Emulation Scenarios on the Effectiveness of Peer Selection

In previous sections, objective video quality assessment metrics are used for measuring the received video quality for both the simulation tests and the real-life emulation tests. However, the results from the objective video quality assessment metrics do not always correlate perfectly with the user perceived quality from human vison, which behaves non-linearly. Using subjective video quality measurement, this section presents the investigation of the effectiveness of peer selection in three different emulation-based scenarios. The three emulation scenarios differ in the hop count of the path between the requesting peer and the destination peer, and the following background traffic load situations are considered: a four-hop link with 200Kbps background load, a two-hop link with 200Kbps background load and a two-hop link with no background load. These scenarios resemble the overlay selection of a non-location aware method, WILCO/WILCO+ and WLO respectively. Video sequences 2 and 3 described in Table 7.2 and Figure 7.9 are used for the emulation-based tests which present a high spatial and temporal complexity sequence and a low spatial and temporal complexity. In each emulation scenario, the video sequences are streamed from the media server using VLC

through the emulated network to the media client and are saved into video files in the media client desktop for subjective video quality assessment tests.

Table 7.4: Mean Opinion Score

MOS	Quality	Impairment
5	Excellent	Imperceptible
4	Good	Perceptible but not annoying
3	Fair	Slightly annoying
2	Poor	Annoying
1	Bad	Very annoying

7.5.5.2.1 Subjective test set-up

1. Watching reference Video   **2. Watching impaired Video**
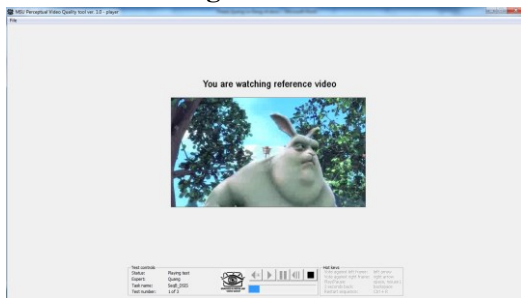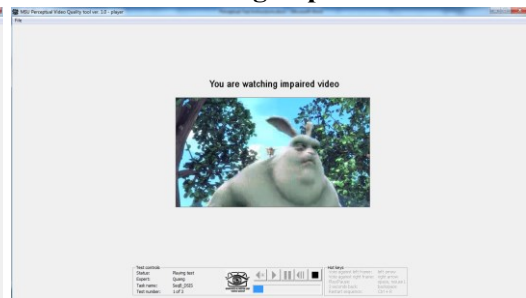
3. MOS rating
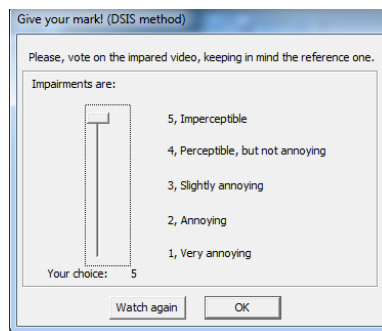
Figure 7.10: DSIS subjective test procedure and interface using MSU Perceptual Video Quality Tool

The subjective tests were done in a separate room without any disturbance form outside. 20 users (12 males and 8 females) were invited to watch the video clips received in the test cases. The ages of the users are distributed between 21 to 44 years old. The occupations of the users include students, technicians, engineers, businesspersons, etc.

MOS [100] is selected for the subjective video quality measurement. The quality scale for MOS is presented in Table 7.4 with the MOS value of 5 indicating the "excellent" quality and the MOS value of 1 indicating the "bad" quality.

The subjective tests follow the *Double Stimulus Impairment Scale (DSIS) method* which is described in ITU-R BT.500-11 [42] and follow all the recommendations from the ITU-T P913 [101]. In DSIS method, videos are shown consequently in pairs: the first video is the reference video, the second video is the impaired video. After each playback, the test participant is asked to give his/her opinion using the MOS impairment scale as in Table 7.4.

The subjective tests are done on the *Media client host* with the configuration as shown in Section 7.5.2 with a 27 inches Asus VG278 monitor. The MSU Perceptual Video Quality Tool [97] is used to automate the test procedure as shown in Figure 7.10. The MOS value for the quality assessment of each video sequence is computed as the average value rated from the 20 users.

7.5.5.2.2 Result Analysis

Error! Reference source not found. illustrates an example of the quality of an original and the received video frame of video sequence 2 affected by the network QoS parameters. The frame was taken in the 2-hop path with 200Kbps background load scenario.

Figure 7.12 illustrates the average MOS values measured for the two video sequences in the network three scenarios. It is illustrated in Figure 7.12 that the longer the path, the worse the video quality is and the lighter the background traffic load, the better the video quality is. In comparison to the 4-hop scenario, the perceived video quality of the 2-hop scenarios is much better. While there are some jerky and blurred video frames in the 2-hop scenario which are perceivable they are still watchable; however, many of the video frames of the 4-hop scenarios are blocky and colour impaired which make the videos almost unwatchable. Furthermore, between the two 2-hop scenarios, the perceived video quality is considerably better in the case of no background load. These results clearly show that both hop count and background load have a great impact on the user perceived video quality. As a result, if overlay peers are

capable of intelligently selecting closest peer or peer on a lighter background load paths to retrieve the video segment from, such as that proposed by WILCO, WILCO+ location-aware segment seeking schemes and WLO scheme, the user perceived video quality is expected to be enhanced.

Original video frame   **Received video frame**

Figure 7.11: An example of the quality of the original and received video frames

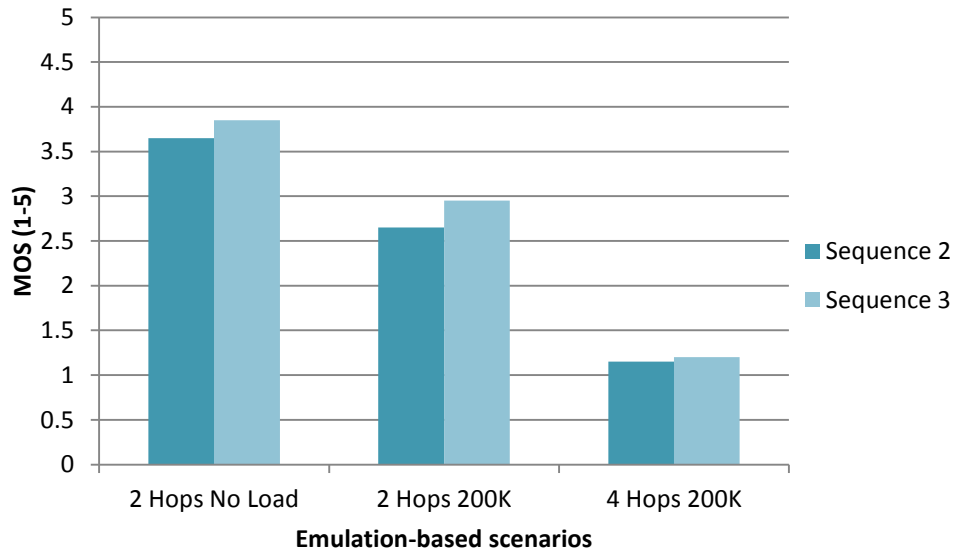**Figure 7.12: MOS results from subjective tests in several network scenarios.**

In comparison to video sequence 2 with high temporal and spatial complexity, the quality degradation of video sequence 3 is harder to perceive. This is because in video sequence 3, the temporal and spatial complexity is low and the consecutive frames are almost identical. This similarity between frames makes it easier for the video player to

conceal the errors, making it harder for the users to notice the degradation in the video quality.

7.6 Conclusion

This chapter proposed MSM, a novel Multiplication Selector Metric. Unlike the traditional summation-based metric, the proposed MSM is capable of detecting bottleneck links, does not have a hop count behaviour and hence is more suitable for selecting the best peer in terms of link quality from multiple overlay peers on different paths. WLO, a cross-layer overlay peer selection mechanism is also proposed which makes use of MSM to select the best peer for overlay video content retrieval. The simulation results show that WLO greatly reduces the packet loss and significantly improves the video quality retrieval in terms of PSNR with different background load levels and degrees of topology incompleteness in comparison with other solutions.

A real-life test-bed is developed to confirm the simulation results with real-life emulation experiments. The emulation results suggest that there is no statistically significant difference between the simulation results and the real-life emulation test results. Subjective video quality assessment tests are also conducted to show the significant impact of overlay peer selection on the user perceived video quality and they confirm the simulation and emulation test results.

CHAPTER 8: Conclusions and Future Works

8.1 Abstract

Chapter 8 summarizes the research work reported in this thesis. First, the problem is briefly described and then, the three main contributions of the thesis are highlighted along with the testing results. The chapter concludes with the presentation of several potential avenues for future work.

8.2 Conclusions

8.2.1 Problem Overview

Wireless Mesh Networks have been widely setup for last-mile network connectivity, especially in urban areas. The benefits of WMN include the ease of use, low-cost deployment, flexibility and scalability. When WMNs are used in conjunction with Peer-to-Peer (P2P) data transfer solutions, many innovative applications can be integrated into the network to enhance the user experience. These innovative applications range from distributed storage to resource sharing applications such as P2P Video on Demand. In P2P VoD applications, many users may watch the same video at the same time. As a result, the same video segment may be simultaneously available at several

places in the network. In this context, by making use of the existing user community and getting the video segments from an overlay peer, the server load could be significantly reduced. Moreover, by getting the content from overlay peers, the traffic balance could be greatly improved as the traffic would concentrate in a few network nodes where the content servers are connected to, creating bottlenecks.

However, in contrast to wired networks, wireless channels are error-prone, time varying and bandwidth limited. These critical characteristics of wireless channels introduce two main challenges for integrating a peer-to-peer overlay network over WMNs.

First, this combination of WMN at lower layers and overlay network at higher layers is not straightforward. As the current overlay protocols are designed for resource-rich wired networks, a high volume of maintenance traffic is required for ensuring the correctness and integrity of the overlay. This high volume maintenance traffic becomes a big issue in wireless multi-hop networks as bandwidth is limited and channels are error-prone. As a result, there is a need for an overlay protocol that is capable of enabling efficient overlay communications on the resource constrained WMNs.

Second, data transfer performance over a wireless multi-hop scenario depends greatly on several factors such as the number of intermediate nodes between the source and the destination node and the network load of the path between the nodes. As a result, an intelligent method of selecting the best peer for content retrieval among the peers that store the same content can significantly improve the data transfer performance. This observation is especially true for video contents in which a degraded bandwidth, delay or packet loss can reduce the video quality significantly. Hence, an overlay content delivery mechanism over WMN should be capable of selecting the best peer among all the available peers to retrieve the content from in order to achieve the best quality of service.

8.2.2 Contributions

In the context of the above problems, this thesis presents solutions to enable an efficient overlay network over WMNs at both levels of overlay communications and overlay data exchange. Three major contributions are proposed in this thesis:

- **Wireless Location-aware Chord-based Overlay (WILCO) mechanism for WMN**. WILCO makes use of the MR locations to integrate the physical topology on to the overlay network for efficient overlay communications, making the overlay network aware of the physical topology. The location-awareness of the proposed mechanism is realized through a novel geographical multi-level Chord ID assignment to the MRs on grid WMNs. An improved finger table is proposed to make use of the WILCO multi-level ID assignment to minimize the underlay hop count of overlay communications and recursively and progressively bound the overlay message to smaller WILCO multi-level area instead of letting the overlay message travel across the entire network.

- **WILCO-based novel geographical location-aware video segment seeking algorithm**. Tackling the issue of choosing the best overlay peer for data exchange, the intuition behind the WILCO-based location-aware video segment seeking algorithm is to choose the peer closest to the requesting peer in terms of hop count to download the requested video segment. The proposed video segment seeking algorithm makes use of the multi-level WILCO ID location-awareness to locate and retrieve video segments from the closest peer to improve video delivery quality. An enhance version of this video segment seeking algorithm (WILCO+) is proposed to mitigate the suboptimal selection of the WILCO video segment seeking algorithm by extracting coordinates from WILCO ID to enable location-awareness.

- **Cross-layer Wireless Link Quality-aware Overlay peer selection mechanism (WLO)**. Picking up the closest peer in terms of hop count for data exchange does not always guarantee the best selection since data retrieval quality also depends on other factors rather than hop count, for instance, traffic load or path quality. Motivated by this observation, the proposed peer selection mechanism aims at providing the requesting peer a measure at link quality of the path to overlay peers so that the requesting peer can select the best peer to get the video segment from. WLO uses a Multiplication Selector Metric (MSM) to overcome the two drawbacks of the traditional summation based metric (i.e., bottle neck link identification and

hop count behaviour) and a cross-layer mechanism to select the best overlay peer based on MSM.

8.2.3 Contribution Benefits and Validations

The performance analysis of the proposed solutions were performed via mathematical analysis, simulation using Network Simulator 3 (NS-3) and real-life experimental tests using objective and subjective quality assessment methods. Simulation models for WILCO, WILCO-based location-aware segment seeking algorithms and WLO peer selection mechanism were developed with the corresponding algorithms implemented.

WILCO was first mathematically analysed to show its lookup efficiency. This study proves that in comparison with the original Chord, WILCO can reduce the maximum number of lookup messages by half and has symmetric lookup behaviour in both the forward and backward directions of the Chord ring. The analytical framework also shows that WILCO has a stretch factor of $O(1)$, which implies that the constructed overlay closely matches the physical topology and significantly outperforms MeshChord another location-aware overlay scheme.

WILCO was also analysed using simulation in terms of the lookup efficiency; i.e., average number of lookup messages, the number of hops a lookup travels on the physical network, lookup time and the stretch factor; and in terms of messaging overhead and overhead balance in the WMN. The simulation results show that WILCO significantly improves (up to 50% and 40% in comparison with Chord and MeshChord, respectively) the lookup efficiency with superior lookup time, number of lookup messages and stretch factor. In terms of messaging overhead, the simulation results show that WILCO noticeably reduces (up to 50% and 20% in comparison with Chord and MeshChord, respectively) the overlay messaging.

WILCO video segment seeking algorithms were first analysed in terms of content retrieval efficiency using a mathematical framework to show the superiority of WILCO and WILCO+. The mathematical analysis results illustrate that WILCO and WILCO+ significantly reduces the hop distance between the requesting peer and the destination

peer in comparison with a non-location aware peer selection. The analysis also shows that WILCO and WILCO+ can productively make use of the number of content replicas in the network to improve the retrieval performance.

Simulation was used to analyse the video delivery performance of WILCO and WILCO+ in terms of PSNR and packet loss in comparison to schemes that retrieve the video from only the server and a non-location-aware scheme. The simulation results show that WILCO and WILCO+ maintains a significantly higher video delivery performance throughout the tests. In particular, without background load, WILCO and WILCO+ improves the video delivery quality by 17dB (82%) in terms of PSNR and reduce the packet loss by 82%. In scenarios with various background loads, WILCO and WILCO+ still outperform the two compared schemes by a significant gap of at least 50% in terms of PSNR and improve the packet loss by 60%. When the number of segment replicas varies, the simulation results show how WILCO and WILCO+ make use of these replicas to further improve the video retrieval quality.

WLO peer selection mechanism was analysed in terms of video retrieval quality using simulation-based tests and real-life emulation-based experiment tests. Using four simple scenarios, the simulations results first show the effectiveness and superiority of MSM metric in mitigating the bottleneck effect and the hop count behaviour. The video retrieval performance of WLO was then analysed in different levels of background loads. The simulation results show how WLO outperforms the WILCO and WILCO+ location-aware mechanism by 10% in PSNR and significantly out performs the other non-location-aware schemes by more than 50% in PSNR. In scenarios with different levels of topology incompleteness, the simulation results show that the rate of reduced PSNR performance of WLO is much slower than that of other schemes. A real-life emulation-based test-bed is developed to confirm the simulation results with the real-life experiment results. The experimental test results show how there was no significantly statistical difference between the simulation results in terms of PSNR and the real-life video streaming using an emulation test-bed. Furthermore, experimental results and subjective video quality assessment tests with different video sequences in various emulation-based scenarios were also conducted and showed that overlay peer selection methods can be used to improve user perceived video quality levels.

8.3 Future Work

The main purpose of the work presented in this thesis is to propose solutions for deploying overlay networks over a wireless multi-hop Wireless Mesh Network. These solutions include both the control plane and data plane aspects. Regarding the control plane aspect, the proposed solution aims at improving the overlay communication efficiency and reducing the messaging overhead. On the data plane, several solutions were proposed aiming at selecting among the available peers with the requested content the best peers to retrieve the content from in order to enhance the user experience, especially in video streaming applications.

However, the solutions proposed in this thesis are mainly heuristic-based. Although the proposed solutions outperform some of the state-of-the-art solutions, the theoretical performance limits were not found. An interesting potential future work could be finding these theoretical performance boundaries, and a working framework that makes it possible to achieve these optimal boundaries. These theoretical optimal limits are very important in network planning in order to maximize the utilizing of network resources and user experiences. The mathematical models defining these theoretical optimal would be a great contribution to the literature. In addition, more extensive simulation scenarios such as considering irregular grids, and testing of the auto-healing capabilities of the overlay networks may also be interesting and could provide a more in depth understanding on how overlay networks react in wireless scenarios.

As wireless devices nowadays are equipped with multiple antennas that can handle multiple channels and frequencies at the same time, multiple transport overlays could co-exist without interference. The coexistence of multiple transport overlays could load balance the traffic to avoid bottlenecks in an overlay from affecting the quality of service of the data transfer sessions, potentially greatly improve the user experience. In this context, a joint optimization method for antenna, frequency, channel provisioning for overlays is mandatory to maximize the network performance. Moreover, in order to achieve the best performance, the constructed overlays have to be aware of the datalink and physical conditions of the underlying network status. As a result, the antenna, frequency, channel provisioning method for overlays has to adaptively adjust to the network conditions, for instance, turning off antennas for energy saving when the traffic

load is light, performing antenna, frequency, channel provisioning under heavy traffic and performing peer selection along with appropriate network optimization to maximize the quality of service of overlay traffic.

Another potential expansion of the thesis could be using the adaptive transcoding on overlay peers to enhance the video retrieval quality. By imposing the assumption of adaptive transcoding on the overlay peers, the stored video segments can be transcode into several quality layers. Depending on the network condition or the feedback from the receiver peer, the sending peer can adaptively send some specific video quality layers to the receiver. For instance, if the background traffic load were high, the video quality would be greatly degraded if the sending peer always sends the highest quality stream since the link bandwidth is insufficient to accommodate the stream. In this case, by sending a lower quality layer, the required transport constraints are more relaxed and hence, it is possible that the received video quality is better due to less packet loss.

Bibliography

[1]   IEEE 802.11™: Wireless LANs standards. [Online]. Available: http://standards.ieee.org/about/get/802/802.11.html

[2]   S. Taylor, "Service Provider Wi-Fi and Small Cells: Discover What Consumers Want from Wi-Fi and Mobile", Cisco research white paper, 2013. [Online]. Available: http://www.cisco.com/web/about/ac79/docs/sp/SP_Wi-Fi_Consumers.pdf

[3]   Cisco Visual Network Index: "Global Mobile Data Traffic Forecast Update", 2013-2018,   2014.   [Online]   -http://www.cisco.com/c/en/us/solutions/collateral/service-provider/visual-networking-index-vni/white_paper_c11-520862.html

[4]   IEEE 802.11ac - 2013 - IEEE Standard for Information technology--Telecommunications and information exchange between systems Local and metropolitan area networks-- Specific requirements--Part 11: Wireless LAN Medium Access Control (MAC) and Physical Layer (PHY) Specifications--Amendment 4: Enhancements for Very High Throughput for Operation in Bands below 6 GHz, December 2013.

[5]   3GPP TS 36.201, "Evolved Universal Terrestrial Radio Access(E-UTRA); Long Term Evolution (LTE) physical layer".

[6]   P. Gupta, P. R. Kumar, "The Capacity of Wireless Networks", *IEEE Transactions on Information Theory*, Vol. 46 (2), pp. 388-404, 2000.

[7]   IEEE 802.11 Working Group – http://www.ieee802.org/11/

[8]   ANSI/IEEE Std 802.11, 1999 Edition (R2003), "Part 11: Wireless LAN Medium Access Control (MAC) and Physical Layer (PHY) Specifications", June 2003.

[9]   IEEE 802.11a-1999, IEEE Standard for Local and Metropolitan Area Networks Specific Requirements – Part 11: Wireless LAN Medium Access Control (MAC) and Physical Layer (PHY) Specifications - High Speed Physical Layer in the 5 GHz Band, 1999.

[10]   IEEE 802.11b-1999, IEEE Standard for Local and Metropolitan Area Networks Specific Requirements –Part 11: Wireless LAN Medium Access Control (MAC) and Physical Layer (PHY) Specifications - High Speed Physical Layer Extension in the 2.4 GHz Band, September 16, 1999.

[11]   IEEE 802.11g-2003, IEEE Standard for Local and Metropolitan Area Networks Specific Requirements – Part 11: Wireless LAN Medium Access Control (MAC)

and Physical Layer (PHY) Specifications - Amendment 4: Further Higher Data Rate Extension in the 2.4 GHz Band, June 27,2003.

[12] IEEE 802.11n-2009, IEEE Standard for Local and Metropolitan Area Networks Specific Requirements – Part 11: Wireless LAN Medium Access Control (MAC) and Physical Layer (PHY) Specifications – Amendment 5: Enhancements for Higher Throughput., October 29, 2009.

[13] R. Bruno, M. Conti, E. Gregori, "Mesh Networks: Commodity Multihop Ad Hoc Networks", *IEEE Communications Magazine*, Vol. 43 (3), pp. 123-131, 2005.

[14] Bert Williams, "Metro Wi-Fi Networks: What are They and How Can They Benefit Your Community?", ICMA publications, Vol. 89 (2), March, 2007.

[15] D. Benyamina, A. Hafid, M. Gendreau, "Wireless Mesh Networks Design – A Survey", *IEEE Transactions on Communications Surveys and Tutorials*, Vol. 14 (2), pp.299-310, 2012.

[16] N. Nandiraju, D. Nandiraju, L.Santhanam, B. He, J.Wang, D. P. Agrawal, "Wireless Mesh Networks: Current Challenges and Future Directions of Web-in-the-Sky", *IEEE Transactions on Wireless Communications*, Vol. 14 (4), pp.79-89, Aug. 2007.

[17] A. S. Reaz, V. Ramamurthi, D. Ghosal, J. Benko, W. Li, S. Dixit, B. Mukherjee, "Enhancing Multi-hop Wireless Mesh Networks with a Ring Overlay", *IEEE Annual Communications Society Conference on Sensor, Mesh and Ad Hoc Communications and Networks Workshops*, pp. 1-6, San Francisco, USA, 2008.

[18] Y. Amir, C. Danilov, M. Hilsdale, R. Musaloiu-Elefteri, N. Rivera, "Fast Handoff for seamless Wireless Mesh Networks", *International Conference on Mobile Systems, Applications and Services*, pp. 83-95, Uppsala, Sweden, 2006.

[19] A.-N. Moldovan, C.-H. Muntean, "Personalisation of the Multimedia Content Delivered to Mobile Device Users", *IEEE International Symposium on Broadband Multimedia Systems and Broadcasting (BMSB)*, pp. 1-6, Bilbao, Spain, May 2009.

[20] D. Johnson, Y. Hu, D. Maltz, "The Dynamic Source Routing Protocol (DSR) for Mobile Ad Hoc Networks for IPv4", IETF RFC 4728, February, 2007.

[21] C. E. Perkins, E. M. Royer, "Ad-hoc On-Demand Distance Vector Routing", *IEEE Workshop on Mobile Computing Systems and Applications*, Los Angeles, USA, pp. 90-100, 1999.

[22] C. E. Perkins, E. B. Royer, S. R. Das, "Ad Hoc On-demand Distance Vector Routing", IETF RFC 3561, July 2003.

[23] C. E. Perkins, P. Bhagwat, "Routing over Multi-hop Wireless Network of Mobile Computers", *Springer Mobile Computing*, Vol. 353, pp. 183-205, 1996.

[24] P. Jacquet, P. Muhlethaler, T. Clausen, A. Laouiti, A. Qayyum, L. Viennot, "Optimized Link State Protocol for Ad hoc Networks", *IEEE Multi Topic Conference*, Pakistan, pp. 62-68, 2001.

[25] T. Clausen, P. Jacquet, "Optimized Link State Routing Protocol (OLSR)", IETF RFC 3626, October, 2003.

[26]   S. Gowrishankar, T. G. Basavaraju, M. Singh, S. K. Sarkar, "Scenario based Performance Analysis of AODV and OLSR in Mobile Ad hoc Networks", *South Easet Asia Regional Computer Conference, Bangkok*, Thailand, 2007.

[27]   C. Mbarushimana, A. Shahrabi, "Comparative Study of Reactive and Proactive Routing Protocols Performance in Mobile Ad Hoc Networks*", IEEE Conference on Advanced Information Networking and Applications*, Ontario, Canada, pp. 679-684, 2007.

[28]   D. B. Johnson, Y. Hu, D. Maltz, "the Dynamic Source Routing Protocol (DSR) for Mobile Ad Hoc Networks for IPv4", IETF RFC 4728, February, 2007.

[29]   J. Haerri, F. Filali, C. Bonnet, "Performance comparision of AODV and OLSR in VANETs urban Environments under Realistic Mobility Patterns", *Mediterranean Ad-Hoc Networking Workshop*, Lipari, Italy, 2006.

[30]   BitTorent – http://www.bittorent.com.

[31]   "Application Usage and Threat Report", Palo Alto Networks, 2014. [Online] – Available: http://researchcenter.paloaltonetworks.com/app-usage-risk-report-visualization/#sthash.38HWmP45.n3Efd4Iq.dpbs

[32]   A. S. Tanenbaum, D. J. Wetherall, "Computer Networks", 5th Edition, Prentice Hall, ISBN-9780132126953, 2010.

[33]   M. Ripeanu, "Peer-to-Peer architecture case study: Gnutella network", *International Conference on Peer-to-Peer Computing*, Linkoping, Sweden, pp. 99-100, 2001.

[34]   Freenet - https://freenetproject.org/

[35]   I. Stoica, R. Morris, D. L. Nowell, D. R. Karger, M. F. Kaashoek, F. Dabek, H. Balakrishnan, "Chord: A Scalable Peer-to-Peer Lookup Protocol for Internet Applications", *IEEE Transactions on Networking*, Vol. 11 (1), pp. 17-32, 2003.

[36]   S. Ratnasamy, P. Francis, M. Handley, R. Karp, S. Shenker, "A Scalable Content-Addressable Network", *Conference on Applications, Technologies, Architectures, and Protocols for Computer Communications*, pp. 161-172, California, USA, 2001.

[37]   A. Rowstron, P. Druschel, "Pastry: A Scalable, Decentralized Object Location and Routing for Large Scale Peer-to-Peer System", *IFIP/ACM Middleware*, pp.329-350, Heidelberg, Germany, 2001.

[38]   D. Malkhi, M. Naor, D. Ratajczak, "Viceroy: A Scalable and Dynamic Emulation of the Butterfly", *Symposium on Principles of Distributed Computing*, pp. 183-192, California, USA, 2002.

[39]   Cisco Visual Networking Index: "Forecasting and Methodology, 2011-2016".

[40]   Real-time Transport Protocol – https://www.ietf.org/rfc/rfc3550.txt

[41]   Real-time Streaming Protocol – https://www.ietf.org/rfc/rfc2326.txt

[42]   ITU BT.500-11: Methodology for the subjective assessment of the quality of television pictures - http://www.itu.int/rec/R-REC-BT.500-11-200206-S/en

[43]   ITU Y.1541 Network performance objectives for IP-based services - http://www.itu.int/rec/T-REC-Y.1541/en

[44] ITU-T: Recommendation P.910: "Subjective Video Quality Assessment Methods for Multimedia Applications," Sept. 1999.

[45] M. J. Sreeman, I. E. G. Richardson, "Digital Video Communications", 1st Edition, Artech House, ISBN- 9780890068908, 1997.

[46] Q. Huynh-Thu, M. Ghanbari, "Scope of validity of PSNR in image/video quality assessment", *IEEE Electronic Letters*, Vol. 44 (13), pp. 800-801, 2008.

[47] S. B. Lee, G. M. Muntean, A. F. Smeaton, "Performance-Aware Relication of Distributed Pre-Recored IPTV content", *IEEE Transactions on Broadcasting*, Vol. 55 (2), pp. 516-526, 2009.

[48] C.H. Ke, C.K. Shieh, W.S. Hwuang, A.Ziviani, "An Evaluation Framework for More Realistic Simulations of MPEG Video Transmission", *Journal of Information Science and Engineering*, Vol. 4 (2), pp. 425-440, 2008.

[49] Z. Wang, L. Lu, A.C. Bovik, "Video quality assessment using structural distortion measurement", International Conference on Image Processing, Vol. 3, pp. 65-68, 2002.

[50] M.H. Pinson, S. Wolf, "A new standardized method for objective measuring video quality", *IEEE Transaction on Broadcasting*, Vol. 50 (3), pp. 312-322, 2004.

[51] A. Klem, C. Lindemann, O. P. Waldhorst, "A Special-Purpose Peer-to-Peer File Sharing System for Mobile Ad Hoc Networks", *IEEE Vehicular Technology Conference*, Florida, USA, pp. 2758-2763, 2003.

[52] I. Gruber, R. Schollmeier, Wolfgang Kellerer, "Performance Evaluation of the Mobile Peer-to-Peer Service", *IEEE International Symposium on Cluster Computing and the Grid*, Illinois, USA, pp.363-371, 2004.

[53] C-C. Hoh, R-H. Hwang, "P2P File Sharing System over MANET based on Swarm Intelligence: A Cross-Layer Design", *IEEE Wireless Communications and Networking Conference*, Hong Kong, China, pp. 2676-2681, 2007.

[54] M. Gunes, U. Sorges, I. Bouazizm, "ARA – the ant-colony based routing algorithm for MANETs*", IEEE, International Workshop on Parallel Processing*, pp. 79-85, Washington DC, USA, 2002.

[55] W. Kellerer, R. Schollmeier, "Proactive Searching Routing for Mobile Peer-to-Peer Networks: Zone-based P2P", *Applications and Services in Wireless Networks*, Paris, France, 2005.

[56] C-L. Liu, C-Y. Wang, H-Y. Wei, "Cross-layer Mobile Chord P2P protocol Design for VANET", *International Journal of Ad Hoc and Ubiquitous Computing*, Vol. 6 (3), pp. 150-163, 2010.

[57] G. Ding, J. Vicente, S. Rungta, D. Krishnaswamy, W. Chan, K. Miao, "Overlays on Wireless Mesh Networks: Implementation and cross-Layer Searching", *IEEE International conference on Management of Multimedia and Mobile Networks and Services*, Berlin, Germany, pp. 171-182, 2006.

[58] S. Ratnasamy, B. Karp, S.Shenker, D. Estrin, R. Govindan, Y. Lin, F. Yu, "GHT: A Geographic hash Table for Data centric Storage in SensorNets", *ACM Workshop on Wireless Sensor networks and Applications*, New York, USA, pp. 78-87, 2002.

[59]   S. Shenker, S. Ratnasamy, B. Karp, R. Govindan, D. Estrin, "Data-Centric Storage in Sensornets", *ACM Workshop on Hot Topics in Networks*, New York, USA, pp. 137-142, 2003.

[60]   S. Ratnasamy, B. Karp, S. Shenker, D. Estrin, R. Govindan, L. Yin, F. Yu, "Data-centric storage in sensornets with GHT, A Geographic Hash table", *Mobile Networks and Applications*, Vol.8 (4), pp 427-442, 2003.

[61]   B. Karp, H.T. Kung, "GPSR: Greedy Perimeter Stateless Routing for Wireless Networks", *IEEE International Conference on Mobile Computing and Networking*, Boston, USA, 2000.

[62]   O. Landsiedel, S. Gotz, K. Wehrle, "Towards Scalable Mobility in Distributed Hash Tables", *IEEE International Conference on Peer-to-peer Computing*, Cambridge, England, pp. 203-209, 2006.

[63]   P. Desnoyers, D. Ganesan, P. Shenoy, "TSAR: A two tier sensor storage architecture using Interval Skip Graphs", *International Conference on Embedded Network Sensor Systems*, New York, USA, pp. 39-50, 2005.

[64]   L. Gallucio, G. Morabito, S. Palazzo, M. Pellegrini, M. E. Renda, P. Santi, "Georoy: A location-aware enhancement to Viceroy peer-to-peer algorithm", *Computer Network*s, Vol. 51 (8), pp. 1998-2014, 2006.

[65]   D. Malkhi, M. Naor, D. Ratajczak, "Viceroy: a scalable and dynamic emulation of the butterfly", *ACM Symposium on Principles of Distributed Computing*, New York, USA, pp. 183-192, 2002.

[66]   S. Burresi, C. Canali, M. E. Renda, P. Santi, "MeshChord: A Location-Aware, Cross-layer Specialization of Chord for Wireless Mesh Networks", *IEEE International Conference on Pervasive Computing and Communication*s, , Hong Kong, China, pp.206-2122008.

[67]   C. Canali, M. E. Renda, P. Santi, S. Burresi, "Enabling Efficient Peer-to-Peer Resource sharing in Wireless Mesh Networks", *IEEE Transaction on Mobile Computing*, Vol. 9 (3), pp. 333-347, 2010.

[68]   C. Canali, M. E. Renda, P. Santi, "Evaluating Load Balancing in Peer-to-Peer Resource Sharing Algorithms for Wireless Mesh Networks", *IEEE International Conference on Mobile Ad Hoc and Sensor Systems*, Atlanta, USA, pp. 603-609, 2008.

[69]   A. Alasaad, S. Gopalakrishnan, V. C. Leung, "Mitigating Load Imbalance in Wireless Mesh Networks with Mixed Application Traffic Types", *IEEE Global Communications Conference*, Miami, USA, pp. 1-5, 2010.

[70]   F. Delmastro, "From Pastry to CrossROAD: CROSS-layer Ring Overlay for AD hoc networks", *IEEE International Conference on Pervasive Computing and Communications Workshops*, Kauai Island, USA, pp. 60-64, 2005.

[71]   I. Gruber, R. Schollmeier, W. Kellerer, "Performance Evaluation of the Mobile Peer-to-Peer Service", *IEEE International Symposium on Cluster Computing and the Grid*, Illinois, USA, pp.363-371, 2004.

[72]   M. C. Castro, E. Villanueva, I. Ruiz, S. Sargento, A. J. Kassler, "Performance Evaluation of Structured P2P over Wireless multi-hop Networks", *IEEE SENSOR COMM*, Cap Esterel, France, pp. 796-801, 2008.

[73]   C. Cramer, T. Fuhrmann, "Performance Evaluation of Chord in Mobile Ad Hoc Networks", *IEEE International workshop on Decentralized resource sharing in mobile computing and networking*, New York, USA, pp. 48-53, 2006

[74]   E. Karasabun, D. Ertemur, S. Sariyidliz, M. Tekkalmaz, I. Korpeoglu, "A Path-Quality-Aware Peer-to-Peer File Sharing Protocol for mobile Ad-hoc Networks: Wi-Share", *International Symposium on Computer and Information Sciences*, Guzelyurt, Turkey, pp. 322-327, 2009.

[75]   A. A. Asaad, S. Gopalakrishnan, V. Leung, "Peer-to-Peer File Sharing over Wireless Mesh Networks", *Processing IEEE Pacific Rim Conference on Communications, Computers and Signal*, Victoria, Canada, pp. 697-702, 2009.

[76]   N. Mastronarde, D. S. Turaga, M. V. D. Schaar, "Collaborative resource Exchanges for Peer-to-Peer Video Streaming Over Wireless Mesh Networks", *IEEE Journal on Selected areas in Communications*, Vol. 25 (1), pp. 108-118, 2007.

[77]   H. Luo, S. Ci, S. Wu, "A Cross-layer Optimized Distributed Scheduling Algorithm for Peer-to-Peer Video Streaming over Multi-hop Wireless Mesh Networks", *IEEE communications society conference on Sensor, Mesh and Ad Hoc Communications and Networks*, Rome, Italy, pp. 619-627, 2009.

[78]   D. Wang, C. K. Yeo, "Exploring Locality of Reference in P2P VoD Systems", *IEEE Global Communications Conference*, Miami, USA, pp. 1-6, 2010.

[79]   D. Wang, C. K. Yeo, "Exploring Locality of Reference in P2P VoD Systems", *IEEE Transactions on Multimedia*, Vol. 14 (4), pp. 1309-1323, 2012.

[80]   W-P. K. Yiu, X. Jin, S-H. G. Chan, "VMesh: Distributed Segment Storage for Peer-to-Peer Interactive Video Streaming", *IEEE Transactions on Selected Areas in Communications*, Vol. 25 (9), pp. 1717-1731, 2007.

[81]   C. Xu, F. Zhao, J.Guan, H.Zhang, G.-M.Muntean, "QoE-driven User-centric VoD Services in Urban Multi-homed P2P-based Vehicular Networks", *IEEE Transaction on Vehicular Technology*, Vol. 62 (5), 2013.

[82]   802.11p – WAVE interface - https://www.standards.its.dot.gov/Factsheets/Factsheet/80

[83]   D. Wang, C. K. Yeo, "Superchunk based Fast Search in P2P-VoD System", *IEEE Global Telecommunications Conference*, Hawaii, USA, pp. 1-6, 2009.

[84]   D. Wang, C. K. Yeo, "Superchunk based Efficient Search in P2P-VoD System", *IEEE Transactions on Multimedia*, Vol. 13 (2), pp. 376-389, 2011.

[85]   Donald Knuth, "The Art of Computer Programming, Volume 3: Sorting and Searching", Third Edition. Addison-Wesley, 1997. ISBN 0-201-89685-0. Pages 458–475 of section 6.2.3: Balanced Trees.

[86]   J. Robinson, E. W. Knightly, "A Performance Study of Deployment Factors in Wireless Mesh Networks", *IEEE International Conference on Computer Communications*, Anchorage, USA, pp. 2054-2062, 2007.

[87]   Y. Chen and H. Kobayashi, "Signal strength based indoor geolocation", *IEEE International Conference on Communications*, pp. 436–439, New York, NY, USA, April–May 2002.

[88]   NS-3 - http://www.nsnam.org/

[89]   Reference videos - http://www2.tkn.tu-berlin.de/research/evalvid/cif.html

[90]   J. Klaue, B. Rathke, A. Wolisz, "EvalVid – A Framework for Video Transmission and Quality Evaluation", *International Conference on Modelling Techniques and Tools for Computer Performance evaluation*, Illinois, USA, pp. 255-272, 2003.

[91]   S. Misra, S. C. Misra, I. Woungang, "Guide to Wireless Mesh Networks", *Computer Communications and Networks*, ISBN 978-1-84800-909-7, pp. 199-230, Springer London, 2009.

[92]   D. S. J. De Couto, D. Aguayo, J. Bicket, R. Morris, "A High-Throughput Path Metric for Multi-Hop Wireless Routing", *International Conference on Mobile Computing and Networking*, New York, USA, pp. 134-146, 2003.

[93]   D. Passos, C. V. N. de Albuquerque, M. E. M. Campoista, L. H. M, K. Costa, O. C. M. B. Duarte, "Minimum Loss Multiplicative Routing Metrics for Wireless Mesh Networks", *Journal of Internet Services and Applications*, Vol. 1 (3), pp. 201-214, 2011.

[94]   NS-2 - http://www.isi.edu/nsnam/ns/

[95]   NS-3   Tap   Bridge   Class   Reference,   Network   Simulator   3   - https://www.nsnam.org/doxygen/classns3_1_1_tap_bridge.html#details

[96]   MSU   Video   Quality   Measurement   Tool   - http://compression.ru/video/quality_measure/video_measurement_tool_en.html

[97]   MSU   Perceptual   Video   Quality   Tool   - http://compression.ru/video/quality_measure/perceptual_video_quality_tool_en.html

[98]   EBU BPN 055: Subjective viewing evaluations of some internet video codecs – Phase 1 Report by EBU Project Group B/VIM (Video In Multimedia), May 2003

[99]   Big Buck Bunny movie - https://peach.blender.org/

[100]   ITU-T Recommendation P.800, "Methods for subjective determination of transmission quality", August, 1996.

[101]   ITU-T Recommendation P913, "Methods for the subjective assessment of video quality, audio quality and audio visual quality of Internet video and distribution quality television in any environment", January, 2014.